THE UNIVERSITY OF CHICAGO

C-TERMINAL PROPERTIES OF TENEURIN, A BACTERIAL TOXIN HOMOLOGUE AT THE SYNAPSE

A DISSERTATION SUBMITTED TO

THE FACULTY OF THE DIVISION OF THE BIOLOGICAL SCIENCES

AND THE PRITZKER SCHOOL OF MEDICINE

IN CANDIDACY FOR THE DEGREE OF

DOCTOR OF PHILOSOPHY

COMMITTEE ON NEUROBIOLOGY

BY

JORGE ANTONIO ALVARADO

CHICAGO, ILLINOIS

JUNE 2025

ABSTRACT

The brain processes information by relaying signals between neurons at the synapse, creating a diverse network of neuronal circuitry. Protein interactions between receptors, ligands, and cell adhesion molecules in the synaptic cleft enable the development of this highly intricate network. A family of highly conserved cell-adhesion proteins called teneurins (TENs) play a role in axon guidance, target selection, and synapse formation via transsynaptic interactions. TENs are comprised of a transmembrane region (TM) and an extracellular region that forms a barrel-like structure followed by a toxin-like domain at the C-terminus. This fold is not found in other eukaryotic proteins but instead bears resemblance to the large barrel structure of bacterial Tc toxins, a set of triple-protein complexes with a C-terminal cytotoxic region that plays an important role in Tc toxin insecticidal function. Furthermore, sequence alignment reveals that a catalytic site in Tc toxins involved in autoproteolysis of the C-terminus is mostly conserved in TENs. Due to this structural and biochemical homology, we investigated the importance of the C-terminus of TENs by targeting the toxin-like domain of the *C. elegans* orthologue, *ten-1*. We observed endogenous expression of Ten-1 at the nerve ring, ventral nerve cord, and tail, and we found that truncation of the toxin-like domain intensified expression. Moreover, defects in M4, NSM, and HSN neurons were observed in both truncation and null mutants. We also observed that protein purification of human TEN2 yielded a C-terminal product when the EGF- and Ig-like domains were deleted, which was abolished when the conserved catalytic residues were mutated. Together, we characterized *C. elegans ten-1* expression and significance of its C-terminus *in vivo* and the autoproteolytic potential of human TEN2 *in vitro*, providing insight into the importance of the toxin-like domain, which may be worthwhile for studying TENs in human disease.

TABLE OF CONTENTS

LIST OF FIGURES

LIST OF TABLES

ACKNOWLEDGEMENTS

When I moved to Chicago in 2019, I never expected the number of obstacles I would face during my journey as a PhD candidate. Not knowing a single person in a new city, overcoming a global pandemic, navigating social and political movement occurring in this country, I never thought as a kid who grew up in Peru and Miami that I would be standing at the precipice of receiving a PhD degree. I could have never done this without the people in my life before Chicago and the new friends and family I made over the years here.

First, I would like to thank the Neurobiology program at UChicago for taking a chance on me and making my dreams come true. To all the member of my committee, I am very grateful for your commitment to seeing me succeed and guiding me in a tumultuous academic journey over the past 5 years. I would like to thank members of the Kratsios and Araç lab for your support as both colleagues and friends. I would like to specially thank Jingxian Li for training me in biochemical assays used in this thesis, and to the whole Kratsios Lab for a crash course in *C. elegans* genetics and maintenance. I would also like to thank Elena Cortés and Indya Weathers for making times in lab a little brighter. And to past members of the lab, Hagerah Malik and Joe Pak, for motivating me to see this journey through.

I would like to thank my loving partner, Matthew Wolf, for being at my side throughout these years, through the good days and the bad days, and making me smile during the typical graduate school down days. It has been a challenging time, but we made it together and have shared a lot of memories together, and I hope many more to come. And, of course, a big hug to our lovely new doggy, Lola, who has become a loving part of our lives so quickly.

Finally, I want to thank my family. We came to the United States more than 20 years ago to set a new life for ourselves, without barely speaking any English or without much family to support us. Mamá, Papá, Kike, Vanesa, los quiero muchísimo, y espero que los haga muy orgullosos de mí. Después de mudarme de la Florida, no paro mucho tiempo con ustedes, pero quisiera aumentar el tiempo que pasamos juntos ya ahora que termino mi doctorado. Y muchos abrazos a Danielito, mi sobrinito, y a Jose, que han agrandado nuestra familia en una manera inolvidable. Y por último, a la familia en el cielo, tía Dula, abuelito Juan, abuelita Sofía, abuelita Luz, tío Freddy, los extraño mucho y ya algún día nos encontraremos otra vez. ¡Saludos y abrazos a mi familia peruana, los quiero mucho!

CHAPTER I: INTRODUCTION

1.1 Background on Neuronal Circuit Assembly in the Brain

The brain is composed of an interconnected network of neurons that receives sensory input from the entire body and processes this information to initiate a response. Neurons form this network by migrating their axons to the correct anatomical position and connecting to each other at a specialized region called the synapse, where the axon or dendrite of one neuron meets the axon or dendrite of another. Intercommunication between neurons occurs at the synapse when presynaptic chemical messengers called neurotransmitters are released from the axon terminal and bind to postsynaptic receptors to induce a chemical or electrical signal, allowing for the transfer of information between neurons. Investigating how neuronal circuitry is established is vital for understanding information processing and proper brain function.

Neuronal circuit assembly can be divided into two steps: axon guidance and synaptic specificity. After neural progenitor cells divide and differentiate into neurons, they migrate along radial glia to reach their final destinations; additionally, extracellular cues in the surrounding environment guide axons to their appropriate anatomical regions via chemical attraction or repulsion. Upon reaching a particular region, axons select specific target neurons through interactions between cell-adhesion molecules, forming the synaptic cleft. Furthermore, transsynaptic crosstalk between cell adhesion molecules directs the type of synapse formed, whether excitatory or inhibitory. Presynaptic cell-adhesion molecules can be classified into at least five major groups, while postsynaptic cell-adhesion molecules emerge from more than 50 genes (Südhof, 2017) Thus, the convergence of dozens of protein-protein interactions give rise to the intricate network of neurons in our brains.

1.2 Role of Teneurins in Neuronal Circuit Assembly

Teneurins (TENs), a family of evolutionarily conserved cell-adhesion proteins, are among the multitude of proteins that play a role in neuronal circuit assembly. They are type-II transmembrane proteins, with an internal N-terminus and external C-terminus, composed of four isoforms in humans, mice, chicken, and other vertebrates (TEN1-4), two isoforms in *Drosophila* (Ten-a and Ten-m), and a single ortholog in *C. elegans* (*ten-1*). TENs are located at the presynaptic side of the synapse, supporting the migration of axons across large distances and directing synaptic specificity at the appropriate region.

1.2.1 Teneurins and Axon Guidance

TENs are widely expressed in the brain during embryonic development, in addition to non-neuronal areas (Kenzelmann et al., 2008; Lossie et al., 2005; Nakamura et al., 2013; Rubin et al., 2002; Tucker & Chiquet-Ehrismann, 2006; Tucker et al., 2001). Expression during development indicates that TENs may play a role in migration of cells and axons necessary for correct neuronal wiring. Indeed, *in vivo* mouse studies reveal that TENs expressed in migrating cortical neurons bind to latrophilin-1, an adhesion G-protein coupled receptor (GPCR), expressed in radial glial cells and contributes to cortical cell migration via contact-repulsion mechanism (Del Toro et al., 2020). Furthermore, the whole extracellular region of TEN2 is proteolytically cleaved and released into the medium, inducing attraction of axonal growth cones via interaction with latrophilin-1 in rat hippocampal neuron cultures (Vysokov et al., 2016; Vysokov et al., 2018). In the mouse visual system, TEN2, TEN3, and TEN4 knockouts (KO) disrupted projection of ipsilateral axons from retinal ganglion cells (RGCs) to the correct targets on the dLGN and superior colliculus (Dharmaratne et al., 2012; Leamey et al., 2007; Young et

al., 2023; Young et al., 2013). TEN3 knockdown in zebrafish also cause morphological and functional defects of retinal ganglion cells in the visual system, while TEN4 point-mutations result in defects in motor axon pathfinding, outgrowth and branching (Antinucci et al., 2013; Antinucci et al., 2016; Hor et al., 2015). In *Drosophila*, *ten-m* mutants cause the inter-segmental nerve to target the incorrect region of the neuromuscular junction (NMJ), which is also observed in ectopic overexpression of *ten-m* (Zheng et al., 2011). *C. elegans ten-1* null mutant exhibits axonal defects in pharyngeal neurons and enhances many axon guidance defective mutants (Drabikowski et al., 2005; Mörck et al., 2010). TENs have a profound role in axon guidance in both vertebrates and invertebrates, influencing motor neuron axon routing, binocular visual circuits, and general neuronal wiring in the developing nervous system.

1.2.2 Teneurins and Synaptic Specificity

While TENs can influence long-range axonal development, they also control short-range synaptic targeting and synapse formation through heterophilic and homophilic interactions. In the mouse hippocampus, Schaffer-collateral axons from the CA3 region and perforant-path axons from the entorhinal cortex project to nonoverlapping dendritic domains of CA1 pyramidal neurons depending on distinct latrophilin expression, respectively: latrophilin-3 in dendritic domains located on the stratum (S.) oriens and S. radiatum layers, and latrophilin-2 in the stratum (S.) lacunosum moleculare. *In vivo* experiments revealed that conditional latrophilin-3 KO mice infected with lentiviral Cre in the CA1 region exhibited a decrease in Schaffer-collateral EPSCs, which was rescued by wildtype latrophilin-3; however, blocking binding of latrophilin-3 to TENs or FLRTs, another cell adhesion molecule that forms the LPHN-TEN-FLRT trimeric complex, prevented rescue of electrophysiological activity, indicating that

coincident binding of TENs and FLRT was necessary for Schaffer-collateral-specific synapse formation via latrophilin-3 GPCR-dependent mechanism. (Sando et al., 2019; Sando & Südhof, 2021). Further studies show that TENs form presynaptic nanoclusters to promote excitatory synapse formation in the hippocampus via heterophilic interactions (Zhang et al., 2022). Mouse TEN3 recruits presynaptic active zone scaffold proteins present as liquid-liquid phase-separated (LLPS) condensates, which was found to be functionally essential for synapse formation alongside latrophilin-3-mediated recruitment of postsynaptic LLPS condensates (S. Wang et al., 2024; Zhang et al., 2025). Moreover, TEN3 *cis*-dimerization generated by disulfide bridges between unpaired cysteines in EGF-like domains was found to be crucial for synapse formation. Alternative splicing of TENs has been postulated as the driving mechanism for determining excitatory or inhibitory synaptic identity by restricting heterophilic binding of latrophilin to a specific splice variant with flexible conformation (Li et al., 2020).

In addition to heterophilic interactions, homophilic interactions between TENs drive circuit assembly. For example, mouse TEN3 is required in both CA1 and subicular neurons of the hippocampus to connect proximal CA1 axons to distal subiculum (Berns et al., 2018). In a similar mechanistic manner, axons from about 50 classes of olfactory receptor neurons (ORNs) form one-to-one connections to dendrites of projection neurons (PNs) in the antenna lobe of Drosophila via homophilic interactions of Ten-m and Ten-a. Mutant KOs of either *ten-m* or *ten-a* result in mismatching ORN-PN pairs, which could not be rescued by overexpression of the other isoform (Hong et al., 2012; Mosca et al., 2012). Furthermore, different expression levels of Ten-m or Ten-a instruct partner matching (DePew et al., 2019). Genetic interaction studies revealed that Ten-m binding to RhoGAP and subsequent activation of Rac1 small GTPase regulate the actin cytoskeleton and drive synaptic partner matching (Xu et al., 2024).

Dimerization has been reported in different TEN isoforms and at multiple domain sites in both *cis* and *trans* conformations, further highlighting how homophilic interactions are integral to TENs function (Feng et al., 2002; Gogou et al., 2024; Li et al., 2023; Meijer et al., 2022). Altogether, TENs drive synaptic specificity in vertebrates and invertebrates through a delicate balance between homophilic and heterophilic interactions.

1.3 Teneurin Structure and Conservation

TENs are single-pass transmembrane proteins with highly conserved domains, sharing an N-terminal intracellular domain (ICD), a single-pass transmembrane region (TM), and a large (over 2000 amino acids) extracellular region (ECR) at the C-terminus (**Figure 1.1A**). The ECR comprises five domains forming a large barrel-like structure and mediates transsynaptic interactions at the synaptic cleft.

1.3.1 The Intracellular Domain and the Nucleus

The ICD is composed of 300-400 residues that contain a nuclear localization sequence (NLS) and proline-rich SH3-binding domain (Tucker, 2018). A furin-like cleavage site is found upstream of the TM, allowing for proteolytic processing and cytoplasmic release of the ICD to the nucleus (Vysokov et al., 2016). *In vitro* studies show that the ICD acts as a transcription regulator at the nucleus by repressing zic, a transcription factor, and binds to CAP/ponsin, a protein involved in cytoskeleton organization and signaling, and MBD1, a methylated DNA binding protein (Bagutti et al., 2003; Nunes et al., 2005). Deletion of the ICD alters the ability of TENs to localize to synaptic sites, implying the ICD contains motifs that bring TENs to synaptic sites (Cheung et al., 2022). Furthermore, the ICD is indispensable for presynaptic active zone

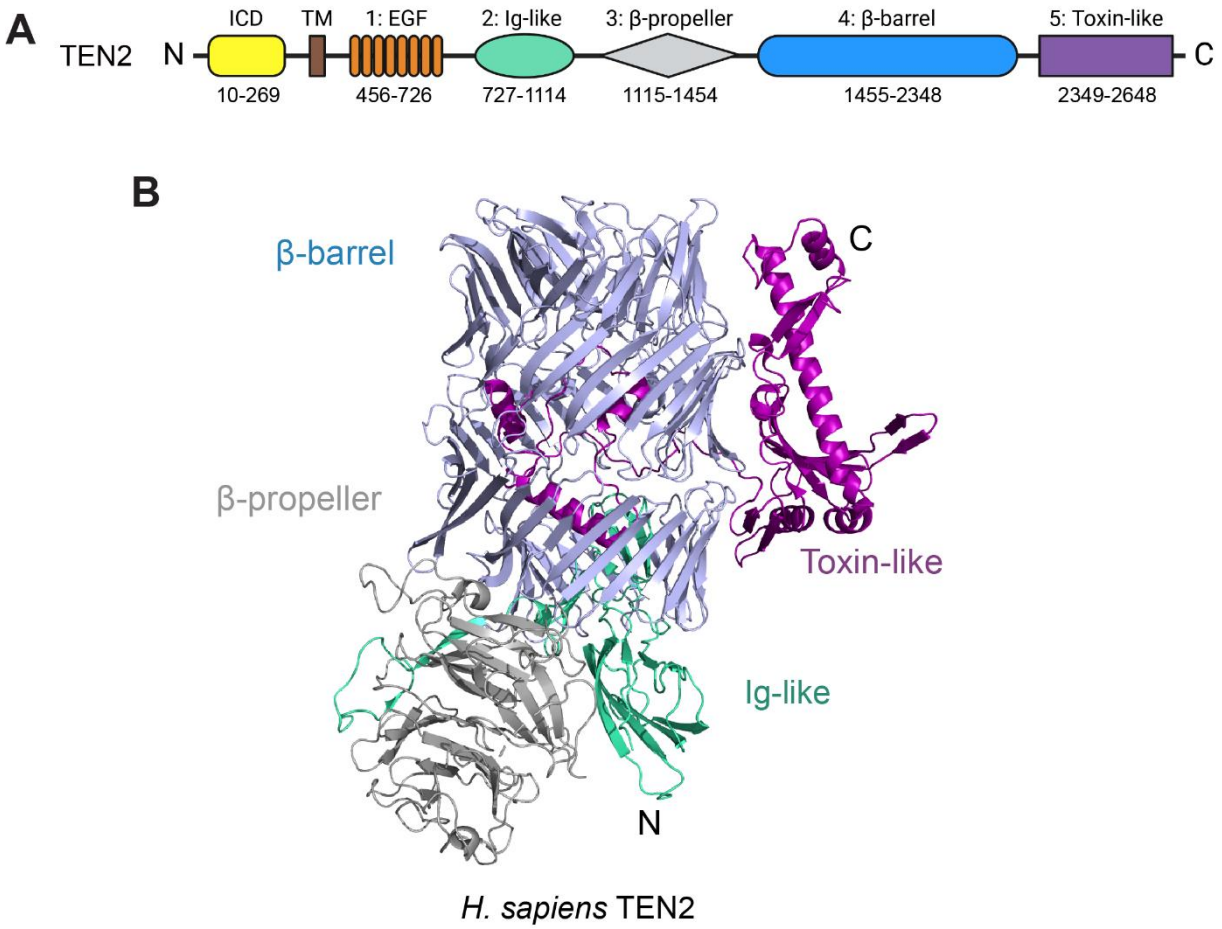

Figure 1.1: Human TEN2 diagram and structure

(A) Linear diagram of full-length human TEN2 protein shows an intracellular domain (ICD) at the N-terminus, single-pass transmembrane (TM), and extracellular region (ECR) comprised of five domains: epidermal growth factor-like domain (EGF), immunoglobulin-like domain (Ig), β-propeller, β-barrel, and toxin-like domain at C-terminus.

(B) Cryo-EM model of human TEN2 ECR monomer without EGF-like domain.

LLPS recruitment necessary for synapse formation alongside latrophilin-3 (Zhang et al., 2025). Alternative splice variants of ICD are present in human and chicken teneurins, while *ten-1* in *C. elegans* is expressed as two isoforms, either the long form (ten-1L) full-length protein or short form (ten-1S) lacking the ICD.

1.3.2 The EGF-like Domain and Dimerization

The ECR of most TENs contains eight epidermal growth factor (EGF) repeats about 200 residues downstream of the TM. Six of these EGF repeats each contain 6 cysteines that form three pairs of disulfide bond, while EGF2 and EGF5 express five cysteines, leaving an unpaired cysteine from each repeat to form a disulfide bridge to lone cysteines from other TENs in *cis* (Feng et al., 2002; Oohashi et al., 1999). Negative stain EM micrographs of full ECR showed two globular domains linked together at their stalk-like ends, while ECR with truncation of the EGF-like domain expressed as a monomeric protein, indicating that the EGF-like domain is responsible for homodimerization in full-length TEN proteins (Li et al., 2018).

1.3.3 The Ig-like Domain and Structure Seal

Downstream of the EGF-like domain, the immunoglobulin (Ig)-like domain (**Figure 1.1B in teal**) spans about 500 residues comprising three subregions: cysteine-rich domain (CRD), transthyretin-related domain (TTR), and fibronectin (FN)-plug. In *Drosophila*, the TTR domain of Ten-m creates an asymmetrical interface with the downstream β-propeller domain of another Ten-1 in a *cis*- or *trans*- orientation, potentially forming long multimer structures, or "zippers" (Li et al., 2023). Furthermore, this Ten-m interface is conserved in arthropods but not in vertebrate TENs. The Ig-like domain plugs the bottom of the barrel-like structure, forming hydrophobic and hydrogen bonds with the shell interior and creating contacts with the toxin-like domain inside the barrel (Li et al., 2018).

1.3.4 The β-propeller and Protein-Protein Interactions

The Ig-like domain holds the flexible β-propeller in place, which resides perpendicular to the barrel (**Figure 1.1B in silver**) (Jackson et al., 2018; Li et al., 2018). This 6-bladed β-propeller contains a series of NCL-1, HT2A and Lin-41 (NHL) repeats that participate in homophilic interactions and directing synaptic specificity. While the β-propeller/Ig-like interface, which allows for homodimerization in *Drosophila ten-m*, is not conserved in vertebrates, TENs express an alternative splice site in an NHL loop of the β-propeller that drives homophilic interactions in *trans* (Beckmann et al., 2013; Berns et al., 2018; Jackson et al., 2018; Li et al., 2020). This alternative splice site is in the same region as the asymmetrical interface in Ten-m, suggesting that regulation of TEN dimerization diverged during evolution (Li et al., 2023). Additionally, alternative splicing in β-propeller influences the ability of TENs to bind to transsynaptic partner latrophilin, controlling synaptic identity as either excitatory or inhibitory (Li et al., 2020).

1.3.5 The β-barrel and Unique Superfold

The β-barrel domain is composed of about 800 residues with more than two dozen tyrosine-aspartate (YD)-repeats forming pairs of β-strands connected by a β-hairpin. These YD-repeat strands coalesce into a spiraling β-sheet, resulting in a hollow cylindrical structure (**Figure 1.1B in sky blue**). The β-barrel is sealed at the bottom by the Ig-like domain but contains an opening at the side, allowing the C-terminus to perforate the barrel outwardly through this exit site. This barrel structure is conserved in all TEN isoforms.

1.3.6 The Toxin-like Domain at the C-terminus

The most C-terminal domain of TENs, the toxin-like domain, is composed of an internal linker about 80 amino acids long that is continuous from the inside of the barrel cavity and exits through a gap in the shell wall (**Figure 1.1B in purple**). More than 200 residues of the toxin-like domain reside outside the barrel exposed to extracellular space. These residues form loops that wrap around α-helices and are tethered to the side of the β-barrel via hydrogen bonds. The final ~40 residues of the toxin-like domain comprise the Teneurin C-terminal Associated Peptide (TCAP), which shares conserved elements with neuropeptides. This TCAP region is conserved among TEN homologs.

Taken together, the extracellular domains of TENs form a unique tertiary structure with multitude of protein-protein interfaces, and the convergence of these structural properties give rise to the functional role of TENs in neuronal circuit formation. Intriguingly, YD-repeats forming the barrel-like structure of TENs are not found in other eukaryotic proteins, leading to questions about the evolutionary origin of TENs and its significance on TEN function.

1.4 Teneurin Origins and Evolution

TEN domain organization is phylogenetically conserved in metazoans. A search for TEN domains in non-metazoan sequences revealed that the single-celled choanoflagellate *Monosiga brevicollis* contains teneurin in its genome, which suggests that TENs evolved from choanoflagellates. Further sequence analysis of choanoflagellate teneurin revealed that its ECR is more analogous to YD repeats in bacteria than ECR of metazoan TENs, suggesting that *M. brevicollis* acquired teneurin from bacterial prey via gene transfer (Tucker, 2013; Tucker et al., 2012). Nevertheless, YD-repeats and β-barrel structure in metazoan TENs share a striking

resemblance to many prokaryotic YD proteins secreted by bacteria. By looking at the function of YD proteins of bacteria, we can gain more insight into TEN structure and function (Tucker, 2018).

1.5 Bacterial Toxin Structure and Functional Implications

One class of YD-repeat proteins consists of bacterial Tc toxins, a group of ABC toxin protein complexes (Araç & Li, 2019). ABC toxins were first discovered in the bacterium *Photorhabdus luminescens* and have since been characterized in various insecticidal bacteria (Bowen et al., 1998; Bowen & Ensign, 1998; Hurst et al., 2011; Pinheiro & Ellar, 2007; Tennant et al., 2005; Waterfield et al., 2001). These bacteria secrete A, B, and C protein components that are individually secreted and assembled into a tripartite ABC complex on neighboring cell membranes (**Figure 1.2**). The A component forms a bell-shaped structure whose funnel-like TcB-binding domain at the top attaches to the β -propeller TcA-binding domain of the B component. The bottom of the A component forms a pore with a target cell upon anchoring to the membrane. The B and C components assemble into a barrel-like structure with a hollow cavity that is closed at both ends; the B end is plugged by its β-propeller domain, and C end is sealed by a conserved RHS- repeat-associated domain sequence. The C-terminus of the C component contains a cytotoxic domain that is enclosed by the TcB-TcC hollow shell, which shields the toxic enzyme from the extracellular environment to maintain its cytotoxic potential (Busby et al., 2013; Meusch et al., 2014).

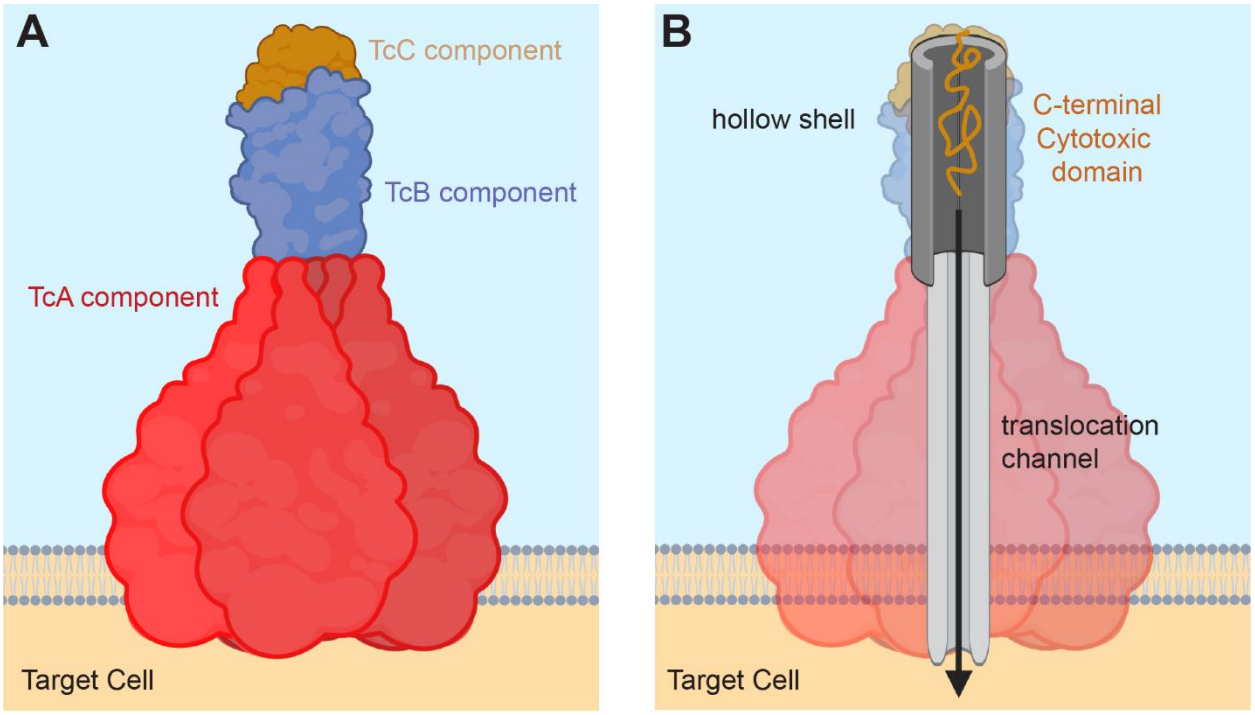

Figure 1.2: ABC toxin components form a hollow cavity and channel

(A) ABC toxins are composed of three A, B, and C protein components that form a tripartite protein complex.

(B) The TcB and TcC components form a hollow shell that encapsulates a cytotoxic domain at the C-terminus. The TcA component contains a translocation cavity that releases the toxin domain into target cells.

1.5.1 C-terminal Cytotoxic Domain Release and Mechanism

When the A component attaches to a target cell, a change in pH triggers opening of the A component at the attachment site and induces conformational change of the inner translocation channel, which opens the gate at the β-propeller gate at the bottom of the TcB-TcC barrel and forms a continuous pore from the inside barrel cavity to the target cell. The cytotoxic domain is jettisoned through the newly opened translocation channel and invades the target cell, inducing insecticidal activity on the infected organism (Gatsogiannis et al., 2018). To release the cytotoxic domain, the C component must first be cleaved inside the hollow shell. The TcB-TcC barrel expresses a catalytic site composed of three residues that induce autoproteolysis of the cytotoxic domain: two aspartate residues that reside near the cleavage site and an arginine residue that

provides structural stability to the adjacent aspartate. These catalytic residues are highly conserved among all bacteria that express C protein, indicating that autoproteolysis is the common mechanism of release for their respective cytotoxic domains (Busby et al., 2013).

1.5.2 C-terminal Cytotoxic Domain Function

Despite sharing autoproteolysis as a mechanism for release, C-terminal cytotoxic domains exhibit different toxic activities. In the case of *P. luminescens,* the cytotoxic domain functions as an ADP-ribosyltransferase, which post-translationally modifies actin in the cytosol and leads to actin clustering and subsequent cell death (Gatsogiannis et al., 2018; Lang et al., 2010; Meusch et al., 2014). On the other hand, *Yersinia entomophaga* produces two chitinases that exhibit endochitinase activity, which may be relevant for insect exoskeleton breakdown (Busby et al., 2012). This disparity can be attributed to the hypervariable nature of the cytotoxic domain sequences across C protein bacteria. The convergence of sequence variability, unique tertiary structure, and conserved proteolytic sites give rise to the multidimensional nature of bacterial toxin activity. This thesis takes these observations into account and applies them to metazoan TENs in search for understanding TEN function at a biochemical and cellular level.

1.6 Structural and biochemical similarities between teneurins and Tc toxins

Comparison between cryo-EM models of TcB and TcC components of *P. luminescens* (TcdB2-TccC3) and human TEN2 demonstrates that, despite a low (13%) sequence identity, TENs are structurally homologous to Tc toxins (**Figure 1.3A-C**). Distance Matrix Alignment (Dali) server is a tool for identifying structurally similar proteins, where a higher Z-score (> 2) indicates a strong structural similarity and a lower RMSD (Root Mean Square Deviation)

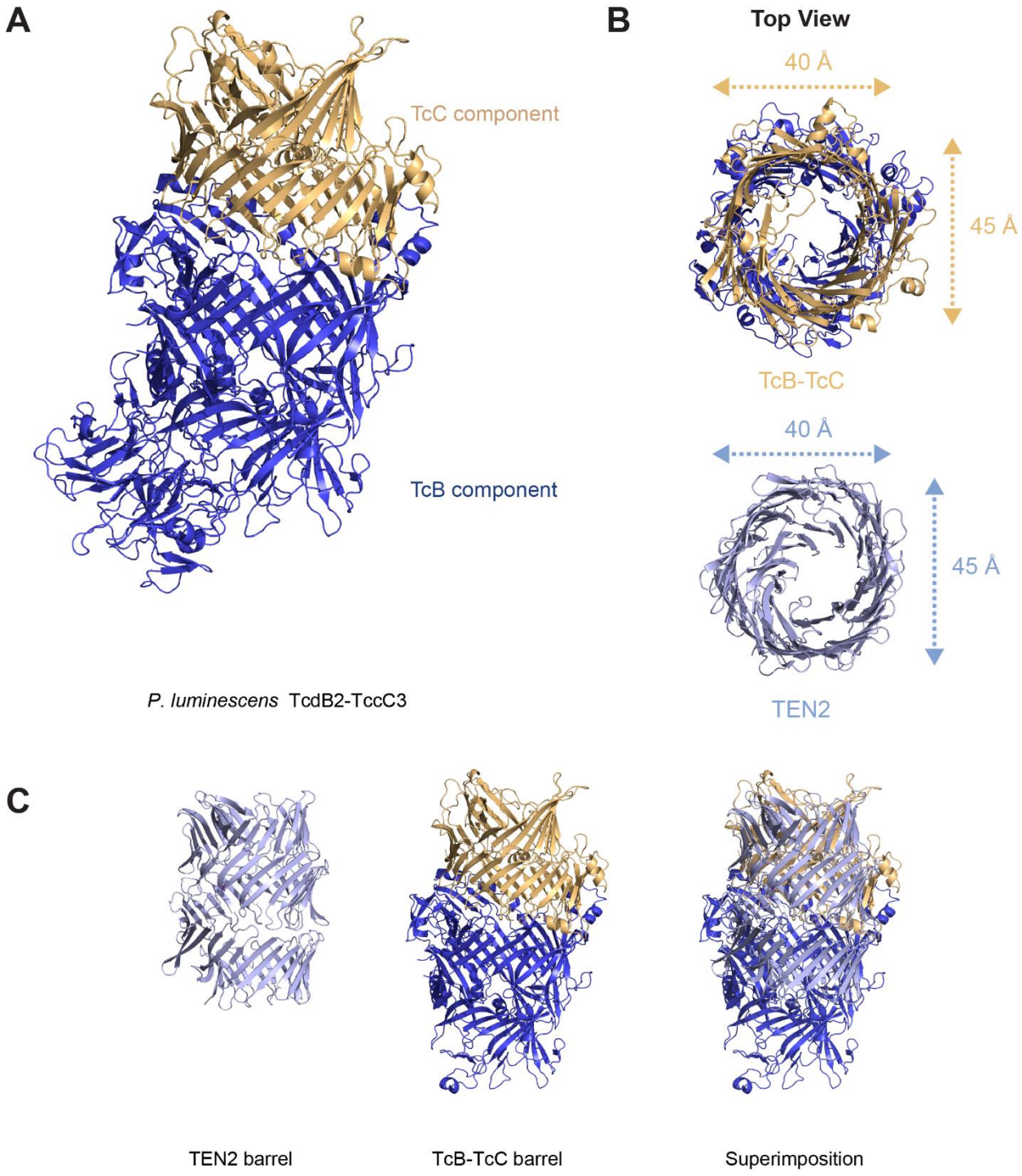

Figure 1.3: Teneurins exihibt structural homology to Tc toxins

(A) Cryo-EM model of TcB and TcC components of *P. luminescens*.

(B) Top view comparison of TcB-TcC and human TEN2 barrel structures shows similar diameters.

(C) Superimposition of TEN2 β-barrel and TcB-TcC barrel.

value, which is the average distance between structurally aligned residues, points to better structural alignment. Dali results for TEN2 compared to TcB-TcC components show a high Z-score of 13.4 and RMSD value of 4.9 Å. Analysis via Pymol, a molecular visualization program for protein structures, shows that TEN2 and TcB-TcC share 40 and 45 Å cylindrical diameters (**Figure 1.3B**). The length of the TcB-TcC barrel, however, is longer than the TEN2 barrel by more than 20 Å. These dimensions may arise from the TcB-TcC barrel housing its lengthy C-terminal cytotoxic domain of about 200 residues, whereas the TEN2 barrel encapsulates only 86 out of about 300 residues of the toxin-like domain (Li et al., 2018).

1.6.1 Similarities in Barrel Plug

In Tc toxins, the TcB-TcC barrel is plugged by a β-propeller domain, which acts as the point of interaction with the A component. Analogously, TEN barrel is plugged by its Ig-like domain. Both the bacterial β-propeller plug and human Ig-like domain contain predicted carboxypeptidase domains, where amino acid sequences align with nearly 50% similarity (Tucker, 2018). Furthermore, the receptor binding domains of toxin A component are composed of Ig-like domains structurally homologous to Ig-like domain on TENs. The receptor binding domains mediate anchoring of the A component to target cells, suggesting that the Ig-like domain in TENs may carry similar functions in protein-protein interactions.

1.6.2 Similarities in C-terminal Domain

Sequence alignment of Tc toxins to species expressing TENs reveals that the catalytic site of Tc toxins is mostly conserved across species (**Figure 1.4).** Chordate TENs express one

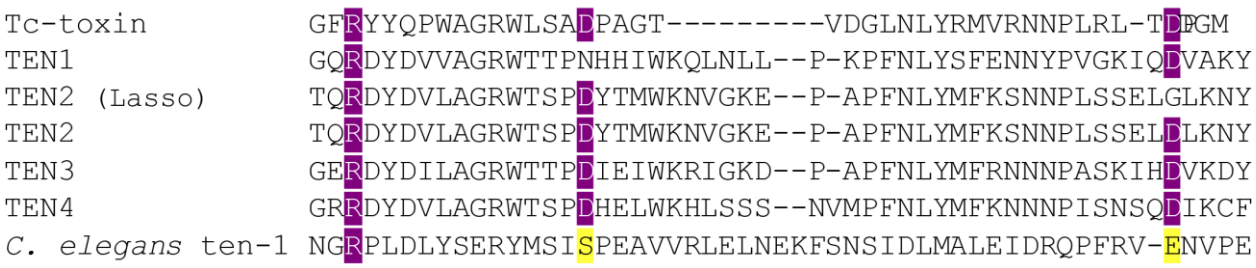

Figure 1.4: Sequence alignment of catalytic residues in Tc toxin and TENs

Catalytic site in Tc toxins, composed of one arginine and two aspartates, is mostly conserved.

arginine and two aspartates that make up the catalytic site in most of their isoforms. Non-chordate TENs like *Drosophila* and *C. elegans* express partial conservation: *Drosophila* have arginine and the first aspartate residues but express glutamate in place of the second aspartate; C. elegans also has an arginine but express serine and glutamate instead of two aspartates. Tc toxins interact with neighboring cells by releasing their C-terminal cytotoxic domain from their barrel structure via autoproteolysis; thus, conservation of these catalytic residues and structural homology in metazoan TENs suggest that the C-terminal toxin-like domain may play a role in TEN function as well.

1.7 Current Knowledge of C-terminal Toxin-like Domain Function

The majority of research on the toxin-like domain has focused on the most C-terminal portion of the domain, the TCAP. This 41-amino-acid peptide region, which is well-conserved across all TENs, has been shown to modulate behavior, stress, and metabolism in both vertebrates and invertebrates (Abramov et al., 2022; Colacci et al., 2015; D'Aquila et al., 2017; Hogg et al., 2019; Mueller et al., 2024; Reid et al., 2019; Tan et al., 2011; Wang et al., 2005). Sequence alignment revealed conserved elements with neuropeptides and corticotrophin releasing factor (CRF); indeed, TCAP-mediated calcium response has been shown to attenuate

CRF-induced stress behavior (Hogg, Casatti, et al., 2022). Interaction between TCAP and latrophilin, the canonical binding partner to TENs, has been speculated as far as their role in astrocytes and tissue repair in the CNS and skeletal muscle contraction, but evidence of direct interaction has not been found (Hogg, Reid, et al., 2022; Husić et al., 2019; Li et al., 2020; Tessarin et al., 2019). Small deletions in the toxin-like domain failed to rescue synaptic defects in cultured neurons from TEN3 and TEN4 double conditional-KO mice, indicating that at least partial toxin-like domain is indispensable for synapse formation (Zhang et al., 2025).

TCAP has been reported to be transcribed as a smaller mRNA transcript, exhibiting its own ATG starting codon. Furthermore, cleavage sites have been identified that yield smaller fragments in mouse brain lysates and hippocampal neurons, leading to speculation that TCAP may be released and post-translationally processed (Chand et al., 2013). Some groups have characterized the C-terminus of TENs to be cytotoxic, similar to their Tc toxin counterpart, where the addition of purified C-terminal TEN increases apoptosis of HEK 293T cells *in vitro*; however, sequence alignment with DNAses shows that TENs lack the HNH catalytic pocket necessary for nuclease activity (Ferralli et al., 2018; Li et al., 2018)

Upstream of the TCAP, the antibody-binding domain (ABD) is expressed, but there are currently no known ligands for this region. The toxin-like domain portion after the barrel-exit site forms hydrogen bonds with the side of the β-barrel and is exposed to the synaptic cleft. It has yet to be determined if this exposed region binds to any post-synaptic receptors or is released into the synaptic cleft, though it is widely speculated by different groups.

Isoform	Perturbation	Associated disorder/disease	Source
TEN1	missense mutaion	congenital general anosmia	Alkelai, et al., 2016
TEN2	overexpression	glioma patients; brain cancer cell lines	proteinatlas.org
TEN3	null mutation	microphthalmia	Aldahmesh, et. al,. 2012
TEN3	null mutation	pediatric autoimmune disease	Li, et. al,. 2015
TEN4	missense mutaion	essential tremor	Hor, et al. 2015
TEN4	risk factor	Parkinson's Disease	Pu, et al., 2020; Liang et al. 2020
TEN2, TEN4	missense mutaion	schizophrenia	Li, et al., 2021; Yi, et al., 2021
TEN4	risk variant	bipolar disorder	Heinrich, et al. 2013
TEN2, TEN4	disregulated expression	ovarian tumor tissue	Graumann, et al., 2017
TEN1, TEN2, TEN4	missense mutation	autism	Iossifov, et al., 2014

Table 1: Summary of TEN mutations and human disease.

All human TEN isoforms are involved in neurological disorders and non-neuronal diseases, as summarized by their literature source.

1.8 Implications on Disease

Human TENs comprise four isoforms whose mutations have been associated with various neurological disorders. Congenital anosmia, a neurological disorder that shuts down the ability to smell, was associated with X-linked missense mutations of TEN1 in the β-barrel (Alkelai et al., 2016). Point mutations for essential tremor (ET) have been found in the Ig-like and β-propeller domains of TEN4, which has been identified as a regulator of oligodendrocyte differentiation and significant for myelination of small-diameter axons in the CNS of mice and zebrafish (Hor et al., 2015; Suzuki et al., 2012). Risk variants and other mutations associated with Parkinson's disease, schizophrenia, autism, and bipolar disorder have been identified in most isoforms (**Table 1**) (Alkelai et al., 2016; Hor et al., 2015; Iossifov et al., 2014; Li et al., 2021; Liang et al., 2021; Pu et al., 2020; Xue et al., 2018). Furthermore, TEN overexpression has been found in glioma patients and brain cancer cell lines, in addition to non-neuronal cancers like ovarian cancer tissue (https://www.proteinatlas.org/ENSG00000145934-TENM2/pathology) (Graumann et al., 2017; Uhlen et al., 2017).

Interestingly, missense mutations in *TEN4* have been identified in schizophrenia patients, meaning that single nucleotide polymorphisms (SNPs) in TEN4 are sufficiently deleterious to TEN4 protein function associated with schizophrenia. One of these variants, Q2735E, is part of the toxin-like domain, indicating that the C-terminus of TENs may be as significant as other TEN domains in neurological disorders than previously thought. Knockdown and overexpression studies of *ten-m* in *Drosophila* show disruption in sleeping behavior, learning ability, and increased aggression, which are schizophrenia-like phenotypes related to cognitive deficits, further supporting TEN4's association with schizophrenia (Carruthers et al., 2021; Ferrarelli, 2020; J. Wang et al., 2024; Yi et al., 2021). Despite the potential implications of the TEN toxin-like domain on brain development and health, the molecular and cellular details for this domain remain to be fully elucidated.

1.9 Teneurin Research in *C. elegans*

To study genes and proteins that underlie neurological disorders, animal models are commonly used as tools for understanding defects in disease, investigating mechanism and function of genes, and searching for potential therapeutic treatments. TENs have been observed to play a role in neurite outgrowth, axon target selection, and synapse identity specification in difference species, which include the canonical model organism *C. elegans* (Antinucci et al., 2013; Del Toro et al., 2020; Drabikowski et al., 2005; Li et al., 2020; Mosca et al., 2012; Sando et al., 2019; Vysokov et al., 2018). *C. elegans* encode a single *ten-1* gene as two isoforms that differ by separate promoters initiating transcription at different points on the N-terminus, resulting in full-length ten-1L and short form ten-1S lacking the ICD (Drabikowski et al., 2005). *Ten-1* has been implicated in basement membrane integrity and proper axon migration of

pharyngeal neurons; additionally, mutations cause embryonic lethality, sterility, infertility, larval arrest, and disrupted neuron targeting (Drabikowski et al., 2005; Mörck et al., 2003; Mörck et al., 2010; Topf & Chiquet-Ehrismann, 2011; Trzebiatowska et al., 2008). Thus, *ten-1* is important for *C. elegans* nervous system and body development.

1.9.1 Current knowledge of C. elegans ten-1 localization

Ten-1L isoform (*F28F5.1*) is driven by the *ten-1a* promoter to produce the full-length protein of 2837 amino acids (aa). This isoform includes translation of the ICD, which contains an NLS, 8 EGF-like repeats, and predicted furin cleavage at 100 and 120aa downstream of TM. Transcriptional GFP reporter using the *ten-a* promoter (BC15001) exhibits GFP expression in mesoderm, pharynx, somatic gonads, and various muscles and neurons. In adults, nervous system expression is specific to 3 marginal cells mc1 and mc3, head ganglion cells, M2 pharyngeal neurons, DVB neurons, and nerve ring interneurons. Body expression is found in intestine, posterior body wall muscles, vulva muscles, gonad and spermatheca sheath cells, utse cells of uterus, and hypodermal cells like rectal hypodermis (Drabikowski et al., 2005; Mörck et al., 2010). RNAi interference of *ten-1a* transcript crossed with *ten-1(ok641)*, a null mutant for *ten-1*, expressed defects in germ line development, somatic gonad formation, meandering distal tip cells, and other morphological abnormalities.

Ten-1b promoter expression, which lack the ICD, differs from *ten-1a*. The alternate transcriptional reporter (BC15000) drives *ten-1b* promoter expression in ectoderm, hypodermis, and extra-pharyngeal neurons. Adult worms exhibit GFP in head and tail neurons, CAN, HSN, lumbar, retro-vesicular ganglion, and some nerve ring interneurons, along with specialized epithelial cells in anterior end and excretory duct. Mutations via RNAi interference and null

mutant present with axonal pathfinding defects, such as wrong direction or turns, defasciculated axons of ventral nerve cord (VNC), abnormal VNC integrity, few or no sperm, and ectopic nerve ring mislocalization to the metacorpus. Together, these reporters demonstrate that *ten-1* is expressed in nervous system and body development of *C. elegans*.

1.9.2 Null mutant for ten-1 exhibit axonal and body morphology defects

The Vancouver Gene Knockout Lab generated hundreds of mutants in *C. elegans* via ethyl methanesulfonate and UV radiation and used large-scale PCR screening to detect deletions, creating a public-domain source of knockout strains for research (Consortium, 2012). Among those mutants was *ten-1(ok641)*, an in-frame deletion of 675aa/2130bp removing 4 EGF-like repeats and part of cysteine-rich region resulting in a null mutant with numerous vitality and morphological defects. This mutant line exhibits embryonic lethality at a rate of about 5%, larval arrest at about 25-30%, vulva defects, sterility, and infertility. Body defects include mispositioned vulva muscle, no open vulva slit, gonad disruption, detachment of epidermis from muscle cells, and basement membrane disruption, indicating *ten-1* is important for basement membrane integrity, adhesion in reproductive organs, and development of proper epidermis (Topf & Chiquet-Ehrismann, 2011; Trzebiatowska et al., 2008). Nervous system defects manifest as misplaced axon bodies, misguided and truncated axons, and conspicuous varicosities in pharyngeal neurons such as M2, M3, M4, I3, and NSM. Increased expression of *unc-129::GFP* in dorsal muscles is present in *ten-1(ok641)* mutants, but no axonal defects are visible in ventral commissures traversing the body to reach dorsal muscles typical of *unc-129* perturbations (Mörck et al., 2010). In fact, body neurons exhibit normal axon guidance, indicating neuronal defects are specific to pharyngeal neurons. Overall, *ten-1* localization and

defects have been studied over the past 20 years, but research has focused on general expression via transcriptional GFP reporters and null mutants that disrupt whole protein. This thesis will focus on specific domains that compose TENs' unique tertiary structure by examining endogenous expression of *ten-1* and the possible influence of its toxin-like domain in *C. elegans* nervous system.

1.10 *C. elegans* as a Model Organism for the Nervous System

The neuroscience field has utilized *C. elegans* for studying the nervous system due to the immense available knowledge and flexibility as an animal model. *C. elegans* contains a total of 302 neurons, 20 of which are pharyngeal neurons and 282 are body neurons. Compared to billions of neurons in the human brain, their small size may appear restrictive and disadvantageous, but the opposite is true. The *C. elegans* genome has been full sequenced, allowing for complete access to the worm for genetic mapping, targeted mutagenesis, and precise genetic manipulation. Typically, genes express fewer isoforms than their vertebrate counterparts, but fewer isoforms mean easier targeting and isolation of genes for study. On a practical level, *C. elegans* worms are relatively easy to maintain in laboratory settings compared to other organisms as they require less space and inexpensive agar plates for feeding and maintenance. Their high reproductive rate and short life cycle grants researchers the ability to address developmental questions, conduct large-scale genetic screenings, and enable swift experimentation.

Despite their small number of neurons, *C. elegans* exhibit a complex nervous system. They contain a tight axon bundle, or nerve ring, around the isthmus of the pharynx that can be interpreted as the "brain" of the worm. While classified as an invertebrate, the worm expresses a VNC, which act as a spinal cord-like structure littered with motor neurons essential for worm

locomotion. Furthermore, axonal processes extend from neurons and form synapses along their trajectory, and over half of these reach the nerve ring, the most synapse-rich part of the animal. The transparency of the worm allows easy visualization of neuronal morphology through microscopy, especially in conjunction with fluorescent reporters. Thus, *C. elegans* is often used in studying synapses, neuronal development, and axonal wiring when addressing questions about orthologs in the nervous system, and this makes the worm a compatible model organism for investigating TENs and neuronal circuitry.

In this study, we examined the *in vivo* endogenous expression pattern of *C. elegans ten-1* and the influence of *ten-1* on proper pharyngeal neuron development. Furthermore, we assessed the importance of the C-terminal toxin-like domain on proper expression and axon morphology. *In vitro*, we used protein purification of TEN2 to address its ability to undergo autoproteolysis at the C-terminus given its strong structural and biochemical homology to Tc toxins. Additionally, we explore the possibility of these C-terminal properties in *C. elegans ten-1*. We aim to expand on the current knowledge of the C-terminal toxin-like domain in TENs and its implications on shaping neuronal circuitry. Among the abundant number of cell adhesion molecules at the synapse, TENs function in all steps of neuronal circuit assembly, which emphasizes their importance in proper brain wiring and need for further study. This thesis couples *C. elegans* genetic modification and microscopy with biochemical experiments to examine the fundamental properties of the C-terminus underlying TEN function, which may contribute to understanding TENs' importance in brain health and disease.

CHAPTER 2: RESULTS

2.1 Endogenous ten-1 expression is *C. elegans*

Previous studies investigated *C.elegans ten-1* expression using transcriptional reporter strains, which fused ten-1 promoters to green fluorescent protein (GFP). However, transcriptional reporters are not always fully representative of gene expression patterns due to spatial and temporal differences. Transgenic animals express GFP in a variable number of cells and at different intensities due to variations in copy numbers. Furthermore, transcriptional reporters will express GFP in the whole cell rather than specifically localize GFP to the protein of interest. To look at endogenous expression of a gene, CRISPR-Cas9 is widely used in *C. elegans* as a gene editing technique for tagging endogenous proteins.

C. elegans ten-1 is located on autosomal chromosome III and contains two promoters that yield two distinct isoforms. The *ten-1a* promoter resides upstream of the exon 1 and transcribes for the full-length protein, called TEN1L or long-form. On the other hand, *ten-1b* is located before exon 10 and allows translation immediately before the TM excluding the ICD and is thus termed TEN1S or short-form (**Figure 2.1**). We used a *C.elegans ten-1* strain tagged with mNeonGreen (mNG) fluorescent protein, *ten-1::mNG*, via CRISPR-Cas9- mediated homologous recombination to observe endogenous ten-1 expression (Keeley et al., 2020). This fluorescence tag is located at the C-terminus of the gene, and thus we expect expression to encompass all isoforms of *ten-1*. Endogenous *ten-1* is expressed in the head, ventral nerve cord (VNC), and tail of C. elegans (**Figure 2.2B**). The punctal fluorescent signal seen in the body of the worm originate from lipids in the digestive system, which emit autofluorescence during excitation of certain wavelengths, and is not part of *ten-1* expression (Clokey & Jacobson, 1986). A closer

look at the head shows that the mNG signal wraps around the isthmus of the pharynx, which connects the two digestive bulbs that make up the mouth of the worm (**Figure 2.2C**). The mNG signal runs along the VNC and ends at the tail as puncta posterior to the anal cavity (**Figure 2.2D**).

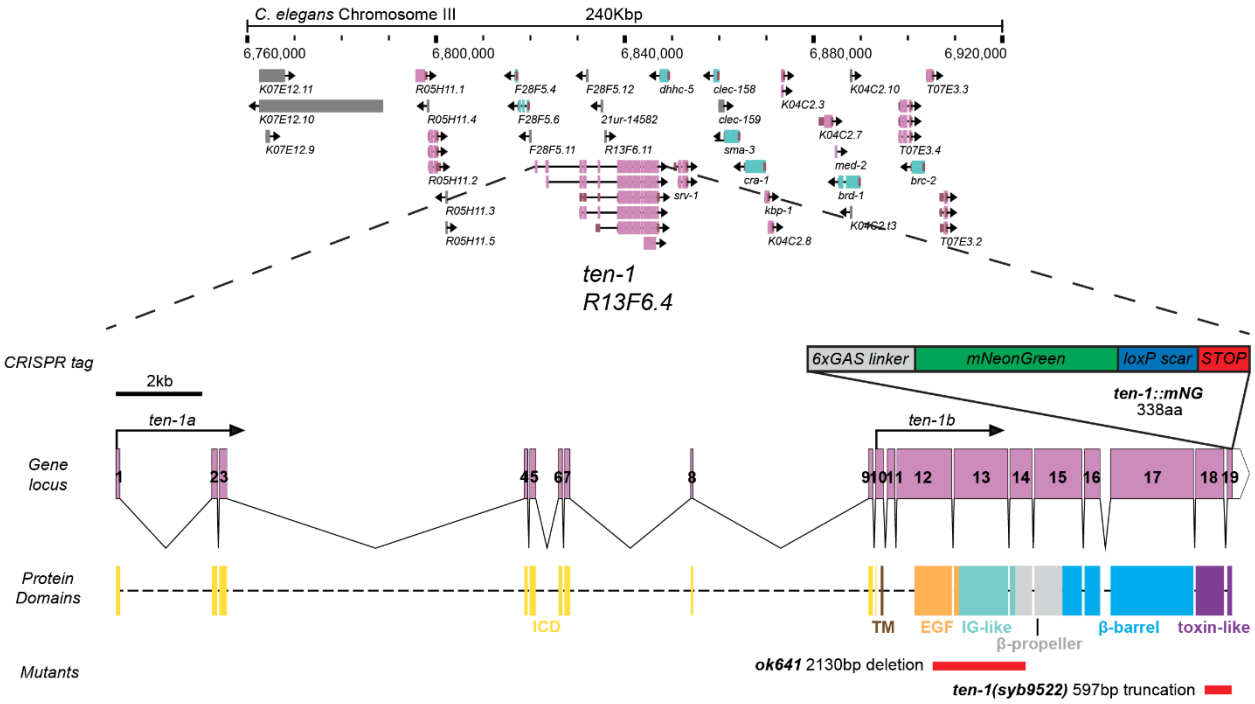

Figure 2.1: Gene locus of *C. elegans ten-1* and genetic modifications

Ten-1 is located on Chromosome III of C. elegans, containing 19 exons across almost 60Kbp and two promoters, *ten-1a* and *ten-1b*. CRISPR-mediated fluorescent tag was introduced at the C-terminus. Protein domains are mapped to gene loci, and mutant locations are shown.

ICD: Intracellular domain; TM: transmembrane; EGF: epidermal growth factor-like domain; IG: immunoglobulin.

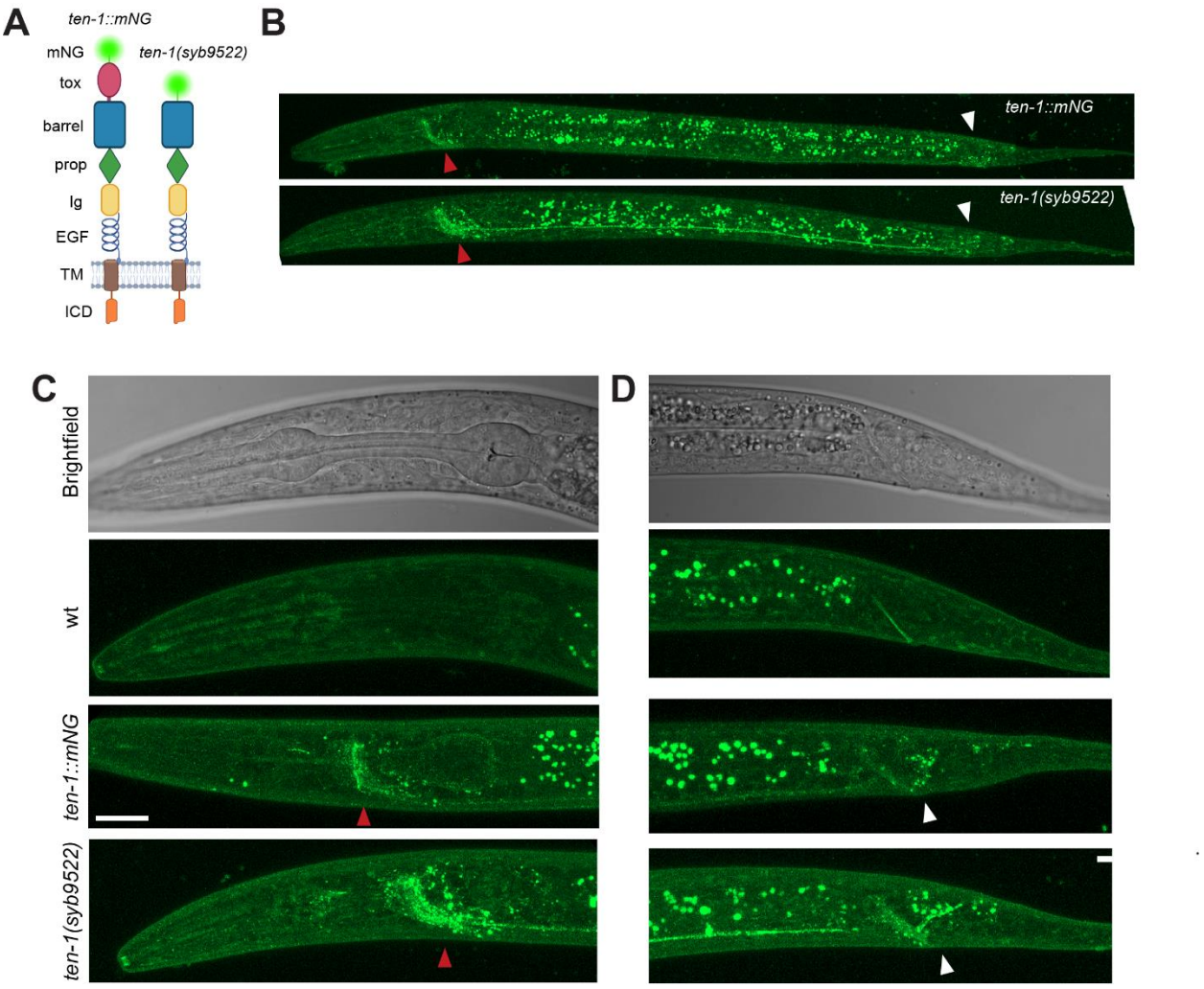

Figure 2.2: *ten-1* is endogenously expressed in the nervous system of *C. elegans* with and without its toxin-like domain

(A) *ten-1* was tagged with mNeonGreen fluorescent protein at its C-terminus, and the toxin-like domain was subsequently truncated via CRISPR-mediated deletion.

(B) L1 worms exhibit expression at pharynx (red arrow), through ventral nerve cord (VNC), and at tail (white arrow) in both full and truncated strains.

(C-D) Anterior *ten-1* expression wraps around the isthmus of the pharynx, indicating nerve ring localization (C), and posterior expression occurs at tail neurons posterior to anal cavity (D).

ICD: Intracellular Domain, TM: Transmembrane; EGF: Epidermal growth factor-like domain; Ig: Immunoglobulin-like domain; prop: β-propeller; barrel: β-barrel; tox: toxin-like domain; mNG: mNeonGreen. Scale bar represents 20 µm in (A) and 10 µm in subsequent images.

2.2 Truncation of the C-terminal toxin-like domain in *C. elegans ten-1*

To investigate the role of the toxin-like domain in C. elegans ten-1, we truncated the C-terminus via CRISPR-Cas9- mediated deletion (**Figure 2.2A**). We targeted exon18 at G2506 and deleted 597bp from 25231-25827. The deletion was performed in-frame to maintain a viably translated mNG protein and the flexible 6X glycine-alanine-serine (GAS) linker. We targeted G2506 right after the barrel exit site at S2501 and not the whole toxin-like domain, which starts at E2583, to minimize the amount of instability a deletion might cause inside the barrel cavity, and to keep most of the extracellular toxin-like domain intact, including the regions most likely to be involved in function.

We found that the truncation mutant strain, *ten-1(syb9522)*, shared similar expression pattern to *ten-1::mNG*, where signal was expressed around the pharynx, extended through the VNC, and ended at the tail (**Figure 2.2B, C**). However, the truncation mutant signal appears more spread out at the pharynx and with higher intensity along the VNC and tail. Quantification

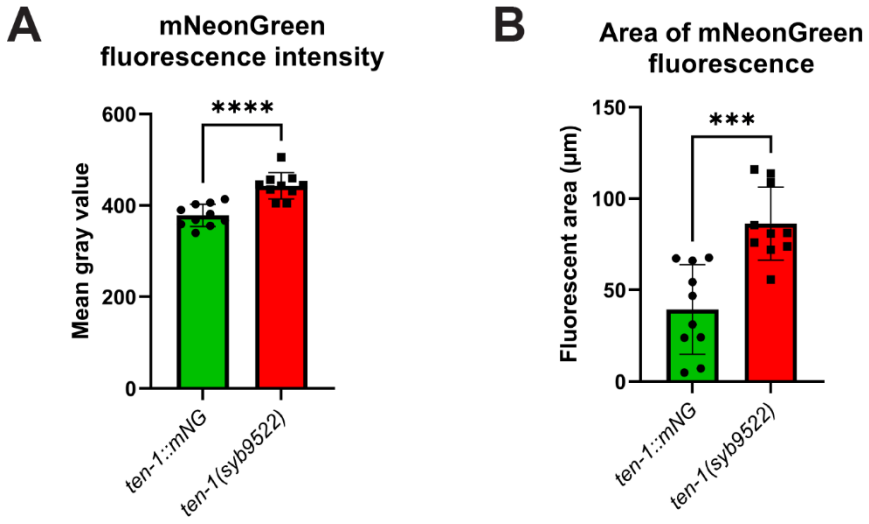

Figure 2.3: Comparison of mNG expression between wildtype ten-1 and truncation mutant

Ten-1(syb9522) truncation mutant exhibits higher fluorescence intensity and larger area of expression (*ten-1::mNG* n = 10, *ten-1(syb9522)* n = 10, ***p < 0.001, ****p < 0.001, Student's t-test).

of mNG expression at the pharynx showed a significantly higher area of expression and intensity between *ten-1(syb9522)* and *ten-1::mNG* (n=10 respectively, ***p < 0.001, ****p, Student's t-test) (**Figure 2.3**).

2.3 Viability of truncation mutant compared to wildtype and null *ten-1* mutants

Previous studies investigated the viability of *ten-1* null mutant *ok641* compared to wildtype and found various deleterious phenotypes such as embryonic and larval lethality (Drabikowski et al., 2005; Mörck et al., 2010; Trzebiatowska et al., 2008). We assessed the viability of our truncation mutant to address whether truncating the C-terminal toxin-like domain of ten-1 produced defective phenotypes as observed in the null mutant. Brood size remained mostly similar among wildtype (N2), *ten-1(ok641)* null mutant, *ten-1::mNG*, and *ten-1(syb9522)* truncation mutant, with a general lower trend in the null (**Figure 2.3B**). Embryonic survivability, which was determined by the percentage of eggs that hatched into larva, showed a significant decrease in *ten-1(ok641)* to 82.53% but no difference in the control or fluorescent strains at about 100% (N2: n=741; *ten-1(ok641)*: n=492, p-value = 0.0205; *ten-1::mNG*: n=295; *ten-1(syb9522)*: n=132) (**Figure 2.3C**). Furthermore, *ten-1(ok641)* experienced a severe decrease in larval lethality, which measures the number of larva that developed into adults, to 58.76% compared to about 100% in N2, *ten-1::mNG*, and *ten-1(syb9522)*. (***p < 0.001, ****p < 0.0001) (**Figure 2.3D**).

In addition to survivability, the *ten-1(ok641)* null mutant exhibited an exploding vulva defect in mature adults, where the vulva protrudes and ultimately explodes, leading to posterior immobility of the worm due to anchoring at the explosion site, and eventual death (**Figure 2.5A, B**). We recapitulated this previously described phenotype by counting the number of adult

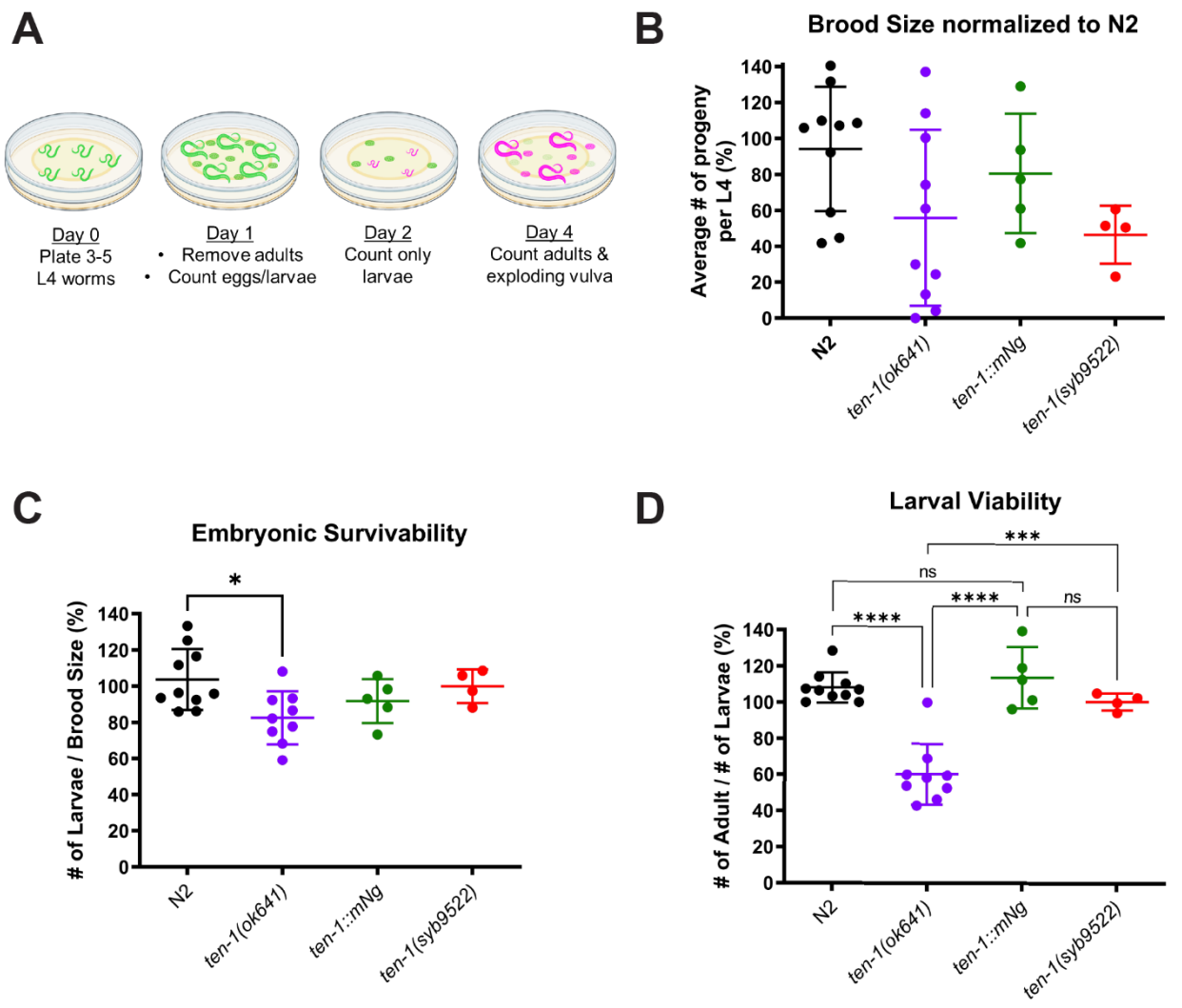

Figure 2.4: Only *ten-1* null mutant exhibits viability defects

(A) Schematic for viability assay counts conducted in wildtype N2, *ten-1(ok641)*, *ten-1::mNG*, and *ten-1(syb9522)* strains.

(B-D) *ten-1(ok641)* shows general decrease in brood size (B), and significant decrease in embryonic survivability (C) and larval viability (D). *ten-1(syb9522)* mutant shows no significant difference in viability compared to wildtype controls.

(N2 n = 741, *ten-1(ok641)* n = 462, *ten-1::mNG* n = 295, *ten-1(syb9522)* n = 132, n.s., not significant, *p < 0.05, ***p < 0.001, ****p < 0.001, One-way ANOVA, Tukey's multiple comparison test).

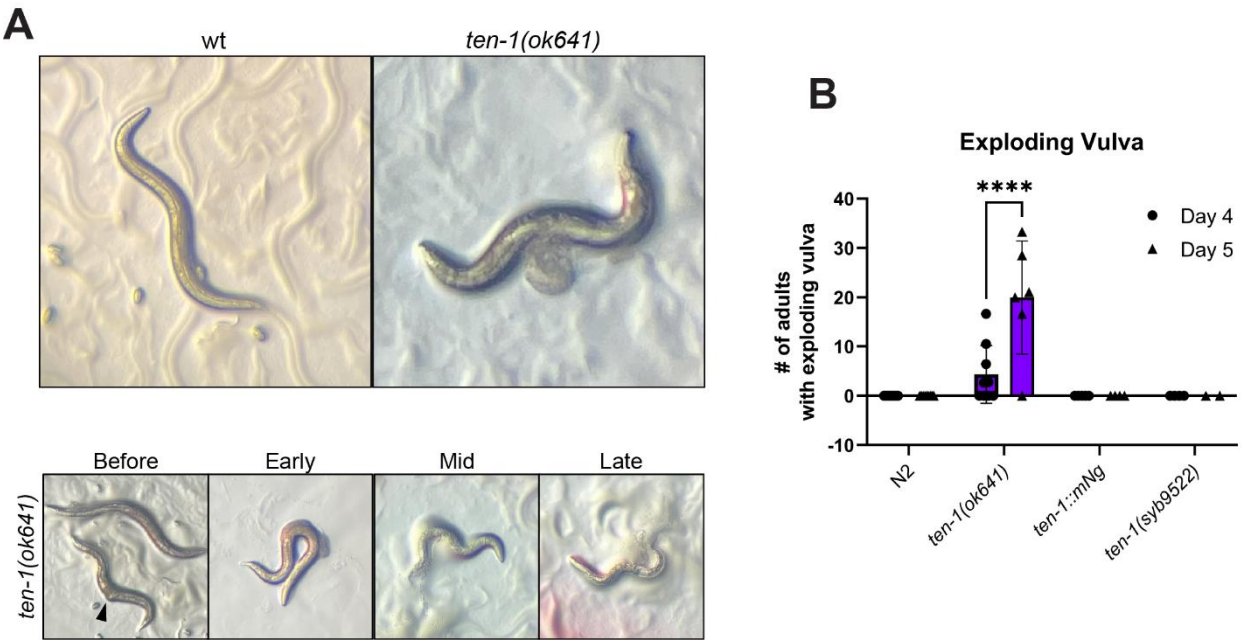

Figure 2.5: *ten-1* null mutants experience an exploding vulva phenotype

(A) *C. elegans ten-1(ok641)* adults exhibit protruding vulva phenotype (Pvl; black arrow).

(B) Adult worms explode at the vulva (*ten-1(ok641)* n = 120). ****p < 0.001, Bonferroni's multiple comparisons test.

worms that exploded after 24hrs as an adult to about 5%, and additionally observed this phenotype significantly grow in severity after 48 hrs to about 20% (n=120, ****p < 0.0001, mixed effects analysis) (**Figure 2.5C**) . No vulva defects were observed in wildtype controls or C-terminal truncation mutant.

2.4 *ten-1* mutants exhibit defective phenotypes in M4 neurons

Pharyngeal neurons in *ten-1* null mutants have been previously described with defective phenotypes ranging from truncated axons to abnormal varicosities (Mörck et al., 2010). M4 neurons are pharyngeal motor neurons important for feeding and peristalsis, and they synapse onto the isthmus and terminal bulb of the pharynx. The cell body sits dorsally at the end of the

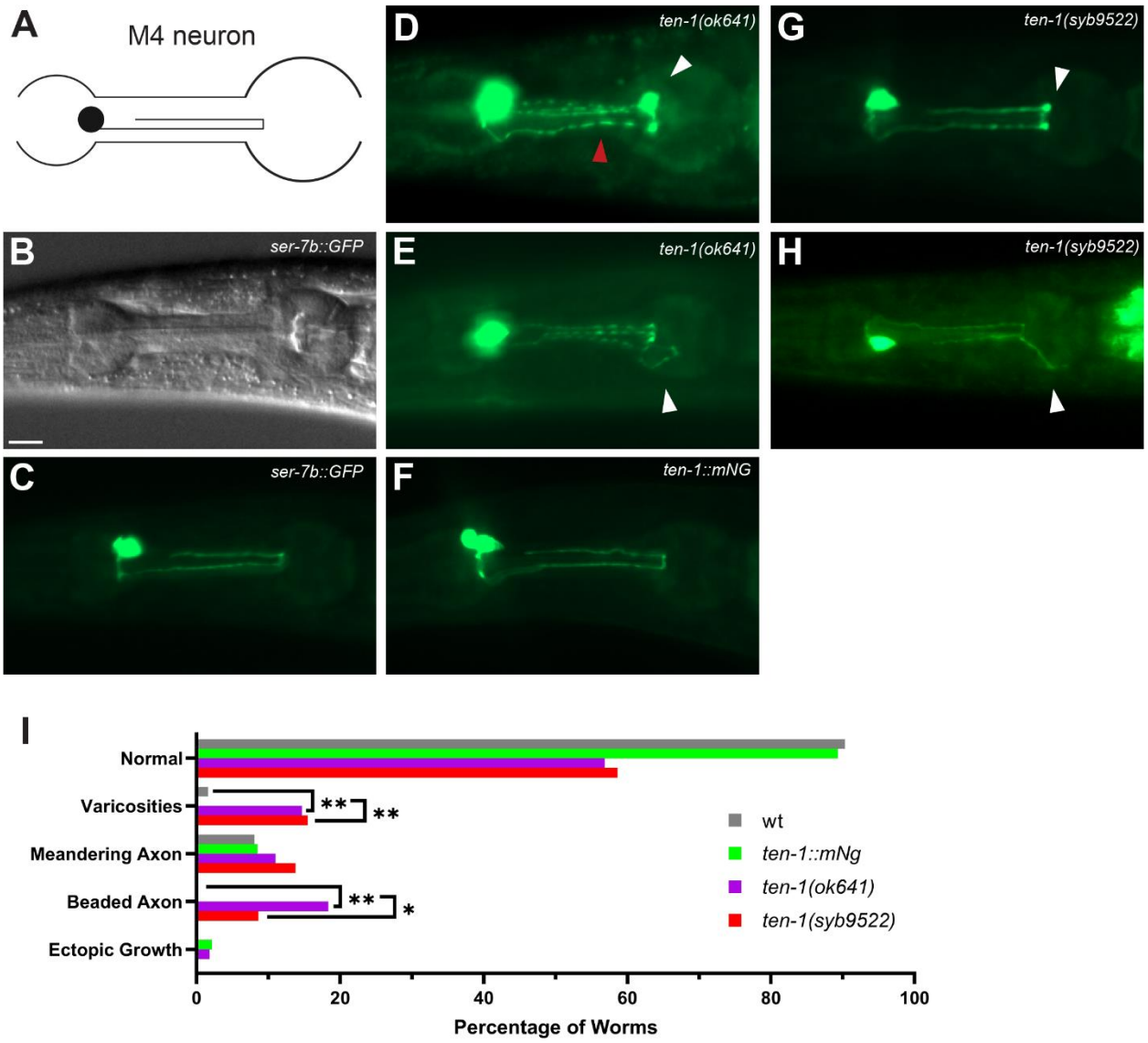

Figure 2.6: M4 neurons exhibit axonal defects in adult *ten-1* mutants

(A) Diagram of normal morphology of M4 neuron, lateral view.

(B-H) Transcriptional GFP reporter *ser-7b::GFP* for M4 neurons was crossed into *ten-1::mNG, ten-1(ok641),* and *ten-1(syb9522)* and imaged for neuronal defects. *Ten-1(ok641)* null mutant exhibits conspicuous varicosities (white arrowhead, D), beaded axons (red arrowhead), and meandering axons (white arrowhead, E). Truncation mutant *ten-1(syb9522)* also shows varicosities (G) and meandering axons (H). Scale bar represents 10 µm.

(I) Comparison of normal axons and axon defect phenotypes between strains. N2 n = 62, *ten-1(ok641)* n = 47, *ten-1::mNG* n = 109, *ten-1(syb9522)* n = 58, *p < 0.05, ***p < 0.001, Fisher's exact test.

anterior bulb and sends two processes across the isthmus of the pharynx until reaching the terminal bulb, where it makes a turn back to toward the initial bulb; a lateral (or side) view of this morphology appears as a single axon extending from the cell body due to 3-dimensional overlap of the two processes (**Figure 2.6A**). *Ser*-7b, a serotonin (5-HT7-like) receptor that enables pharyngeal pumping, is exclusively expressed in M4 neurons (Hobson et al., 2003). Using *ser-7b::GFP* transcriptional reporter, we can observe M4 neuron morphology when crossed into *ten-1* strains.

Ten-1(ok641) null mutant exhibits conspicuous varicosities along the axon most commonly at the turn in the terminal bulb, beaded axon phenotype (red arrowhead), and meandering axons that stray from the usual axonal trajectory (**Figure 2.6D, E**). Similar defects are observed in *ten-1(syb9522)* truncation mutant whereas *ten-1::mNG* exhibits normal morphology akin to the wildtype GFP reporter, indicating that these phenotypes arise when the C-terminal toxin-like domain is truncated (**Figure 2.6F-H**). In fact, the number of animals with varicosities and beaded axon defects seen in the ten-1 mutants is significantly higher than wildtype controls (**Figure 2.6I, Table 2**). Moreover, these mutants display meandering axons generally more than observed in wildtype but not to a significant extent. Taken together, we observe that wildtype strains produce normal M4 neurons about 90% of the time, while the mutant strains exhibit about 60% normal morphology.

2.5 *ten-1* mutants exhibit defective phenotypes in NMS neurons

Neurosecretory–motor (NSM) neurons are bilateral pair of pharyngeal neurons that release and reuptake serotonin and are involved in mediating feeding response (Axäng et al., 2008). *Tph-1* gene, which encodes for tryptophan hydroxylase ubiquitously expressed in

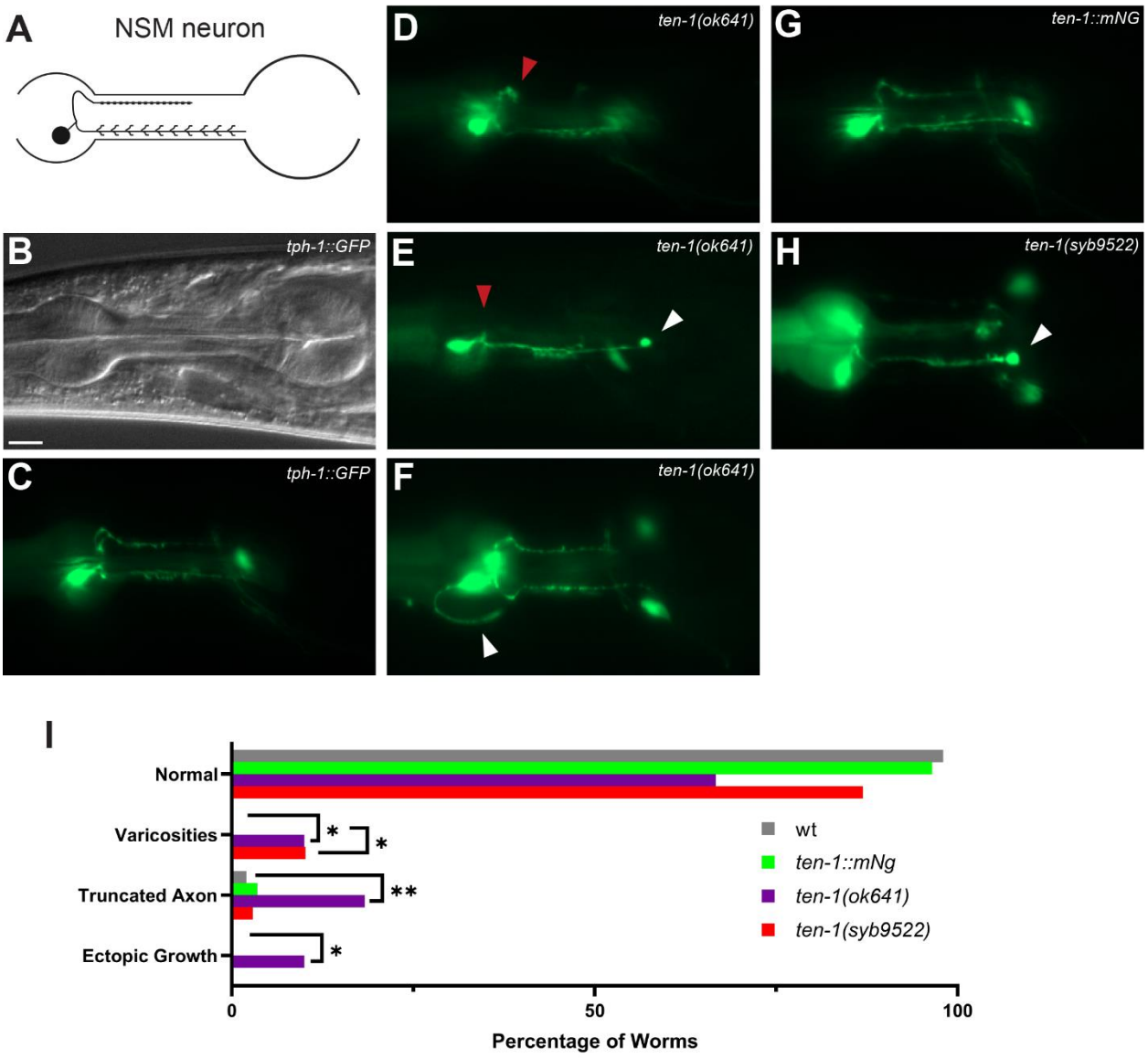

Figure 2.7: NSM neurons exhibit axonal defects in adult *ten-1* mutants

(A) Diagram of normal morphology of NSM neuron, lateral view.

(B-H) Transcriptional GFP reporter *tph-1::GFP* for NSM neurons was crossed into *ten-1(ok641)*, *ten-1::mNG*, and *ten-1(syb9522)* and imaged for neuronal defects. *Ten-1(ok641)* null mutant exhibits truncated axons (red arrowhead, D), varicosities (white arrowhead, E), and ectopic growths (white arrowhead, F). *Ten-1::mNG* shows similar morphology as wildtype (G), while truncation mutant *ten-1(syb9522)* shows varicosities (H). Scale bar represents 10 µm.

(I) Comparison of normal axons and axon defect phenotypes between strains. N2 n = 50, *ten-1(ok641)* n = 61, *ten-1::mNG* n = 57, *ten-1(syb9522)* n = 69, *p < 0.05, ***p < 0.001, Fisher's exact test.

serotonergic neurons, is used as a reporter for NSM expression. Thus, we use *tph-1::GFP* transcriptional reporter to observe changes in NSM morphology from mutation in *ten-1*.

NSM neurons are composed of a cell body at the anterior bulb with an axon that bifurcates into two major processes extending either dorsally or ventrally toward the terminal bulb (**Figure 2.7A**). NSM's are found symmetrically in both the left and right side of the C. elegans body, resulting in appearing as a single cell body and two processes due to their overlap when observed laterally. When imaged, *ten-1(ok641)* null mutant exhibits truncation of the major dorsal process almost 20% of the time, significantly higher than the 3% seen in wildtype (**Figure 2.7D, I; Table 2**). This natural variation in wildtype is consistent with previous studies (Axäng et al., 2008). The null mutant also exhibits bright varicosities, typically at the end of processes, and ectopic growths such as extra processes threading around the anterior bulb (**Figure 2.7E, F**). Both fluorescent strains display the natural variation in truncated dorsal axon seen in wildtype, but the truncation mutant exhibits a significant number of varicosities like the null mutant at about 10% (**Figure 2.7H, I, Table 2**). Ectopic growths are not observed in either *ten-1::mNG* or *ten(syb9522)* strain.

Overall, both ten-1 mutants have a less-than-normal number of NSM neurons with normal morphology, where the C-terminally truncated strain shows only about 87% normal NSMs while the null mutant is more severe at only about 67% normal NSMs. Wildtype and mNG-tagged wildtype showed a typical natural variation of normal NSM neurons at about 97%.

2.6 *ten-1* mutants show varicosities along the VNC processes of HSN neurons

Tph-1::GFP not only expresses in NSM neurons but also in hermaphrodite specific motor neurons (HSN). HSNs are a set of left/right symmetrical motor neurons that innervate the vulva

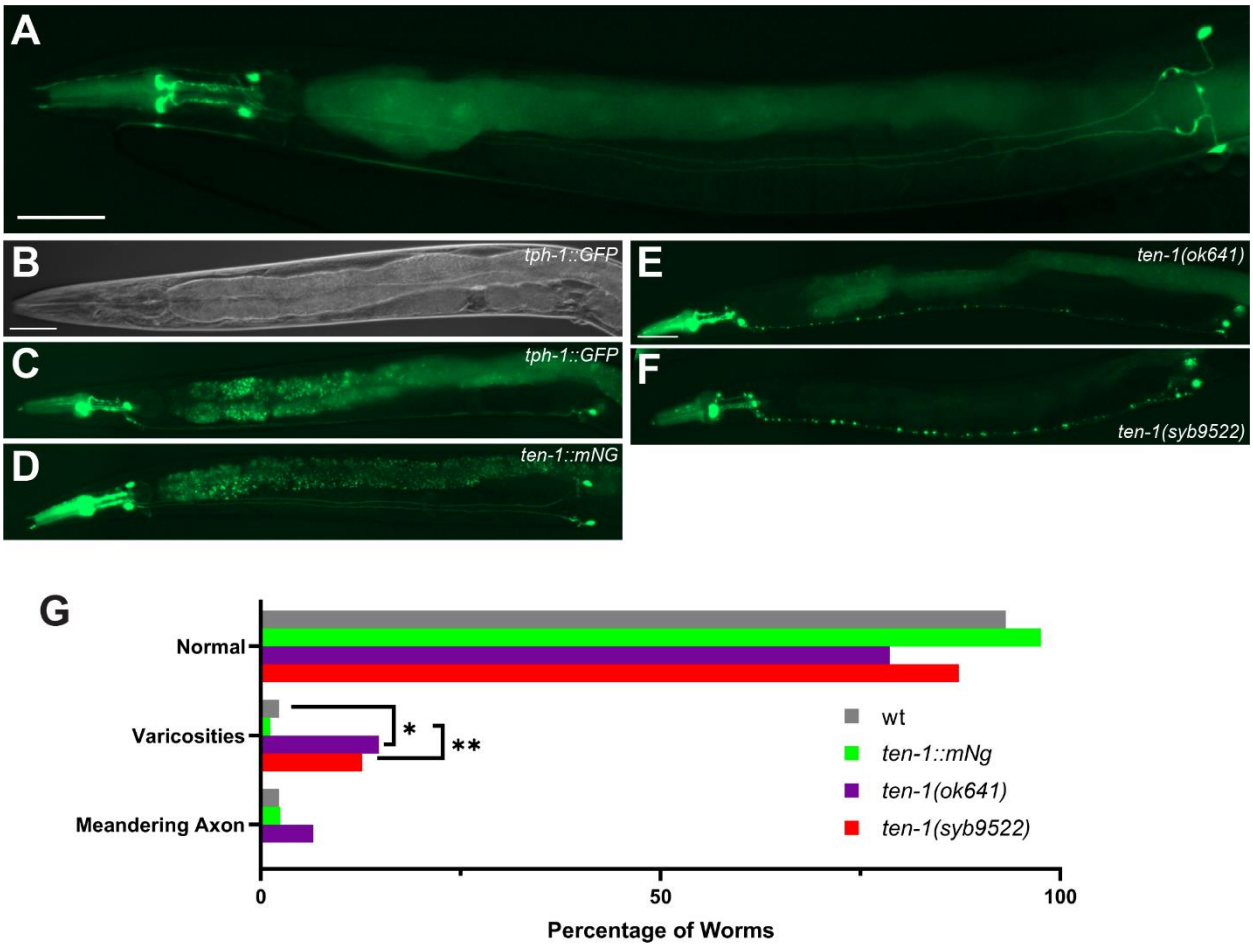

Figure 2.8: HSN axons exhibit conspicuous varicosities in adult *ten-1* mutants

(A) Representative image of a normal HSN neuron in an adult *C. elegans* worm, ventral view.

(B-F) Transcriptional GFP reporter *tph-1::GFP* was crossed into *ten-1(ok641)*, *ten-1::mNG*, and *ten-1(syb9522)* and imaged for neuronal defects. Wildtype *ten-1::GFP* exhibited cell bodies at the vulva extending axons along the VNC until reaching the nerve ring (B, C). *Ten-1(ok641)* null mutant and *ten-1(syn9522)* truncation mutant presented with varicosities along the VNC and the vulva (E, F), while *ten-1::mNG* expressed similar morphology as wildtype (D). Images in lateral view. Scale bar represents 50 µm.

(G) Comparison of normal axons and axon defect phenotypes between strains. N2 n = 44, *ten-1(ok641)* n = 61, *ten-1::mNG* n = 82, *ten-1(syb9522)* n = 71, *p < 0.05, ***p < 0.001, Fisher's exact test.

muscles and contribute to egg-laying. The cell bodies of HSNs reside sub-ventrally just posterior to the vulva and extend axons that branch and synapse onto the vulva. The main processes enter and run along the VNC anteriorly until reaching the nerve ring (**Figure 2.8A**). HSN neurons from *ten-1(ok641)* null mutant exhibited conspicuous varicosities in their axons along the VNC and in processes near the vulva (**Figure 2.8E**). Similarly, *ten-1(syb9522)* truncation mutant expressed HSN axons with varicosities along the VNC. Wildtype and *ten-1::mNG* strains exhibited normal morphology, indicating that varicosities can be attributed the mutations in *ten-1* (**Figure 2.8B, C, E**). Meandering axons were also observed in the null mutant and wildtype, but this phenotype may be due to natural variation. On the other hand, varicosities in both *ten-1* mutants were statistically significant , indicating a defective phenotype in the axons of HSN manifest when *ten-1* protein is truncated or null (**Figure 2.8G, Table 2**).

Neuron	Genotype	Normal	Varicosities	Meandering axon	Beaded axon	Truncated axon	Ectopic growth	n
M4	wt	90.32%	1.61%	8.06%				62
	ten-1::mNG	89.36%		8.51%			2.13%	47
	ten-1(ok641)	56.88%	14.68% **	11.01%	18.35% **		1.83%	109
	ten-1(syb9522)	58.62%	15.52% **	13.79%	8.62% *			58
NSM	wt	98.00%				2.00%		50
	ten-1::mNG	96.49%				3.51%		57
	ten-1(ok641)	66.67%	10.00% *			18.33% **	10.00% *	60
	ten-1(syb9522)	86.96%	10.14% *			2.90%		69
HSN	wt	93.18%		2.27%				44
	ten-1::mNG	97.56%		2.44%				82
	ten-1(ok641)	78.69%	14.75% *	6.56%				61
	ten-1(syb9522)	87.32%	12.68% **					71

Table 2: Summary of scoring pharyngeal and body neurons in ten-1(ok641) null and ten-1(syb9522) truncation mutant

Statistical significance tests were conducted for all strain comparisons. Stars for *ten-1(ok641)* correspond to comparisons against wt, and *ten(syb9522)* to comparisons against *ten-1::mNG*.
*p < 0.05, **p < 0.01, Fisher's exact test.

2.7 TEN2 ECR produces a C-terminal product when EGF- and Ig-like domains are absent

As a type-II transmembrane protein, the C-terminus of TENs is exposed to the outside of the cell, attached to the membrane via its single-pass TM region; in turn, this ECR interacts transsynaptically via homophilic and heterophilic interactions (Berns et al., 2018; Li et al., 2023; Li et al., 2020; Zhang et al., 2022). To study the C-terminus of TEN2, we used an insect cell expression system to purify secreted protein composed of only the five ECR domains. Sf9 cells were transfected with TEN2 full ECR construct with a C-terminal His-tag to produce baculovirus, which was subsequently used to infect Hi5 cells and secrete TEN2 protein into the media. The His-tagged protein was purified via nickel beads and processed by size exclusion chromatography (SEC), where larger molecules are eluted earlier than smaller products. The protein fractionations contained a large 245 kDa product corresponding to the full ECR in Comassie blue staining and a single absorbance peak in the chromatogram (**Figure 2.9A**).

Because TENs form *cis*-dimers due to disulfide bonds between EGF domains, we also purified TEN ECRΔ1, which lacks the EGF-like domain, to test whether TEN2 monomer produces a C-terminal product. Similar to the full ECR, purified ECRΔ1 contained only a single protein product at the expected size of 215 kDa (**Figure 2.9B**). We then looked at the Ig-like domain, which plugs TEN2 at the bottom of the β-barrel and makes contacts with residues inside the barrel cavity, including those belonging to the C-terminal toxin-like domain (Li et al., 2018). TEN2 ECR with both EGF- and Ig-like domains deleted was purified and analyzed via SEC to test whether a C-terminal product would be present in TEN2 monomer lacking the Ig-like domain. We observed ECRΔ1,2 protein at 170 kDa and an additional product about 30 kDa in size (**Figure 2.9C**). Furthermore, an additional absorbance peak was observed in ECRΔ1,2 at elution volumes 14-16 mL, which was not seen in chromatograms of neither the full ECR or

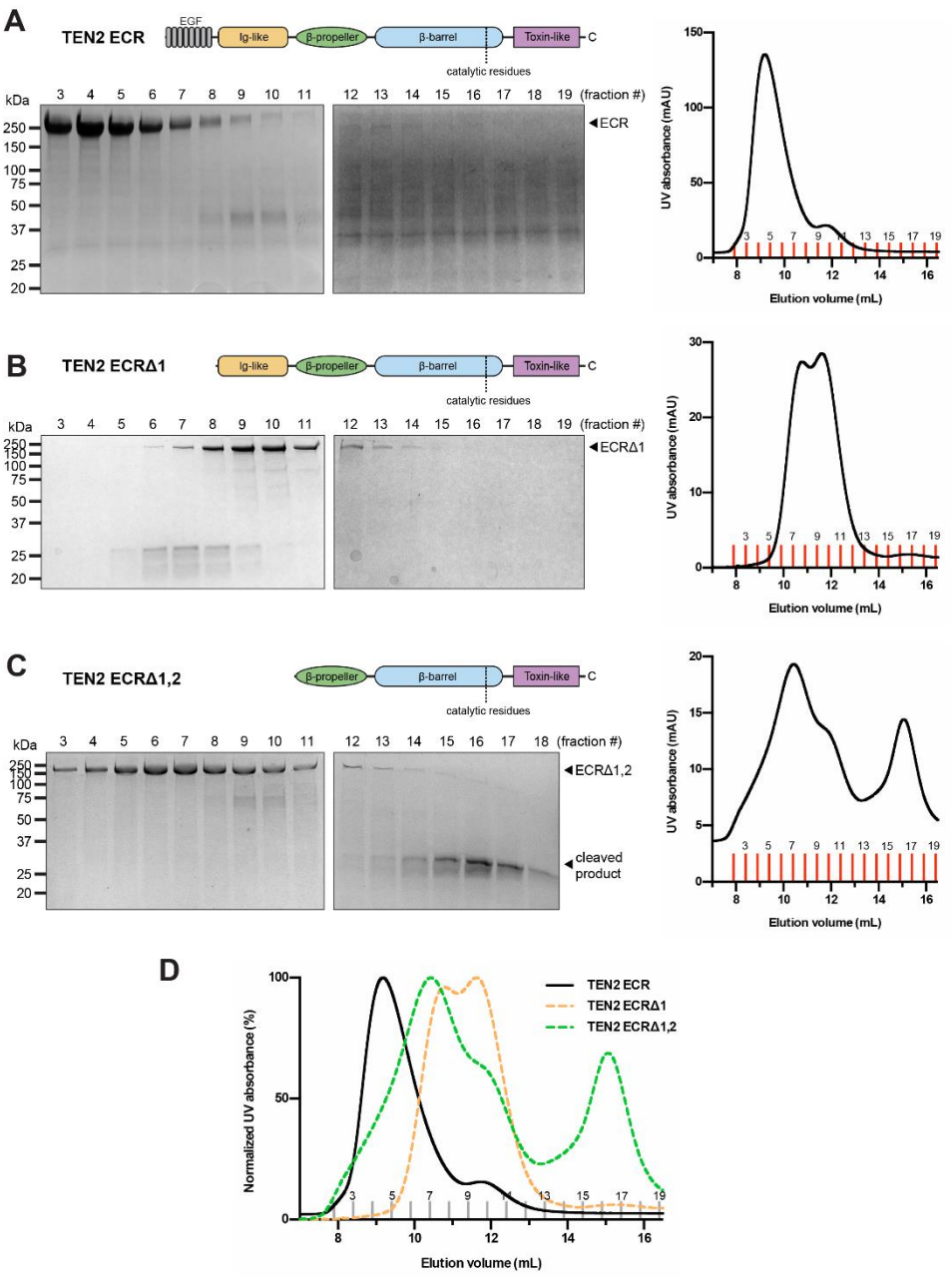

Figure 2.9: TEN2 exhibits a C-terminal cleavage product when EGF- and Ig-like domains are deleted

(A-C) Size exclusion chromatography of (A) TEN2 ECR, (B) TEN2 ECRΔ1, and (C) TEN2 ECRΔ1,2 protein purifications. Red bars in chromatograms indicate fractions collected.

(D) Comparison of size exclusion chromatograms of TEN2 ECR (black), ECRΔ1 (orange), and ECRΔ1,2 (green) normalized to 100%.

UV: Ultraviolet; mAU: mili-Absorbance units

ECRΔ1 lacking the EGF-domain. A peak shift to the left in was also observed in full TEN2 ECR and ECRΔ1,2 compared to ECRΔ1 monomer.

These constructs contain a 6x His tag at the C-terminus, and thus we used His-antibody to test whether the protein products came from the C-terminus. Western blot against His-antibody showed staining at the expected size of the full construct 170 kDa and the additional protein product of 30 kDa, which suggests that this smaller product is part of the C-terminus of ECRΔ1,2 (**Figure 2.10**). Furthermore, mass spectrometry of this protein product revealed peptides present at the toxin-like domain (**Figure 2.11**). These data indicate that the identity of the 30 kDa product belongs to the toxin-like domain of TEN2 and is only produced when both the EGF- and Ig-like domains are ablated from the ECR.

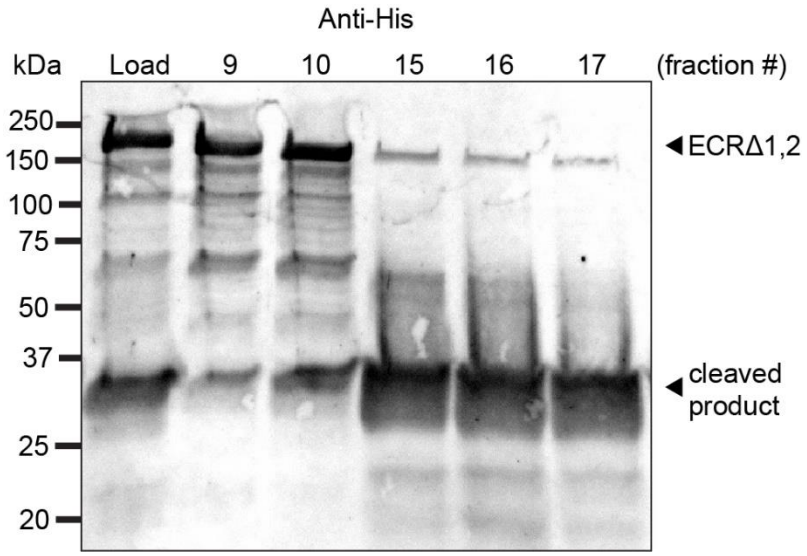

Figure 2.10: TEN2 exhibits a C-terminal cleavage product when EGF- and Ig-like domains are deleted

Fractions of TEN2 ECRΔ1,2 immunostained with His-488 antibody. Load sample control before size-exclusion chromatography. Arrowheads indicate expected size bands for TEN ECRΔ1,2 (170 kDa) and cleavage product (34 kDa).

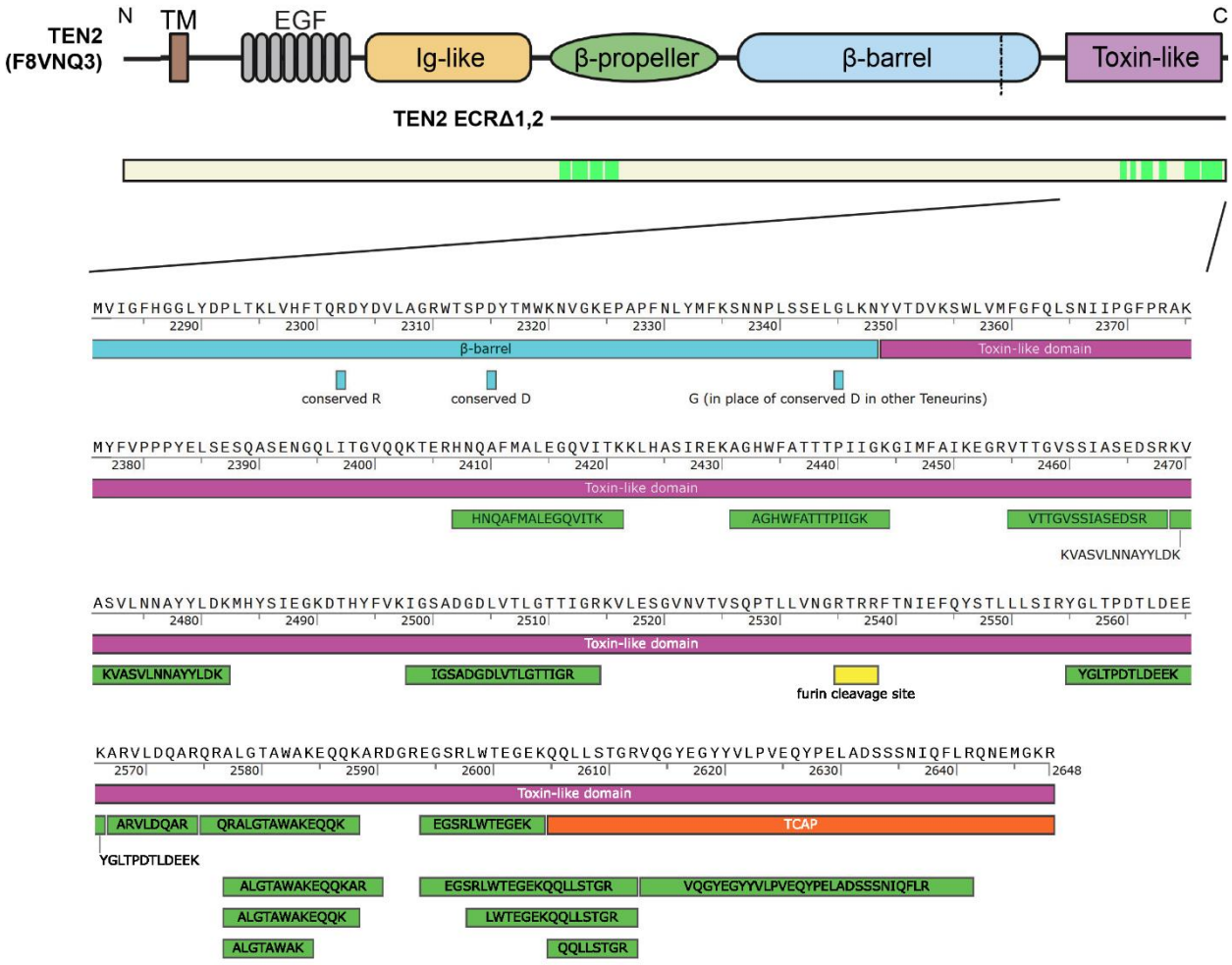

Figure 2.11: Mass spectrometry of 30kDa protein product from TEN2 ECRΔ1,2 purification .

Mass spectrometry for cleavage product produced from ECRΔ1,2 purification. Peptide mass results compared to TEN2 (UniProt: F8VNQ3). Peptide matches highlighted in green. β-barrel (blue) with catalytic residues, toxin-like domain (purple), furin cleavage site (yellow), and TCAP (orange). TCAP: Teneurin C-terminal-associated peptide

2.8 TEN2 undergoes C-terminal autoproteolysis via conserved catalytic residues

Tc toxins contain a set of catalytic residues that induce autoproteolysis of the C-terminus of the C component, which is released into the cytoplasm of neighboring cells to induce insecticidal activity (Busby et al., 2013; Meusch et al., 2014). This catalytic site is evolutionarily conserved across species, from partial conservation in *C. elegans* to high conservation in all isoforms of human TENs (Li et al., 2018). TEN proteolytic activity and its effect on TEN function have been thoroughly characterized at the N-terminus, but the C-terminal autoproteolytic potential of TENs remains undetermined (Bagutti et al., 2003; Kenzelmann et al., 2008; Schöler et al., 2015; Vysokov et al., 2016; Vysokov et al., 2018).

Tc toxins cleave the C-terminus of their C component through an aspartate dyad located inside its barrel structure (Busby et al., 2013; Meusch et al., 2014). This cleavage is abolished when either of the two aspartates or a nearby arginine are mutated to a neutral amino acid, indicating that these three residues are responsible for C-terminal cleavage in Tc toxins. Through structure alignment, we noted that the conserved catalytic residues are conserved in TEN2

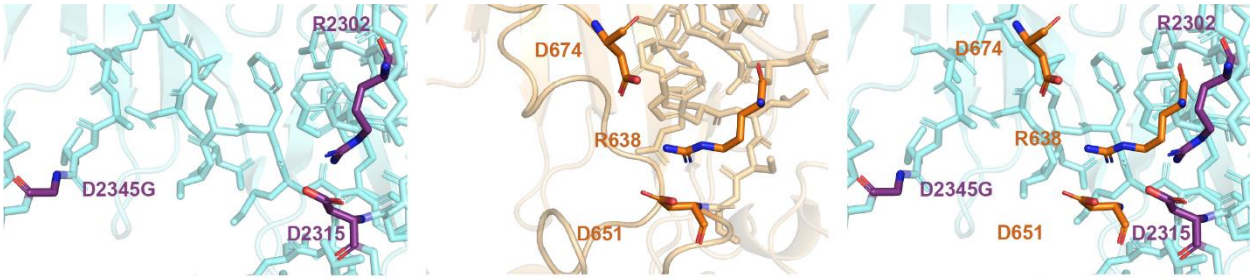

Figure 2.12: TEN2 conserved catalytic residues reside in similar positions as Tc toxin autoproteolysis site

Comparison of catalytic residue positions in TEN2 (purple) and *P. luminescens* (orange). TEN2 exhibit R2302 and D2315 at similar structural positions as corresponding R638 and D651 toxin catalytic residues. This TEN2 isoform contains a glycine in place of aspartate at a different spatial position.

(R2302, D2315, and D2345) are spatially located in similar positions as the autoproteolysis site of Tc toxins (**Figure 2.12**). Thus, we hypothesized that the C-terminal product observed from TEN2 ECRΔ1,2 was cleaved via autoproteolysis by these conserved catalytic residues.

We targeted R2302 and D2315 for mutation to neutral alanine amino acid (R2302A and D2315A) to test whether these residues were responsible for C-terminal product in wildtype ECRΔ1,2. The mutant ECRΔ1,2_RD protein was purified and separated by SEC to check if protein product was present at the same elution volumes (14-16 mL) as the cleavage product observed in wildtype. Comparison of chromatograms revealed that the peak corresponding to C-terminal product observed in ECRΔ1,2 was absent in the mutant construct (**Figure 2.13B**).

Mutation of these catalytic residues (R2302A and D2315A) prevented formation of the 30 kDa protein product observed in wildtype (**Figure 2.13**), Moreover, SEC showed that the protein peak corresponding to the C-terminal product observed in ECRΔ1,2 was absent in mutant construct ECRΔ1,2_RD, suggesting that the conserved catalytic residues are responsible for C-terminal product release. To further investigate this observation, we used His-antibody to show a reduction in C-terminal product for ECRΔ1,2_RD as compared to wildtype ECRΔ1,2 (**Figure 2.14**). Taken together, these data show that mutating R2302 and D2315 abolished autoproteolysis in TEN2 ECRΔ1,2, indicating that release of the toxin-like domain occurs in TEN2 lacking EGF- and Ig-like domains via these conserved catalytic residues. Furthermore, this proteolytic mechanism of release appears to be evolutionarily carried over from Tc toxins as a C-terminal property of TENs.

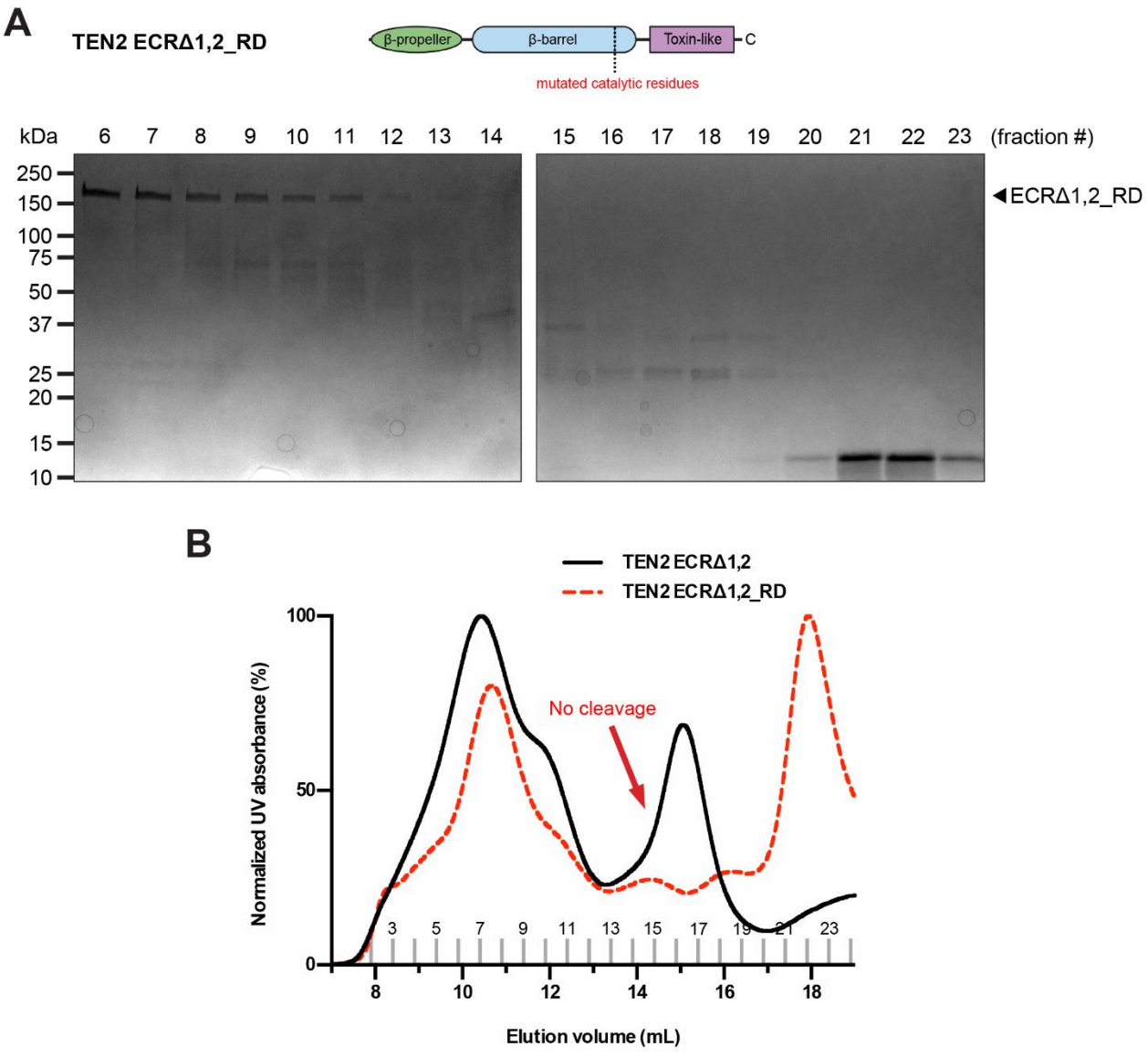

Figure 2.13: Mutagenesis of TEN2 conserved catalytic residues abolish autoproteolysis

(A) Size exclusion chromatography of purified TEN2 ECRΔ1,2_RD.

(B) Chromatogram comparison of TEN2 ECRΔ1,2 (black) and ECRΔ1,2_RD (red) normalized to 100%.

RD: R2302A, D2315A mutagenesis.

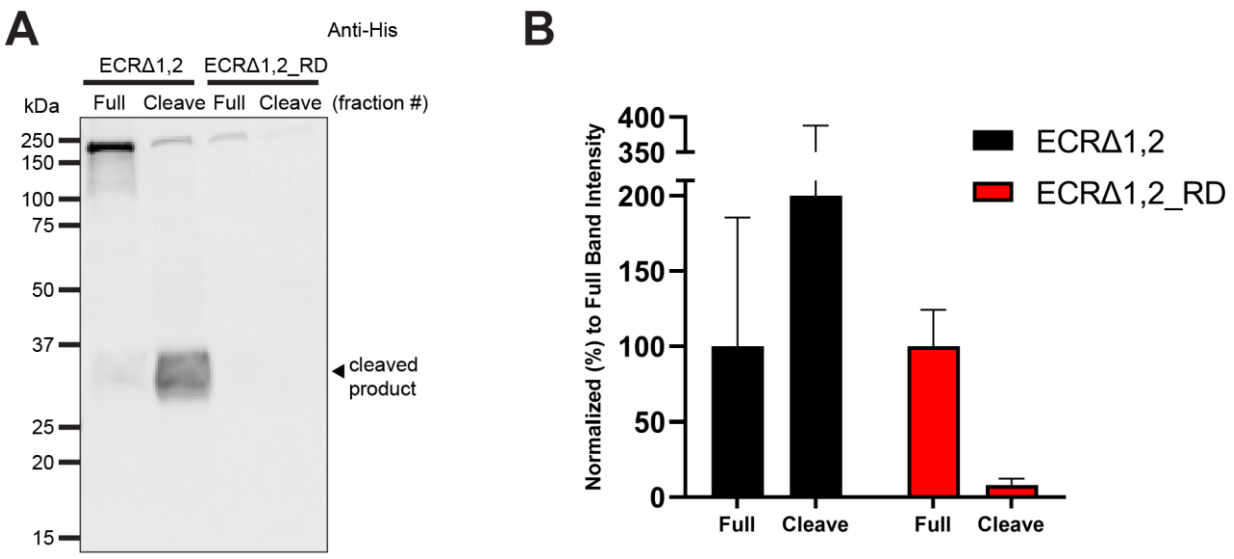

Figure 2.14: Mutagenesis of TEN2 conserved catalytic residues abolish autoproteolysis

(A) Fractions containing full construct or cleavage product of TEN2 ECRΔ1,2 and ECRΔ1,2_RD immunostained with His-488 antibody. Arrowhead indicates expected size band for cleavage product (34 kDa).

(B) Quantification of cleavage band intensity normalized to full construct, respectively.

RD: R2302A, D2315A mutagenesis.

2.9 Ig-like domain may contribute to C-terminal product release

The TcB-TcC barrel of Tc toxins is plugged by a β-propeller domain that is integral to the release of the C-terminal cytotoxic domain (Gatsogiannis et al., 2018; Meusch et al., 2014). The Ig-like domain is reported to make contacts with the β-barrel and toxin-like domain when it plugs the barrel at the bottom of the structure (Li et al., 2018). Earlier we observed that TEN2 releases its C-terminal toxin-like domain only when the Ig-like domain is deleted. Thus, we hypothesize that the Ig-like domain is involved in regulating toxin-like domain release.

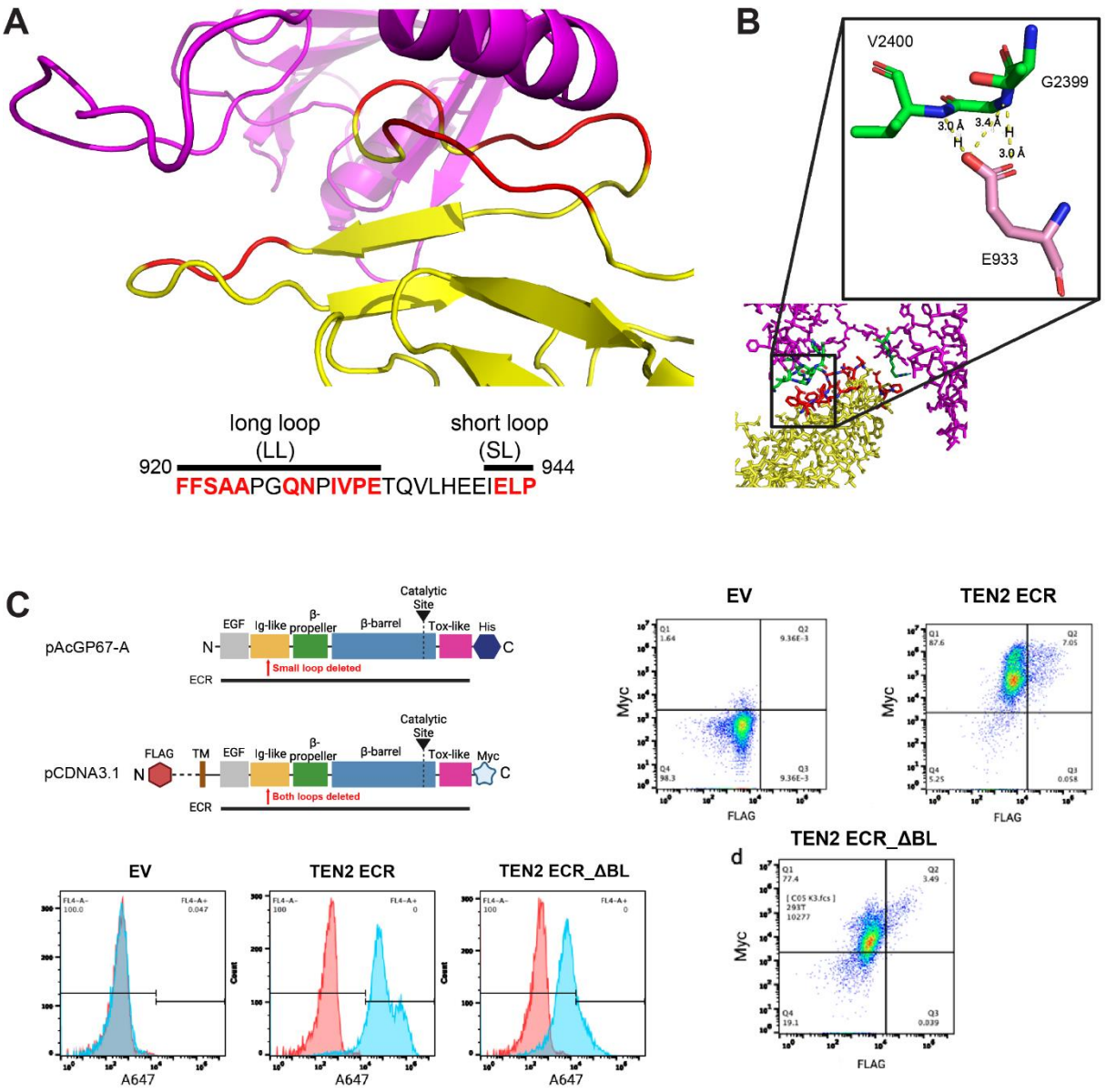

Figure 2.15: TEN2 Ig-like domain makes contacts with the toxin-like domain at two loops

(A) The Ig-like domain (yellow) contains a long (LL) and short loop (SL) (red) that form a possible interface with the toxin-like domain (magenta).

(B) Example of hydrogen bonds connecting the Ig-like domain interface residues (pink) with toxin-like domain interface residues (green).

(C) Deletion of the small loop in insect vector and both loops (BL) in mammalian vector. BL deletion exhibits cell surface expression in HEK 293T cells via flow cytometry of against Myc-antibody. EV: Empty vector.

2.9.1 Ig-like domain makes contacts with the toxin-like domain

Using PDBePISA, which identifies interfaces in crystal structures, we find that 14 residues in the Ig-like domain of TEN2 form an interface with the toxin-like domain, which corresponds to two loops that sandwich a β-sheet (**Figure 2.15A**). The long loop (LL) from F920-E933 and the short loop (SL) from I941-P944 are predicted to make contacts with a single loop and an α-helix/loop combination in the toxin-like domain, respectively. The interface residues are within distance of 5 Å, where five of them are within 4 Å and predicted to form hydrogen bonds via Pymol analysis (**Figure 2.15B)**. We cloned TEN2 with deletion of the predicted Ig- and toxin-like domain interface into a mammalian vector tagged and used flow cytometry to show that deletion of both loops expressed at the cell surface in mammalian cells, implying mutations of these loops produce a stable protein (**Figure 2.15C**).

2.9.2 Deletion of a small loop in Ig-like domain results in possible C-terminal product

We cloned TEN2 with deletion of only the small loop (TEN2 ECR_ΔSL) into insect cell expression vector to test whether the predicted interface between the Ig-like and toxin-like domain influenced C-terminal product release. Wildtype TEN2 ECR and mutant ECRΔSL were purified from insect cells and separated by SEC, and we observed a 270 kDa band corresponding to the size of whole ECR in the ΔSL construct under Coomassie blue conditions (**Figure 2.16A**). C-terminal product in the earlier wildtype ECRΔ1,2 experiments was found at elution volumes 14-16 mL; if C-terminal product was released in ΔSL, we expect to find it in the same fractions corresponding to those elution volumes. Comparison of chromatograms shows full ERC peaks, albeit eluted at different volumes, in both constructs and a small peak at volumes 14-16 mL in the ECR_ΔSL mutant (**Figure 2.16B**). His-antibody staining of fractions containing these

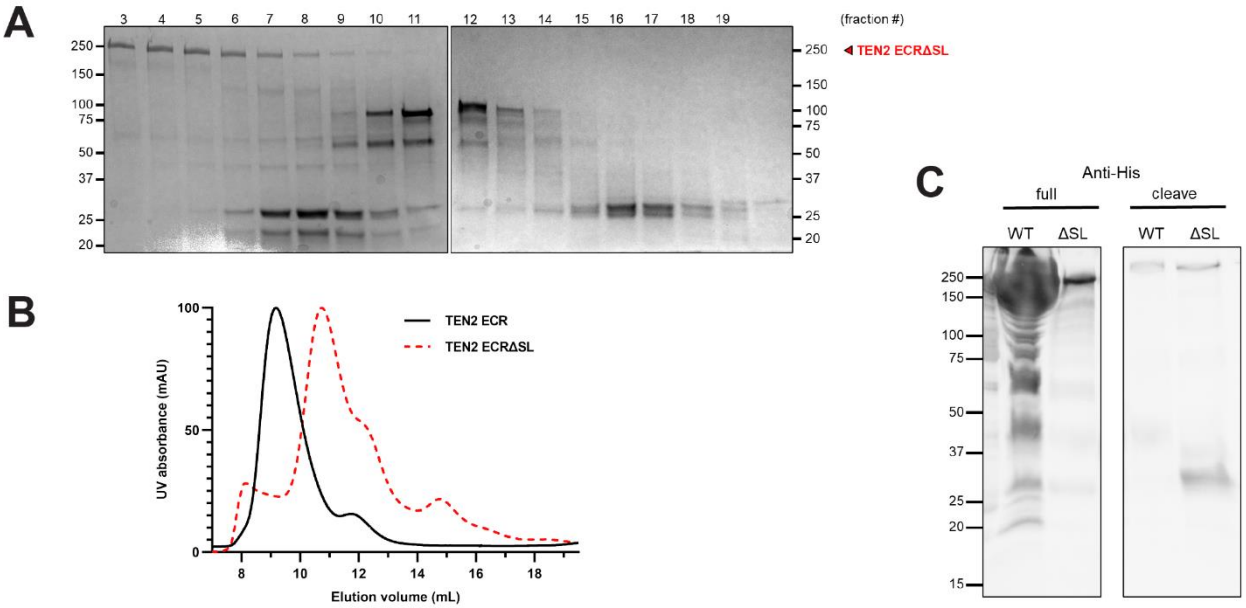

Figure 2.16: Deletion of small loop in Ig-like domain results in C-terminal product

(A) Coomassie blue gel of eluted fractions of TEN2 ECR_ΔSL after SEC (B). Chromatogram shows small peak at elution volume expected for cleavage.

(C) His-antibody staining of fractions expected to contain either the full ECR (left) or the cleaved product (right). WT full fraction contained too much protein, hence the distorted band.

volumes (cleave) exhibited a band at about 30 kDa in ECR_ΔSL but not wildtype, suggesting that deletion of the small loop contributed to the emergence of a C-terminal product (**Figure 2.16C)** . Further tests such as mass spectrometry or N-terminal are necessary to confirm the identity of this band.

DISCUSSION

3.1 *Ten-1* toxin-like domain plays a role in *C. elegans* nervous system development

Endogenous expression of *ten-1* in *C. elegans* has not been previously described post-embryogenesis, and here we show that worms at L1 larval stage express *ten-1* around the isthmus of the pharynx, where the nerve ring is located. Furthermore, *ten-1* runs along the VNC and reaches the end of the tail posterior to the anal cavity. This pattern corroborates the expression seen in transcriptional reporters, though more acutely instead of throughout the cell. Ten-1 is a type II transmembrane protein, meaning the C-terminus resides outside the membrane; thus, the endogenous C-terminal mNG tag sits at the cell surface with the ECR. Because *ten-1* expression is observed at the nerve ring, which is composed of a tight bundle of axons with dozens of synapses, we expect Ten-1 plays a role at the synaptic cleft.

3.1.1 Deletion of the toxin-like domain on C. elegans as a neomorphic effect

The expression pattern of endogenous *ten-1* differs when the toxin-like domain is deleted, where *ten-1* is more spread out around the isthmus and exhibits higher intensity, confirmed quantitatively. The truncated mutant also appears overly expressed at the VNC and in the tail regions. Overall, the truncated protein is overexpressed compared to WT, which suggests that truncation of the toxin-like domain results in a more stable protein. It is not unheard of for structural flexibility of TENs to change dramatically; in fact, some functions depend on the ability of TEN genes to encode for structurally disparate isoforms. For example, an alternative splicing site (+SS) at the β-propeller of the ECR was identified and confirmed to affect the steric potential of the teneurin backbone, thereby preventing the binding of TEN2 to LPHN3 (Li et al.,

2020). Transfection of TEN2 +SS isoform in HEK 293T cells results in inhibitory synapse formation when co-cultured with cortical neurons, while the absence of splice site (-SS), which allows for LPHN3 binding, leads to excitatory synapse formation. Thus, alternative splicing directs synaptic specificity in TENs through shape-shifting mechanism.

It is possible that truncating the toxin-like domain leads to overexpression or neomorphic effects. In our viability assays, we see a decrease in average brood size for the truncation mutant strain. While the variance of the brood size assay is too high to show statistical significance, this observation is worth noting when considering neomorphic effects of the truncation mutant, especially when the fluorescent WT strain, t*en-1::mNG*, retains an average brood size similar to WT control. The embryonic survivability and larval viability of the truncation mutant remain steady when compared to controls, implying that the truncation of toxin-like domain bears no negative effect on embryonic or body development as observed in *ten-1* null mutant; thus, the toxin-like domain is not necessary for viability of the worm as is full-length Ten-1. Another previously described *ten-1* mutant allele, *et5*, is composed of point mutation that introduces a premature stop codon just downstream of the EGF-like domain, producing a strain with milder post-embryonic phenotype than *ok641* null mutant, where 70% of worms *et5* progeny grow into fertile adults (Mörck et al., 2010). The *ok641* strain contains a 2130 bp deletion that removes the last four EGF repeats until part of the β-propeller (**Figure 2.1**) and results in a more severe post-embryonic phenotype, indicating an important function for these last four EGF repeats present in the *et5* hypomorph. Moreover, the *ok641* mutant is an in-frame deletion, which means the toxin-like domain is still present in the translated mutant protein and yet still produces severe viability defects. This corroborates our finding that toxin-like domain has no bearing on embryonic

development or post-embryonic phenotype and most likely produces a stable protein, and truncation of the toxin-like domain may actually produce a more stable protein.

It is also feasible that truncation of toxin-like domain results in increased transcriptional feedback to produce more Ten-1 protein. While this possibility seems unlikely because it would require the extracellular toxin-like domain to communicate with the intracellular nucleus, we could test this by crossing our *ten-1::mNG* and *syb9522* lines to transcriptional GFP reporters for *ten-1a* and *ten-1b* promoters and measuring the amount of GFP expression. If the toxin-like domain downregulates *ten-1* promoter activity, then we expect *syb9522* to induce more GFP intensity, which is driven by *ten-1a* or *ten-1b* promoter. It is also possible that the toxin-like domain interacts with an intermediate molecule to downregulate activity of *ten-1a* and/or *ten-1b* promoters. If there is no change in transcriptional GFP reporters, then truncation of toxin-like domain may indeed induce a neomorphic effect on ten-1 by increasing its stability as previously hypothesized.

3.1.2 Truncation mutant produces defects similar to null mutant in pharyngeal or body neurons

TENs are known for their ability to form homo- and heterophilic interactions in *cis* along the cell membrane or in *trans* across the synapse, and we surmise that Ten-1 may be important for proper axon morphology in *C. elegans* due to its localization at the nerve ring and along the VNC. The null mutant has been previously characterized to show axonal defects in pharyngeal neurons, and we demonstrate that these defects are not unique to the null. Partial truncation of C-terminal *ten-1* domain produced varicosities and beaded axons in M4 neurons comparable to the null mutant, both at a significantly higher rate than wildtype strains, indicating that the toxin-like domain is at least partially responsible for these phenotypes. Meandering axons were observed

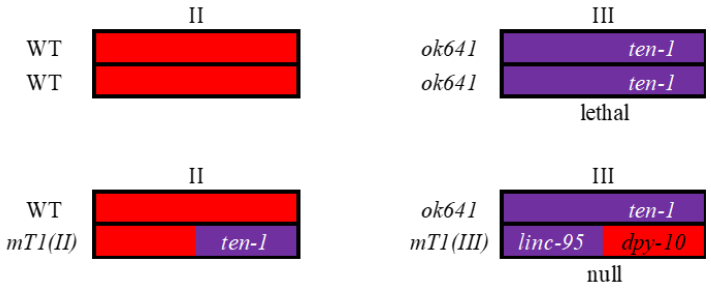

Figure 3.1: Ch. 2 and Ch.3 pair alleles for homozygous *ten-1* and *ten-1(ok641)* mutants

Homozygous ten-1 mutant (top) in ch. 3 results in embryonic lethality, but when balanced with mT1(II;III) translocation, a single *ten-1* mutant allele yields a null mutant strain. mT1(III) allele is marked by *dpy10* and *linc-25*.

more in mutants than wildtype but not to a significant extent, although a general higher trend of this defect is present in the mutants.

Interestingly, *ten-1(ok641)* is an in-frame deletion far upstream of the toxin-like domain that is balanced by the translocation of chromosome II and III [*mT1(II;III)*] because the mutation is otherwise homozygous lethal (Consortium, 2012; Edgley & Riddle, 2001). The right arm of one allele in ch. II is exchanged with the right arm of one allele in ch. III to prevent recombination. *Ten-1* genetic position is at the right arm of ch. III, which means the *ok641* mutation is found in the ch. III allele paired with the chimeric *mT1(III)* allele, while wildtype ch. II allele is paired with the chimeric *mT1(II)* allele containing translocated wildtype *ten-1* (**Figure 3.1**). While the resulting *ok641* strain contains a single copy of both wildtype and mutant *ten-1* alleles, it behaves as a null mutant, suggesting that the mutation is dominant negative. The mutant protein is still translated but likely interferes with the wildtype copy. We do not observe the same embryonic, larval, and vulva defects in our C-terminal truncation mutant, *syb9522*, that are present in *ok641*, yet we see defects in M4 neurons almost as severe, suggesting the toxin-like domain plays a role in proper axon morphology.

Similarly, we observed varicosities in axons of NSM neurons in both mutants, but only the null mutant exhibited truncated axons and ectopic growths at a higher rate than the normal variation found in wildtype. Nevertheless, scRNA-Seq from the CeNGEN project reports *ten-1* expression in NSM neurons, suggesting that the toxin-like domain exerts influence over NSM axons in a cell-autonomous manner (Taylor et al., 2021). Furthermore, NSMs express a dorsal and a ventral axon extending from the soma, and the truncation we observed was of the dorsal branch, which has been reported to be most sensitive to mutations that affect growth cone guidance and function (Axäng et al., 2008). This truncation implies *ten-1* may play a role in NSM axon guidance or interaction with synaptic partners, which necessitates further study via genetic interaction studies.

In addition to NSM, the *tph-1::GFP* reporter allowed us to examine HSN neuron morphology in relation to *ten-1* mutations. HSN neurons are a key part of the egg-laying circuit of *C. elegans*, synapsing onto VC neurons and vulva muscle wall and extending axons from two cell bodies near the vulva all the way to the nerve ring (**Figure 2.7A**) (Huang et al., 2023). They control timing of egg-laying, high locomotion during egg-laying behavior, low-dwelling motion in response to food, and release serotonin that is taken up by NSM neurons at the nerve ring. As such, HSNs orchestrate multiple functions in *C elegans,* and this multifaceted control over motor circuits and neurotransmitter release makes them a crucial target for study.

Ten-1 mutants displayed conspicuous varicosities in HSN axons along the VNC and at the vulva, which was not previously reported. Abnormalities are more severely present in *ok641*, suggesting that the toxin-like domain of *ten-1* is only partially responsible for axonal defects. We previously discussed that missense mutations in multiple domains of TEN4 have been identified as risk variants for schizophrenia, which suggests that multiple domains, not necessarily a single

domain, contribute to structure stability and protein-protein interactions in combination. Thus, although the truncation mutant experienced these defects to a slightly lesser degree than the null, the difference compared to wildtype is still significant enough to suggest that the toxin-like domain may be an important component of HSN neurons and pharyngeal neurons, perhaps in conjunction with other domains. This aligns with *in vivo* studies in mice, where the ICD, EGF-like, and toxin-like domain of TEN3 were identified as indispensable for synapse formation (Zhang et al., 2025).

3.1.3 Lack of full penetrance indicates functional redundancy between multiple players

It must be noted that these neurons develop mostly normal axons in these mutant strains (**Table 2**). The highest degree of penetrance was about 43% in NSM neurons, then 33% in M4 neurons, and a little over 10% in HSN neurons. However, *ten-1(ok641)* has been reported to enhance defects in the pharyngeal M2 neurons when combined with mutations in *mig-14*, *unc-5*, *unc-51*, *unc-52* and *unc-129* (Mörck et al., 2010). Furthermore, *ok641* is synthetic lethal with mutations in *sax-3, unc-34, unc-73, phy-1*, *ina-1*, *dgn-1*, *epi-1*, and *nid-1*, which encode for hypodermal cell morphogenesis, basement membrane components, and pharyngeal development, and double mutants enhance non-neuronal defective phenotypes (Topf & Chiquet-Ehrismann, 2011; Trzebiatowska et al., 2008). Thus, it is highly likely that *ten-1* mutants are not fully penetrant because *ten-1* is working in conjunction or share redundancy with other genes involved in nervous system development. Genetic studies are needed to identify which genes when mutated enhance axonal defects reported here.

3.1.4 Protein-protein interactions of ten-1

Interactions between TENs and other receptors is complicated in both vertebrates and invertebrates and remains to be fully understood. Mammalian TENs canonically bind to LPHNs to mediate certain functions during neurodevelopment, such as cell migration with redial glial cells, axon targeting in the mouse hippocampus, and synaptic specificity to determine excitatory synapse identity. On the other hand, presynaptic TEN2 +SS alternative splicing variant that cannot bind to LPHN induces inhibitory synapse formation in mammalian cell cultures, implying an unknown postsynaptic partner. In *C. elegans*, binding partners of *ten-1* remain to be identified. *Lat-1*, the *C. elegans* homolog of vertebrate LPHNs, is expressed in multiple neurons and neuronal support cells, and transcriptome analyses of *lat-1* null-mutants revealed downregulated genes associated with neurodevelopment and mechanosensation (along with body morphology and copulation) (Matúš et al., 2022). Furthermore, abnormal dendritic morphology and anterior shift of the nerve ring was observed in *lat-1* mutants. The N-terminus of *lat-1*, which resides on its extracellular part exposed to the synaptic cleft, was identified as the responsible region for regulating sperm guidance, ovulation, and germline apoptosis, which contribute to reproduction and brood size control, and morphogenesis of sensory structures in the C. elegans nervous system (Matúš et al., 2024). This N-terminal dependent regulation indicates a *trans* function for *lat-1*.

Past literature describes the interaction of *ten-1* and *lat-1* as in parallel rather than the trans interactions seen in vertebrates TENs (Schöneberg & Prömel, 2019). While genetic interaction studies in *C. elegans* imply interaction between *ten-1* and *lat-1*, no direct binding has found (Mörck et al., 2010; Prömel et al., 2012). Double mutants of *lat-1; ten-1* exhibited almost completely penetrant developmental arrest and a greatly reduced brood size. Heterozygous

animals, which carry at least one wild-type allele for either loci, exhibited significant defects in embryogenesis and fertility in a dose-sensitive manner (meaning that *lat-1 +/-; ten-1+/+* exhibited low penetrance of about 10%, *lat-1 +/+; ten-1+/-* showed about 25%, *lat-1 +/-; ten-1+/-* about 40%, until full penetrance reached in mutant homozygotes), which implies that both genes are acting at least partly in parallel during development and germline function. This non-complementation implies a synergistic rather than linear interaction between both genes. Furthermore, patterning of *ten-1* expression in neurons does not coincide with *lat-1* according to early studies, and non-neuronal expression is present in early hypodermal cells, implying possible interaction in *cis* rather than in *trans* (Schöneberg & Prömel, 2019).

When looking at CeNGEN reports of *lat-1* and *ten-1* expression, however, we see that expression coincides in NSM pharyngeal neurons as they contain both *lat-1* and *ten-1*. Moreover, while HSN body neurons cells do not express ten-1, they do carry *lat-1*, implying that if an interaction were to exist between *ten-1* and *lat-1*, it could be in *trans*. NSM and HSN neurons synapse with each other, whose interaction is crucial for egg-laying behavior, and thus a possible connection between *ten-1* and *lat-1* could be further investigated to explain the neomorphic effect we see in decreased brood-size of our truncation mutant. Furthermore, NSM neurons synapse onto I6 and M3 neurons, which express *lat-1*, and M3 axonal defects have been previously described with regards to *ten-1* null-mutants; additionally, M4 neurons, whose axonal defects were described here, synapse onto M1 neurons that express *lat-1*. Therefore, the possible interaction between *ten-1* and *lat-1* remains to be full disentangled, whether in *cis* or in *trans*.

While there is no evidence of binding between *lat-1* and *ten-1*, the former has been reported to interact with other receptors. In vertebrates, UNC5 interacts with FLRT and LPHN in cell adhesion assays, while FLRT and LPHN form a trimeric complex with TENs to induce

synapse formation (Li et al., 2018; Lu et al., 2015). Genetic interaction studies in *C. elegans* imply interaction between *ten-1* and *unc-5* and *lat-1*, but direct binding has yet to be determined (Mörck et al., 2010; Prömel et al., 2012). Lat-1 has been reported to bind to Tol-1, a cell-surface receptor, and this interaction is important for embryonic development and brood size (Carmona-Rosas et al., 2023). It is possible that *ten-1* does not interact with *lat-1* and instead act in parallel with each other, where Lat-1 binds to other receptors to maintain functions similar to Ten-1. Many genes in *C. elegans* act in redundancy with each other, which would explain the lack of full penetrance seen in our axon defect phenotypes.

While most of the discussion here and in the literature surrounds *lat-1*, *C. elegans* also expresses a paralog called *lat-2*. While both *lat-1* and *lat-2* encode seven transmembrane domain G protein-coupled receptors with characteristics of LPHNs, they share only 21% amino acid identity with each other (Willson et al., 2004). *Lat-2* is expressed in the pharynx and gland cells of the excretory system, but its function is still unknown, where its deletion has no obvious phenotype except for enhancing penetrance of the late embryonic and larval defects observed in *lat-1* deletion (Langenhan et al., 2009; Topf & Drabikowski, 2019). Vertebrate TENs interact with different isoforms of LPHNs, which is essential for correct axon targeting, and while *ten-1* has not been found to interact with *lat-1*, interaction with *lat-2* remains unexplored and thus remains a possibility for functionality of *ten-1* in *C. elegans*.

3.1.5 Establishing cell autonomy of ten-1 in axonal development

We previously described that NSM neurons express ten-1 according to CeNGEN scRNA-Seq data, and the axon defects observed in NSM due to *ten-1* mutants imply cell autonomy. To fully establish whether ten-1 functions cell-autonomously, RNA interference (RNAi)

experiments could be performed that target ten-1 in specific neurons of C. elegans. Previously, RNAi has been used to test whether Ten-1 acts cell autonomously or nonautonomously in sperm development (Drabikowski et al., 2005). Mutant strain *rrf-1*, which is known to be defective in somatic RNAi, was injected with RNAi directed against both ten-1a and ten-1b transcripts or GFP-RNAi, and no significant difference was observed in the number of progeny of injected worms from either group, implying non-cell autonomy. However, the authors concluded that this result was not an indication of non-cell autonomy because the somatic gonad is already developed at time of injection and *ten-1* is expressed in developing sperm, and *rrf-1* mutant worms are not hypersensitive in the germ line and expected to react as wild-type worms. Regardless, we can apply RNAi to test to cell autonomy of *ten-1* in NSM neurons. First, we would globally remove *ten-1* from wildtype N2 worms by using RNAi directed against both promoters, where we predict NSM axonal defects as observed in the *ten-1* mutants earlier in this thesis. Then, we would inject a cosmid carrying the entire genomic region of the *ten-1* gene (or empty control) that is only expressed in NSM neurons. If *ten-1* is acting cell autonomously in NSM neurons, then we expect *ten-1* expressed only in NSM to rescue the NSM axon defects.

Because we observed similar phenotypes in our C-terminal truncation mutant, we could further test cell autonomy specific to the toxin-like domain by injecting *ten-1* gene with deletion of the C-terminus. If this truncated *ten-1* gene fails to rescue the axonal defects, then we could attribute *ten-1* function in NSM morphology to the toxin-like domain. Likewise, cosmid with only the *ten-1* toxin-like domain part of the gene could be injected into ten-1 knockdown worms to test whether only the toxin-like domain is necessary for NSM function, as the varicosities phenotype is present at the 10% rate in both null and truncation mutants (**Figure 2.7**).

Cis interaction between TENs residing on the same side of the membrane have been observed in other organisms such as Drosophila and mammals. Thus, it is possible that *ten-1* in NSMs may be acting cell autonomously in *cis*. In this case, it would be important to also probe the importance of the ICD and its role in cell autonomy of *ten-1* in NSM neurons, which can be accomplished by targeting RNAi only to ten-1a transcript and comparing to RNAi of both transcripts.

In contrast, if no rescue is observed, then *ten-1* is likely acting non-cell autonomously, which could be confirmed by using RNAi that specifically targets *ten-1* in NSM neurons. Synapses form onto NSM neurons from HSN body neurons and I1, I2, I3, I4, and I6 interneurons in the pharynx. Non-cell autonomy would be consistent with interactions in *trans*, and at least I1 and I6 express *ten-1* according to CeNGEN. Using RNAi to target *ten-1* knockdown in I1 and I6 and probe for NSM axon defects would show if *ten-1* function in NSM neurons is non-cell autonomous.

Although *ten-1* is not present in M4 neurons according to CeNGEN, this absence could be attributed to a drawback in collecting pharyngeal neurons for scRNA-Seq, where not enough pharyngeal neurons may have been collected, and thus a lack of expression is not necessarily the correct conclusion. M4 neurons receive synapses from I3, I5, I6, NSM and synapse onto M1, of which I6 and NMS neurons express *ten-1*. These connections could be targets for establishing cell or non-cell autonomy of ten-1 function in M4 neurons. HSN neurons follow similar logic, where no expression of *ten-1* was detected in CeNGEN data, implying cell autonomy. Due to HSNs extending axons all the way from the vulva to the pharynx, they make numerous connections with other neurons, receiving synapses from BDU, AVL, PLM, AVB, AVJ, PVQ, PVN, AVG, and synapsing to VUL, NMJ, VC5, SABV, AVD, SABD, VC2, AS5, VA6, DA6. In

this case, it would be interesting if targeted expression of *ten-1* in these individual neurons could rescue axonal defects in HSNs from *ten-1* RNAi knockdown. This type of observation would imply a *trans* interaction of Ten-1 in *C. elegans*.

3.1.6 ten-1 mutants and C. elegans reproduction

Ten-1(ok641) worms exhibit exploding vulva, sterility, and infertility, and although these phenotypes appear unrelated to egg-laying, vulva explosion and death only happen in early adults, which coincides with the onset of egg-laying behavior. Furthermore, *ten-1* is found in VC4 and VC5 neurons according to CeNGEN, which synapse onto HSN neurons and vulva egg-laying muscles, and which have been reported to induce the egg-laying phase via serotonin release (Waggoner et al., 1998; Zhang et al., 2008). The null mutant also showed a general decrease in brood size (with the truncation mutant to a lesser extent), which could be attributed to fewer eggs laid or lower rate of egg-laying. Thus, it might be worth exploring egg-laying speed by measuring it in *ten-1* mutants to investigate whether *ten-1* plays a role in egg-laying behavior.

When HSN axons are cut anterior to the vulval presynaptic region, egg-laying rate remained intact while increased locomotion, which is coupled to egg-laying, was weakened (Huang et al., 2023). Varicosities were observed not only close to the vulva but along the HSN axons extending to the nerve ring, suggesting that *ten-1* may be important to HSN motor output independent of egg-laying behavior. Measuring increased locomotion in *ten-1* mutants could be explored to further assess the role of *ten-1* during egg-laying process. Additionally, HSN axons project to the nerve ring and synapse onto NSM neurons, which together promote slow dwelling behavior as feeding response in worms via serotonin release and reuptake. AVL neurons, which

are GABAergic motor neurons that start at the nerve ring and run along the VNC until reaching the posterior end at the tail, form synapses with HSN, coordinating the defecation motor program. Behavioral assays can be performed with *ten-1* mutants to address whether Ten-1 contributes to function via these specific neurons. Furthermore, the possible interaction between *lat-1* and *ten-1* could be further explored with regards to HSN neurons, as *lat-1* is crucial for regulating components of reproduction in *C. elegans*.

3.1.7 The connection between ten-1 and unc-129 regulation

Ten-1 null mutant has also been reported to increase *unc-129* levels in the dorsal muscles, which suggests that *ten-1* may influence TGF-β levels on the *unc-129* locus (Mörck et al., 2010). DA and DB motor neurons project commissural axons from the VNC circumferentially to the dorsal wall muscles, facilitated by *unc-129* enhancing the UNC5/UNC40 heterodimers dorsally in oppositional gradient to ventrally-concentrated UNC6. This allows axon grown cones to migrate from the high UNC6 ventral levels to the dorsal side with low UNC6 and reach dorsal muscles (Colavita & Culotti, 1998; Colavita et al., 1998; MacNeil et al., 2009). Although *ten-1(ok641)* increases *unc-129* expression, axonal defects in DA/DB neurons are absent in the null mutant, despite other studies showing that changes in *unc-129* levels result in axon guidance defects. The influence of *ten-1* toxin-like domain on *unc-129* could be explored by crossing our truncation mutant with a proper *unc-129::GFP* reporter to address whether *ten-1* suppression of *unc-129* is specific to the toxin-like domain. In preliminary data, we observe that *unc-129::GFP* expression along the dorsal is increased in the truncation mutant (**see Appendix A**). This change in expression from WT reporter to truncation mutant is similar to the 20-fold increase visible in the null mutant from previous study. Thus, we speculate that the toxin-like domain may at least

be responsible for the influence of *ten-1* over unc-129 levels. Control strain for the fluorescent protein (*unc-129::GFP with ten-1::mNG*) must be generated to make a definite conclusion. If this observation is attributed to the truncation of toxin-like domain, then we could speculate that the C-terminus of *ten-1* somehow influences the innervation of commissural axons from DA/DB to dorsal muscles, and perhaps a deeper connection between ten-1 and TGF-β exists that accounts for this phenotype.

3.2 C-terminus of human TEN exhibits autoproteolytic potential

When referring to cleavage in TENs, the N-terminus is often discussed, as it has been thoroughly studied and found to coordinate several functions at different cleavage sites. In an isoform of TEN2, furin-mediated cleavage (S3) occurs before the EGF-like domain during processing at the Golgi complex, but this cleavage product remains non-covalently attached to the N-terminal fragments at the transmembrane (TM) region (**Figure 3.2A**). To release the whole ECR, an additional cleavage site (S2) at the TM breaks up the membrane-anchored fragment and is thought to be mediated by a matrix metalloproteinase. Cleavage of this TEN2 ECR contributes to axon pathfinding in developing hippocampal neurons by attracting LPHN-1-expressing axonal growth cones via a concentration gradient (Vysokov et al., 2016; Vysokov et al., 2018). Another cleavage site (S1) is found in the cytosolic side of the protein just before the TM, which releases the ICD from the rest of the anchored TEN2 into the cytoplasm. The ICD contains a nuclear localization signal that allows its translocation into the nucleus, where it enacts transcriptional activity (Bagutti et al., 2003; Kenzelmann et al., 2008; Schöler et al., 2015).

Cleavage sites at the C-terminus of TENs are predicted at the toxin-like domain (**Figure 3.2B**). A furin-cleavage site is found that would release the toxin-GHH domain of the C-

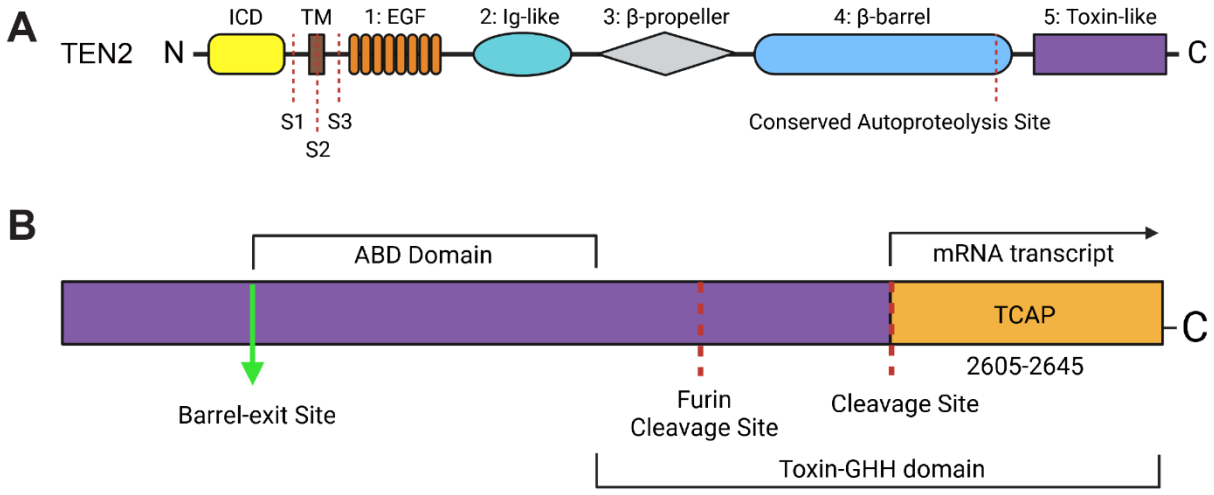

Figure 3.2: Cleavage sites found in N-terminus and C-terminus of TEN2

(A) N-terminal cleavage sites at TEN2 reside near the TM only: S1, S2, S3.

(B) C-terminal cleavage sites in the toxin-like domain located at the toxin-GHH domain and TCAP. Conserved autoproteolysis site is predicted to release most of the toxin-like domain.

ICD: intracellular domain; TM: transmembrane; EGF: epidermal growth factor-like domain; Ig-like: immunoglobulin-like domain (Ig); ABD: antibiotic-binding-like domain; GHH: glycine-histadine-histadine domain; TCAP: teneruin C-terminal associated peptide.

terminus, named after the Glycine-Histadine-Histadine amino acid motif responsible for DNAse activity in Tc toxins. Sequence alignment showed that this GHH sequence is not conserved in human TENs, but an adjacent GYE/D motif, which is found in the GHH toxin from *Bacillus thuringiensis*, is found in all vertebrate TENs. Mammalian HEK 293T cells transfected with human TEN1 or TEN2 toxin-GHH domain exhibited apoptotic activity, meanwhile purified chicken TEN1 or TEN2 toxin-GHH-domain linearized pcDNA3 plasmid and hydrolyzed plasmid containing murine mitochondrial DNA at short or overnight incubation times, respectively (Ferralli et al., 2018). Interestingly, when the whole ECR of chicken TEN2 was purified and incubated with DNA, no nuclease activity was observed, indicating that toxin-GHH

domain is cytotoxic only when separated from the full-length ECR. This evidence suggests that a stimulus or event is necessary for the release of teneurin C-terminus into the synaptic cleft region.

In Tc toxins, a change in pH triggers the opening of the TcA component and a subsequent conformational change of the inner translocation channel. This structural shift opens the β-propeller gate at the bottom of the TcB-TcC barrel, allowing for the cleaved C-terminal cytotoxic domain to flow down the newly continuous pore from inside the barrel cavity to the target cell (Gatsogiannis et al., 2018). Once inside the cell, the cytotoxic domain exerts its insecticidal activity depending on species of bacteria. For example, the cytotoxic domain from *P. luminescens* acts as an ADP-ribosyltransferase, which post-translationally modifies actin that leads to increased actin polymerization and clustering and subsequent cell death (Gatsogiannis et al., 2018; Lang et al., 2010; Meusch et al., 2014). While an insecticidal role for the C-terminal cytotoxic domain exists in bacterial Tc toxins, the need for a cytotoxic role in higher organisms is unclear. If the cleaved toxin-like domain of TENs is detrimental to cells in living organisms, especially in areas where TENs are localized such as the brain, then perhaps a mechanism is in place to prevent autoproteolysis or release of teneurin C-terminus. On the other hand, an argument could be made that cytotoxicity is required only at specific times and thereby initiated by a particular event or trigger; for instance, pruning of inappropriate contacts during neurodevelopment could be a result from programmed cell death or the disruption of mitochondrial DNA induced by cleavage and release of toxin-like domain from TENs.

Some groups claim C-terminal cleavage is absent in TENs, while others report cleavage at the TCAP site (**Figure 3.2B**) (Chand et al., 2013; Vysokov et al., 2016; Vysokov et al., 2018). While cleavage is predicted at the TCAP, the appearance of this small protein product in brain

lysates may be due to TCAP acting as its own mRNA transcript independent of TEN translation. Furthermore, TCAP does not exhibit any nuclease activity and instead acts in opposite fashion as a neuromodulatory agent in both vertebrates and invertebrates. Most of these groups utilize murine brain lysates and neuronal tissue culture lines to examine the catalytic potential of TENs. Following suit, we observed no C-terminal cleavage when transfecting mammalian cells with full-length TEN2 constructs or purifying full ECR from insect cells. However, once the EGF- and Ig-like domains were removed, a C-terminal product was detected in TEN2, and we identified conserved catalytic residues responsible for the appearance of this product, R2302 and D2315. This evidence strongly suggests that the toxin-like domain is cleaved via autoproteolysis comparable to Tc toxins, and likewise a mechanism may exist in human TENs that regulates C-terminal release.

The Ig-like domain has increasingly become a point of interest for studying TENs, due to its carboxypeptidase-like sequence conservation, TTR domain, and β-propeller interface for dimerization in flies (Li et al., 2023; Tucker, 2018). We targeted the Ig-like domain as a possible modulator of toxin-like domain release because of putative interface between domains inside the barrel structure. We saw evidence that the full ECR produced a C-terminal product when the small loop in the interface was deleted. Furthermore, we saw very preliminary evidence that specific residues N928A/E933A/Q2402A/R2406A may contribute to releasing the C-terminal product (**see Appendix B**). However, further investigation is needed to make this claim and establish a concrete interface between the Ig-like and toxin-like domain. Nevertheless, these data point to the Ig-like domain as a possible regulatory domain for autoproteolytic release of the toxin-like domain in TENs. Whether the Ig-like domain influences autoproteolysis itself or directs the release of an already-cleaved toxin-like domain remains to be determined. If we look

at Tc toxins for comparison, the cytotoxic domain is cleaved regardless of an open or closed translocation channel, but autoproteolysis is required for translocation to occur, hinting that the Ig-like domain interface with toxin-like domain is influencing C-terminal release rather than autoproteolysis. To test this possibility, we could mutate the catalytic residues R2302 and D2315 in the ECR_ΔSL construct and observe whether C-terminal product is absent from purified protein. Furthermore, the effect of pH on cytotoxic domain release in Tc toxins suggests pH may be important for toxin-like domain release. The cytotoxic domain is released only when a change in pH triggers the opening of the translocation channel (Gatsogiannis et al., 2018). Additionally, the C-terminal domain is dissociated from the TcB-TcC complex only when dialysed with low pH buffer rather than at pH 7.5 (Busby et al., 2013). It is possible that a certain event triggers release of the toxin-like domain, such as a change in pH or interactions with an unknown ligand. All these unexplored possibilities could be the reason for the lack of C-terminal cleavage reported by various groups. These future experimental considerations for the Ig-like and toxin-like domain could reveal a physiologically relevant mechanism for autoproteolysis of the C-terminus.

C-terminal processing of *ten-1* has yet to be determined, but here we see some early evidence of potential C-terminal cleavage in *C. elegans*. Similar to TEN2, we observed a possible C-terminally His-tagged product when the EGF- and Ig-like domains were deleted, suggesting a potential for C-terminal release (**see Appendix C**). While the catalytic site is only partially conserved, serine participates in enzymatic activity through serine proteases in conjunction with histadine and aspartic acid. When we examined an Alpha-fold model of Ten-1, we did not locate histadines or asparates within 4 Å, a typical distance for protease residue positions. However, it is possible TENs undergoes some conformational shifts to activate a

catalytic site. Tc toxin studies of catalytic residues exceeded a distance of 4 Å in their crystal structure but were still confirmed to induce autoproteolysis. Furthermore, limitations of Alpha-fold modeling may be at play. It is not unheard of that invertebrate TENs diverged in evolution from vertebrates. For example, the asymmetrical interface in *Drosophila* that regulates dimerization is not conserved in vertebrates, but vertebrate TENs contain an alternative splice site in the same position that regulates dimerization (Li et al., 2023). However, we fully acknowledge that C-terminal autoproteolysis may not be present in *ten-1* as we have yet to confirm it via our biochemical studies. It should be noted that we observed a smaller 15 kDa product in the *ten-1* ECR_Δ1, 2 construct, suggesting that TCAP is cleaved in *C. elegans* similarly to other TENs, which has been previously unreported (**see Appendix C**). The modulatory effects of TCAP on stress behavior has been studied in other invertebrates, which leaves TCAP and its functional role in C. elegans as worthy of further investigation.

While *ten-1* in *C. elegans* is usually described as an extracellular matrix component affecting basement integrity and body morphology, our data hints at *ten-1* as playing a possible axon guidance role or a component of egg-laying behavior. Furthermore, *ten-1* has been identified as part of the neuroprotective gene pool that promotes axonal regeneration in touch receptor neurons (Delgado et al., 2023). Thus, a multitude of functions remains to be fully explored in *C. elegans* with respect to *ten-1* and its domains.

TENs have risen in popularity as a target of study in recent years due to its role in neuronal circuitry development. Its complex and unique tertiary structure has attracted much speculation about how TENs function and the implications for diseases. In this thesis, we explored the C-terminal properties of TENs, where we found axonal defects in *C. elegans* nervous system when the toxin-like domain was truncated and found evidence of potential

autoproteolytic processing of a vertebrate isoform. The toxin-like domain may shed into the synaptic cleft and undergo further proteolytic processing or post-translational modifications to produce an active TCAP, or itself act as a ligand across the synapse with post-synaptic receptors. The C-terminal properties recorded in this thesis can lead to further studies of TENs in their biochemistry and their potential functions, which ultimately could be important for understanding the role of TENs in disease.

MATERIALS AND METHODS

4.1 Worm Handling and Strains

Worms were grown under standard conditions at 20° C on nematode growth media (NGM) plates with bacteria (*E. coli* OP50) as food source (Brenner, 1974). All worms used in this study were hermaphrodites. L1 worms were obtained from recently hatched eggs. Adult worms were picked at Day 1 after maturation from L4, which were identified by DIC or fluorescence based on vulval morphology. N2 Bristol strain was used as wildtype. In addition, the following strains were used: NK2502 [*ten-1::mNG*], PHX9522 [*ten-1(syb9522)*], *ten-1::mNG; otIs544[cho-1(fosmid)::SL2::mChOpti::H2B + pha-1(+)]*, VC518 [ten-1(ok641)], *ser-7b::GFP*, *ser-7b::GFP; ten-1::mNG*, *ser-7b::GFP; ten-1(syb9522)*, *ser-7b::GFP; ten-1(ok641)*, *tph-1::GFP*, *tph-1::GFP; ten-1::mNG*, *tph-1::GFP; ten-1(syb9522)*, *tph-1::GFP; ten-1(ok641)*, *evIs79(unc-129::GFP).* Some strains were provided by the CGC, which is funded by NIH Office of Research Infrastructure Programs (P40 OD010440), unless otherwise stated: *ser-7b::GFP* was a generous gift from Dr. Peter G. Okkema, *ten-1(syb9522)* was procured from SUNY Biotech, *unc-129::GFP* was a generous gift from Dr. Marc Pilon.

4.2 Generation of CRISPR Strain

Truncation of the C-terminus in *ten-1(syb9522)* was conducted on *ten-1::mNG*, which has been previously described (Keeley et al., 2020). Briefly, *ten-1::mNG* strain was previously generated by insertion of an 18 amino acid flexible linker (6x glycine-alanine-serine) and mNeonGreen fluorophore at the C-terminus of the *ten-1* genetic loci via CRISPR-mediated genome editing. *Ten-1::mNG* was then modified by truncating 597 nucleotides starting in exon

18 and completely ablating exon 19 (25231-25827), which corresponds to the toxin-like domain of *ten-1* located outside the barrel-exit site. Truncation was conducted in frame upstream of the linker region.

4.3 Microscopy

Animals were anesthetized using 100mM sodium azide (NaN_3) and mounted on 4% agarose (w/v in water) on glass slides. Images of neuronal GFP reporter lines were taken with an automated fluorescence microscope at 20X magnification for pharyngeal neurons and 10X for body neurons (Zeiss, Axio Imager Z2). Several z-stacks were taken with each image (0.32 μm intervals between stacks) with Zeiss Axiocam 503 mono using the ZEN software (Version 2.3.69.1000, Blue edition). Images of ten-1 fluorescent strains were obtained with a confocal microscope at 63X magnification with oil (Zeiss LSM 880). Representative images shown were obtained by either single layer or maximum intensity projection of 8-11 μm Z-stacks. Image reconstruction was performed using Image J/FIJI software.

4.4 Quantification Analysis on ImageJ/FIJI

CZI files of images containing both fluorescent strains, *ten-1::mNG; otIs544* and ten-1*(syb9522),* side-by-side were imported directly to FIJI. The region of interest (ROI) was set between the anterior and terminal bulbs length-wise and between the dorsal and ventral edges height-wise. Images were processed using Z-project to obtain Sum of Slices image with boundaries manually set per Z-stack. Only worms that were sitting laterally were selected to maintain a consistent pattern of expression between images at the ROI. Threshold of 300 was

globally applied and values were set to NaN to reduce background fluorescence. Mean Gray Value and Area were measured to extract fluorescence intensity and total area of expression.

4.5 Cell Culture

High-Five insect cells (Trichoplusia ni, female, ovarian) (Thermo Fisher, B85502) were cultured in Insect-Xpress medium (Lonza, 12-730Q) supplemented with 10 μg/mL gentamicin at 27°C and were used for production of recombinant proteins. HEK293T mammalian cells (Homo sapiens, female, embryonic kidney) were cultured in Dulbecco's modified Eagle's medium (DMEM; GIBCO) supplemented with 10% (v/v) fetal bovine serum (FBS) (Sigma) at 37°C in 5% CO2 and were used for cell-surface flow cytometry and protein expression.

4.6 Cloning and Expression in Insect Cells

ECR constructs of human TEN2 variant Lasso (UniProt: Q9NT68-2) and *C. elegans ten-1* (UniProt: G5EGQ6) were cloned into pAcGP67A vector containing a 6x His tag at the C-terminus for affinity purification. Spodoptera frugiperda (Sf9) cells (Thermo Fisher, 12659017) were transfected with TEN constructs and linearized baculovirus DNA (Expression Systems, 91-002) using Cellfectin II (Thermo Fisher, 10362100) transfection reagent. Baculovirus was amplified in Sf9 cells with 10% FBS in SF900-III medium (Gibco). Large-scale protein expression was performed by infection of High Five cells in Lonza medium at a cell density of 2 × 10^6 cells/ml for 72 hr at 27 °C. The media containing the secreted recombinant protein was collected and centrifuged at 900 g for 15 min at room temperature. After centrifugation, the supernatant was transferred into a beaker, and the following were added (to final concentrations): 50 mM Tris pH 8.0, 5 mM $CaCl_2$ and 1 mM $NiCl_2$. After 30 minutes of stirring, the protein

solution was centrifuged at 8,000 g for 30 min, and the supernatant was collected and incubated with nickel-nitrilotriacetic agarose resin (QIAGEN) for 3 hr at room temperature. The resin was transferred to a glass Buchner funnel and rinsed with HBS buffer containing 20 mM imidazole, then transferred to a smaller poly-prep chromatography column (Bio-rad). His-tagged protein was eluted with HBS buffer at 200 mM imidazole and then processed by size-exclusion chromatography (Superdex 200 10/300 GL; GE Healthcare). The separated protein was eluted in fractions in a final buffer at 10 mM Tris pH 8.5, 150 mM NaCl.

4.7 Cloning and Expression in Mammalian Cells

Wildtype TEN2 ECR and Ig- and toxin-like interface mutants were cloned into pcDNA3.1 vector with an N-terminal FLAG tag and C-terminal myc tag. Constructs were transfected into HEK 293T cells using Lipofectamine and used for Western Blot or flow cytometry cell-surface confirmation.

4.8 Western Blots

Protein from various TEN constructs were mixed with 6x sodium dodecyl sulfate (SDS) sample buffer, boiled at 95 °C for 5 min, and loaded into 12% polyacrylamide gel for SDS-PAGE electrophoresis. Gel was run at 150V for 60 min, and proteins were then transferred to nitrocellulose membrane using via either wet transfer (20% methanol transfer buffer at 100V at 4 °C for 1 hr) or semi-dry transfer (7 min at room temperature). Membrane was blocked in 4% bovine serum albumin (BSA) in tris-buffered saline with Tween-20 (TBST) for 1 hr at room temperature. Primary antibody in 4% BSA was added and incubated overnight at 4 °C: mouse anti-His 1:1000, conjugated His-488 1:5000, conjugated FLAG-488 1:2000, chicken anti-Myc

1:1000. Membranes were washed 4x in TBST for 5 min, probed with secondary antibody, and washed again: Alexa Fluor 488 Donkey Anti-Mouse IgG (H+L) (Invitrogen A21202) 1:5000, Alexa Fluor 647 Anti-Chicken 1:5000. Proteins were visualized with BioRad Chemidoc system.

4.9 Statistical Analysis

Student's t-test was used for calculating difference in mNG fluorescence expression between wildtype and truncation mutant. One-way ANOVA and Tukey's multiple comparison test were used to compare viability differences across four ten-1 strains. Bonferroni's multiple comparisons test was used for comparing vulva defects across days. Fisher's exact test was used to compare binary conditions for axon scoring. Resulting p values <0.05 were considered significant. Data was analyzed using software GraphPad Prism.

APPENDIX A

A.1 *unc-129::GFP* expression in the *ten-1(syb9522)* truncation mutant

In previous studies, *unc-129::GFP* expression was shown to increase 20-fold when crossed into *ten-1(ok641)* null mutant (Mörck et al., 2010). To test whether the truncation of the toxin-like domain could reproduce a similar phenotype as the null mutant, *ten-1(syb9522)* was crossed into *unc-129::GFP* reporter strain. We found that GFP in the dorsal muscles increased in the truncation mutant when compared to the WT reporter. Thus, truncation of the toxin-like domain was able to recapitulate the same increase in *unc-129::GFP* expression seen in the null mutant, indicating that the toxin-like domain is at least partially responsible for downregulation of *unc-129* on dorsal muscles.

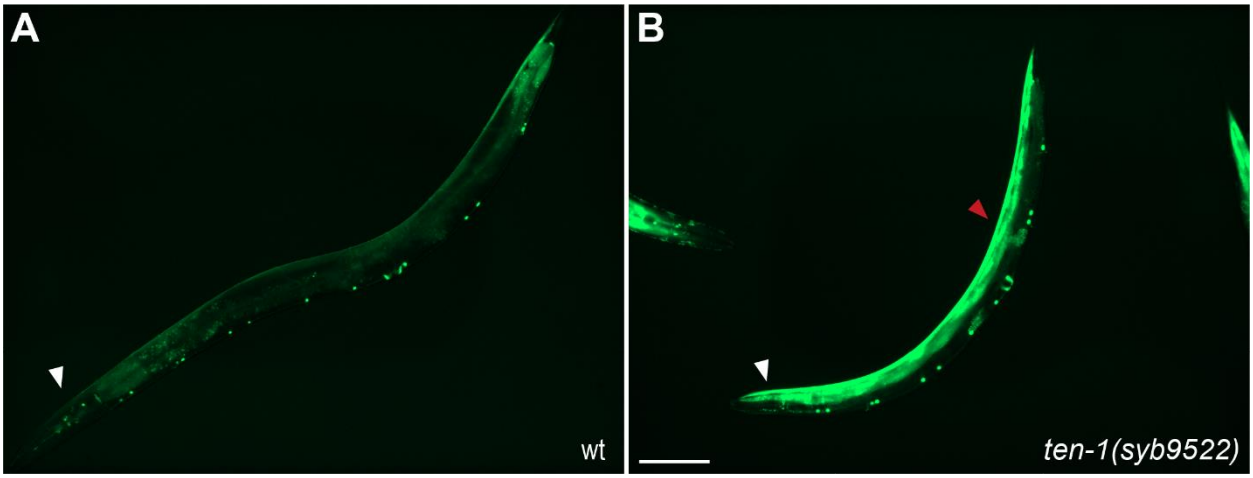

Figure A.1: *unc-129::GFP* expression is increased in adult *ten-1* truncation mutant

(A) WT transcriptional reporter *unc-129::GFP* shows expression at DA/DB neurons along VNC and dorsal muscles. White arrowhead points to head of worm.

(B) *ten-1(syb9522)* truncation mutant shows increased *unc-129::GFP* expression along the dorsal muscles. Red arrowhead points to increased dorsal muscle expression. Scale bar represents 100 µm.

APPENDIX B

B.1 Mutagenesis of specific residues at the Ig-like/toxin-like interface may produce a C-terminal product

To investigate which residues influence the Ig-like/toxin-like domain interface, we targeted amino acids predicted to form hydrogen bonds across the interface for mutagenesis. N928 and E933 in the Ig-like domain potentially form hydrogen bonds with I2397 and I2397/G2399/V2400 in the toxin-like domain, and Q2402A and R2406A of the toxin-like domain may interact with A923 and F921 of the Ig-like domain. We chose residues that use their side chain to form hydrogen bonds instead of their amino group because disturbing the amino group may lead to destabilization of secondary structure of the protein. We cloned double mutant N928A/E933A, Q2402A/R2406A, and quadruple mutant N928A/E933A/Q2402A/R2406A into TEN2 ECR mammalian construct and transfected into HEK 293T cells. We observed a very faint band at about 30 kDa in NEQR mutant that may be absent in EV or other combination of mutated residues (**Figure B.1**). Because the Western blot signal was low, we cannot make a definitive conclusion about these mutations, but this preliminary evidence may point to specific residues crucial for establishing the Ig-like/toxin-like interface.

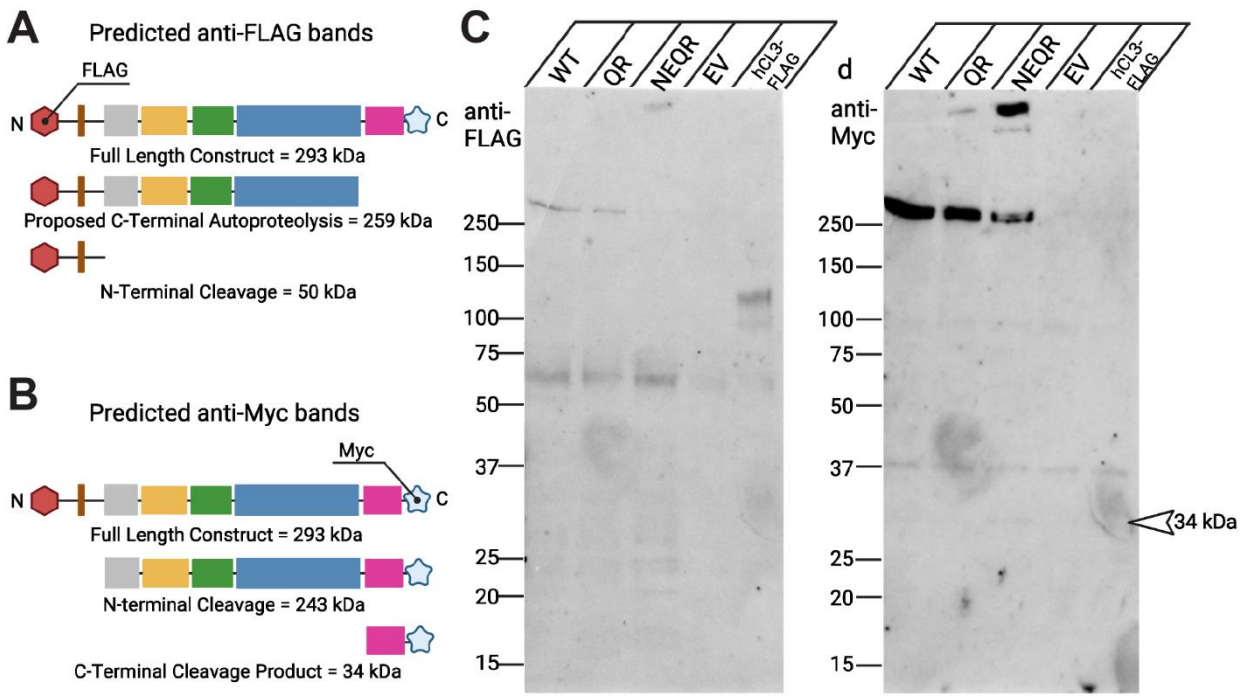

Figure B.1: Specific interface residues may contribute to C-terminal product release

(A-B) Predicted bands for FLAG and Myc antibody staining of mammalian TEN2 constructs

(C) Western blots for FLAG (left) and Myc (right) antibodies. QR: Q2402A/R2406A; NEQR: N928A/E933A/Q2402A/R2406A; EV: empty vector; hCL3-FLAG: Latrophilin-3 positive control for FLAG.

APPENDIX C

C.1 *C. elegans ten-1* may exhibit a C-terminal product

While the C-terminal autoproteolysis site is conserved in human TENs, the catalytic residues are only partially conserved in *C. elegans ten-1*: arginine (R2381) is conserved, serine (R2394) takes the place of the first aspartate, and glutamate (E2426) substitutes the second aspartate. Serine is not involved in the canonical aspartic dyad found in aspartic proteases, but it participates as a catalytic residue in other active sites, being the nucleophilic center of serine proteases in conjunction with other residues like histidine and aspartate. Moreover, glutamate and aspartate both contain a negatively charged carboxyl group in their side chains, allowing glutamate to act as a substitute for aspartate in catalytic reactions. Furthermore, we looked at Ten-1 structure using Alpha-fold and found that the putative catalytic residues R2391, S2394,

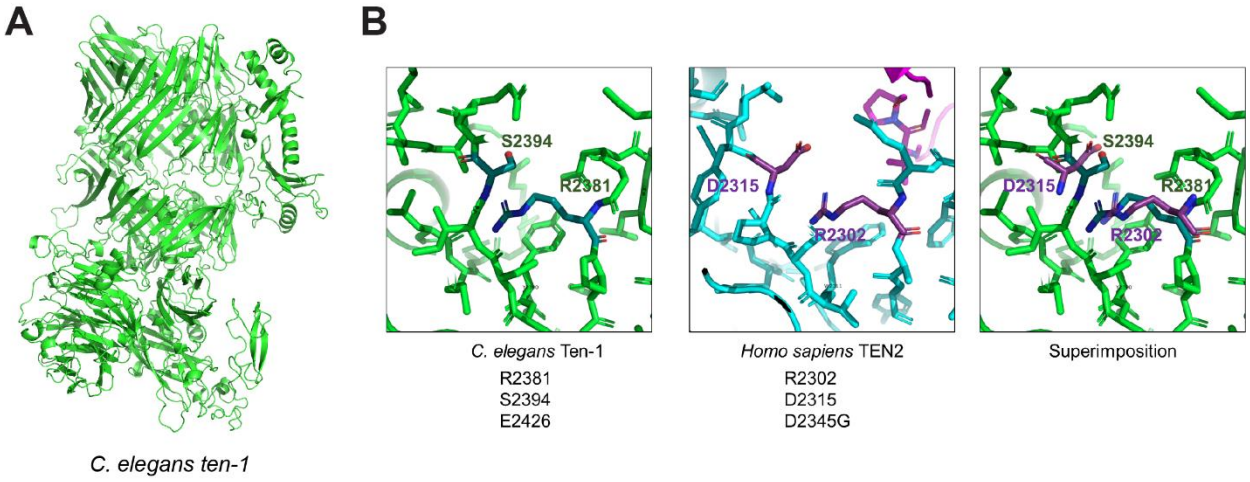

Figure C.1: Autoproteolysis site is partially conserved in *C. elegans ten-1*

(A) Alpha-fold model of *C. elegans ten-1*.

(B) Putative catalytic residues arginine and serine reside at similar structural positions as their partially conserved counterparts in TEN2.

and E2426 lie spatially in similar position as the catalytic residues in TEN2 responsible for autoproteolysis (**Figure C.1**). Thus, we tested the potential of *C. elegans ten-1* to produce a C-terminal product as observed in human TEN2.

Size-exclusion chromatography of the full Ten-1 ECR resulted in protein product corresponding to the expected size of 270 kDa (**Figure C.2A**). When the EGF-like domain was deleted, we observed a protein product at about 210 kDa and an absorbance peak to the right of the full construct, which indicates that *ten-1* ECRΔ1 protein is purified as a monomer while the full ECR as a dimer (**Figure C.2B**). Dimerization is most likely due to unpaired cysteines found in the EGF-like domain, which are conserved in other TENs. We then deleted the Ig-like domain to test whether a small C-terminal product is present akin to TEN2 protein purification. While we did not fully resolve a peak at the predicted elution volume for potential cleavage product, His-antibody staining showed a band a 37 kDa in the ECRΔ1,2 fractions corresponding to the expected elution volumes small-sized protein product (**Figure C.3A**). This light band was partially present in the full ECR and missing in ECRΔ1 (**Figure C.3B**). Additionally, ECRΔ1,2 yielded a clear band about 14 kDa in size, the expected weight of TCAP-cleavage product. These constructs contain a 6x His tag at the C-terminus, suggesting that these bands may be part of *ten-1* C-terminus. However, more testing, such as cleaner protein purifications and mass spectrometry, needs to be conducted before reaching a proper conclusion.

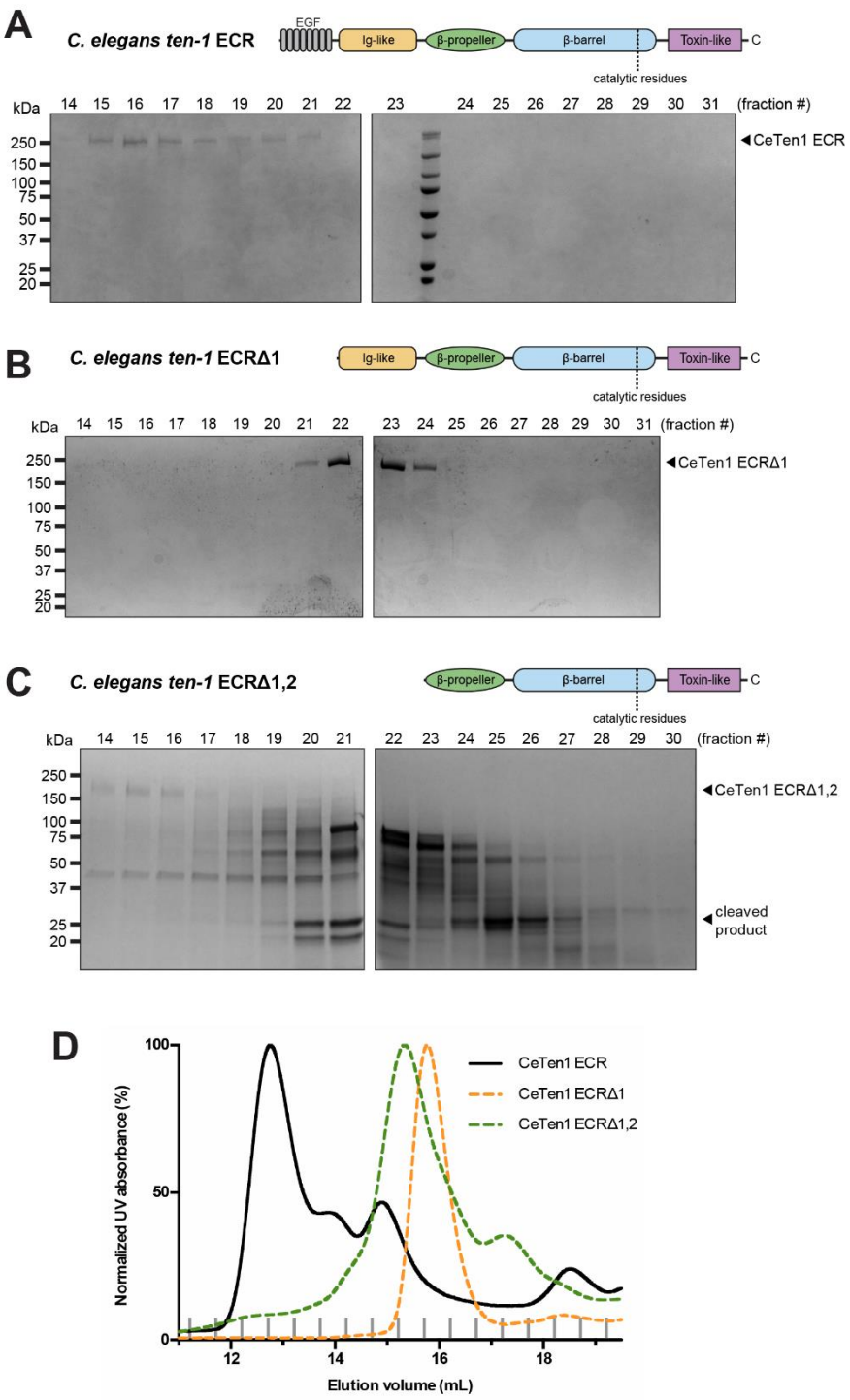

Figure C.2: Size-exclusion chromatography of *C. elegans ten-1* protein purifications

(A-D) Fractions from size exclusion chromatography of *ten-1* ECR (A), ECRΔ1 (B), and ECRΔ1,2 (C) protein purifications. Red bars in chromatograms indicate fractions collected. Comparison of chromatograms normalized to 100% show a peak-shift left in ECR (black) compared to ECRΔ1 (yellow). UV: Ultraviolet; mAU: mili-Absorbance units.

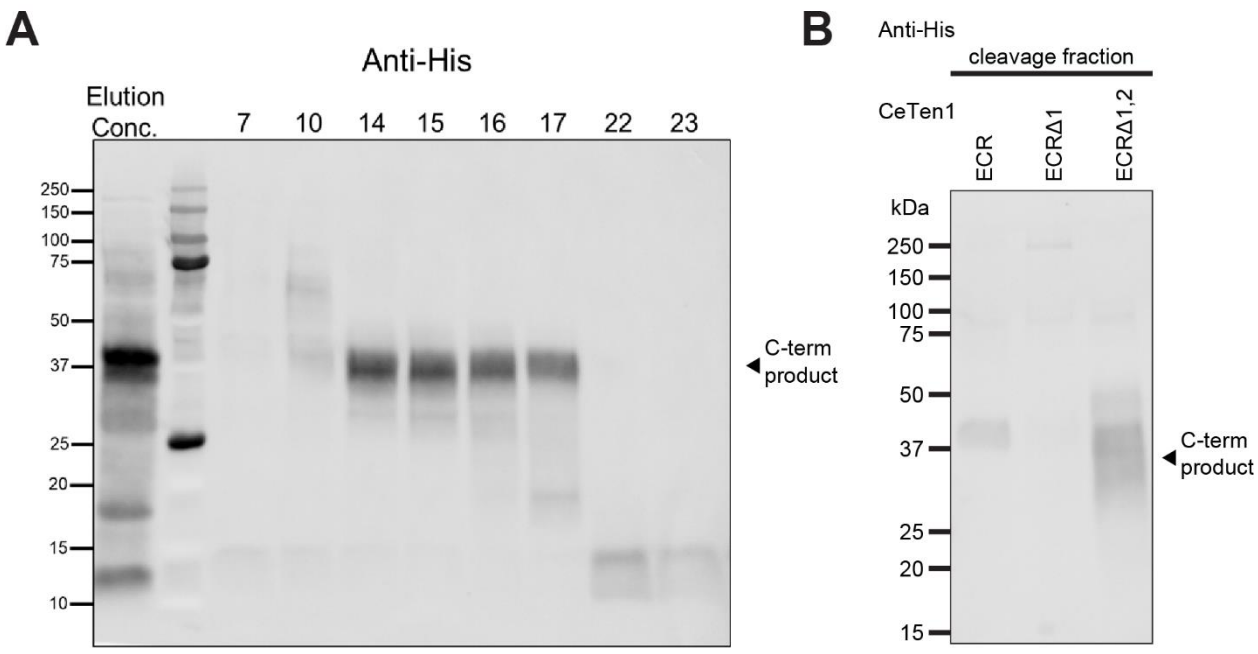

Figure C.3: His-antibody staining of C-terminally His-tagged *ten-1*

(A) Eluted fractions from SEC of ECRΔ1,2 were probed with anti-His and show 37 kDa bands in expected cleavage fractions. Elution Conc. is concentrated elution before SEC separation.

(B) Comparison between *ten-1* purifications shows no His-staining in ECRΔ1 and partial band in full ECR.

REFERENCES

Abramov, T., Suwansa-Ard, S., da Silva, P. M., Wang, T., Dove, M., O'Connor, W.,…Elizur, A. (2022). Teneurin and TCAP Phylogeny and Physiology: Molecular Analysis, Immune Activity, and Transcriptomic Analysis of the Stress Response in the Sydney Rock Oyster (*Front Endocrinol (Lausanne)*, *13*, 891714. https://doi.org/10.3389/fendo.2022.891714

Alkelai, A., Olender, T., Haffner-Krausz, R., Tsoory, M. M., Boyko, V., Tatarskyy, P.,…Lancet, D. (2016). A role for TENM1 mutations in congenital general anosmia. *Clin Genet*, *90*(3), 211-219. https://doi.org/10.1111/cge.12782

Antinucci, P., Nikolaou, N., Meyer, M. P., & Hindges, R. (2013). Teneurin-3 specifies morphological and functional connectivity of retinal ganglion cells in the vertebrate visual system. *Cell Rep*, *5*(3), 582-592. https://doi.org/10.1016/j.celrep.2013.09.045

Antinucci, P., Suleyman, O., Monfries, C., & Hindges, R. (2016). Neural Mechanisms Generating Orientation Selectivity in the Retina. *Curr Biol*, *26*(14), 1802-1815. https://doi.org/10.1016/j.cub.2016.05.035

Araç, D., & Li, J. (2019). Teneurin Structure: Splice Variants of a Bacterial Toxin Homolog Specifies Synaptic Connections. *Front Neurosci*, *13*, 838. https://doi.org/10.3389/fnins.2019.00838

Axäng, C., Rauthan, M., Hall, D. H., & Pilon, M. (2008). Developmental genetics of the C. elegans pharyngeal neurons NSML and NSMR. *BMC Dev Biol*, *8*, 38. https://doi.org/10.1186/1471-213X-8-38

Bagutti, C., Forro, G., Ferralli, J., Rubin, B., & Chiquet-Ehrismann, R. (2003). The intracellular domain of teneurin-2 has a nuclear function and represses zic-1-mediated transcription. *J Cell Sci*, *116*(Pt 14), 2957-2966. https://doi.org/10.1242/jcs.00603

Beckmann, J., Schubert, R., Chiquet-Ehrismann, R., & Müller, D. J. (2013). Deciphering teneurin domains that facilitate cellular recognition, cell-cell adhesion, and neurite outgrowth using atomic force microscopy-based single-cell force spectroscopy. *Nano Lett*, *13*(6), 2937-2946. https://doi.org/10.1021/nl4013248

Berns, D. S., DeNardo, L. A., Pederick, D. T., & Luo, L. (2018). Teneurin-3 controls topographic circuit assembly in the hippocampus. *Nature*, *554*(7692), 328-333. https://doi.org/10.1038/nature25463

Bowen, D., Rocheleau, T. A., Blackburn, M., Andreev, O., Golubeva, E., Bhartia, R., & ffrench-Constant, R. H. (1998). Insecticidal toxins from the bacterium Photorhabdus luminescens. *Science*, *280*(5372), 2129-2132. https://doi.org/10.1126/science.280.5372.2129

Bowen, D. J., & Ensign, J. C. (1998). Purification and characterization of a high-molecular-weight insecticidal protein complex produced by the entomopathogenic bacterium photorhabdus luminescens. *Appl Environ Microbiol*, *64*(8), 3029-3035. https://doi.org/10.1128/AEM.64.8.3029-3035.1998

Brenner, S. (1974). THE GENETICS OF CAENORHABDITIS ELEGANS. *Genetics*, *77*(1), 71-94. https://doi.org/10.1093/genetics/77.1.71

Busby, J. N., Landsberg, M. J., Simpson, R. M., Jones, S. A., Hankamer, B., Hurst, M. R., & Lott, J. S. (2012). Structural analysis of Chi1 Chitinase from Yen-Tc: the multisubunit

insecticidal ABC toxin complex of Yersinia entomophaga. *J Mol Biol*, *415*(2), 359-371. https://doi.org/10.1016/j.jmb.2011.11.018

Busby, J. N., Panjikar, S., Landsberg, M. J., Hurst, M. R., & Lott, J. S. (2013). The BC component of ABC toxins is an RHS-repeat-containing protein encapsulation device. *Nature*, *501*(7468), 547-550. https://doi.org/10.1038/nature12465

Carmona-Rosas, G., Li, J., Smith, J. J., Cheng, S., Baltrusaitis, E., Nawrocka, W. I.,…Özkan, E. (2023). Structural basis and functional roles for Toll-like receptor binding to Latrophilin adhesion-GPCR in embryo development. *bioRxiv*, 2023.2005.2004.539414. https://doi.org/10.1101/2023.05.04.539414

Carruthers, S. P., Brunetti, G., & Rossell, S. L. (2021). Sleep disturbances and cognitive impairment in schizophrenia spectrum disorders: a systematic review and narrative synthesis. *Sleep Med*, *84*, 8-19. https://doi.org/10.1016/j.sleep.2021.05.011

Chand, D., Casatti, C. A., de Lannoy, L., Song, L., Kollara, A., Barsyte-Lovejoy, D.,…Lovejoy, D. A. (2013). C-terminal processing of the teneurin proteins: independent actions of a teneurin C-terminal associated peptide in hippocampal cells. *Mol Cell Neurosci*, *52*, 38-50. https://doi.org/10.1016/j.mcn.2012.09.006

Cheung, A., Schachermayer, G., Biehler, A., Wallis, A., Missaire, M., & Hindges, R. (2022). Teneurin paralogues are able to localise synaptic sites driven by the intracellular domain and have the potential to form. *Front Neurosci*, *16*, 915149. https://doi.org/10.3389/fnins.2022.915149

Clokey, G. V., & Jacobson, L. A. (1986). The autofluorescent "lipofuscin granules" in the intestinal cells of Caenorhabditis elegans are secondary lysosomes. *Mechanisms of Ageing and Development*, *35*(1), 79-94. https://doi.org/https://doi.org/10.1016/0047-6374(86)90068-0

Colacci, M., De Almeida, R., Chand, D., Lovejoy, S. R., Sephton, D., Vercaemer, B., & Lovejoy, D. A. (2015). Characterization of the teneurin C-terminal associated peptide (TCAP) in the vase tunicate, Ciona intestinalis: A novel peptide system associated with energy metabolism and reproduction. *Gen Comp Endocrinol*, *216*, 161-170. https://doi.org/10.1016/j.ygcen.2015.01.021

Colavita, A., & Culotti, J. G. (1998). Suppressors of ectopic UNC-5 growth cone steering identify eight genes involved in axon guidance in Caenorhabditis elegans. *Dev Biol*, *194*(1), 72-85. https://doi.org/10.1006/dbio.1997.8790

Colavita, A., Krishna, S., Zheng, H., Padgett, R. W., & Culotti, J. G. (1998). Pioneer axon guidance by UNC-129, a C. elegans TGF-beta. *Science*, *281*(5377), 706-709. https://doi.org/10.1126/science.281.5377.706

Consortium, C. e. D. M. (2012). large-scale screening for targeted knockouts in the Caenorhabditis elegans genome. *G3 (Bethesda)*, *2*(11), 1415-1425. https://doi.org/10.1534/g3.112.003830

D'Aquila, A. L., Hsieh, A. H., De Almeida, R., Lovejoy, S. R., & Lovejoy, D. A. (2017). Expression and actions of corticotropin-releasing factor/diuretic hormone-like peptide (CDLP) and teneurin C-terminal associated peptide (TCAP) in the vase tunicate, Ciona intestinalis: Antagonism of the feeding response. *Gen Comp Endocrinol*, *246*, 105-115. https://doi.org/10.1016/j.ygcen.2016.06.015

Del Toro, D., Carrasquero-Ordaz, M. A., Chu, A., Ruff, T., Shahin, M., Jackson, V. A.,…Seiradake, E. (2020). Structural Basis of Teneurin-Latrophilin Interaction in

Repulsive Guidance of Migrating Neurons. *Cell*, *180*(2), 323-339.e319. https://doi.org/10.1016/j.cell.2019.12.014

Delgado, S. E., Urrutia, A., Gutzwiller, F., Chiu, C. Q., & Calixto, A. (2023). Microbiota and Diapause-Induced Neuroprotection Share a Dependency on Calcium But Differ in Their Effects on Mitochondrial Morphology. *eNeuro*, *10*(7). https://doi.org/10.1523/ENEURO.0424-22.2023

DePew, A. T., Aimino, M. A., & Mosca, T. J. (2019). The Tenets of Teneurin: Conserved Mechanisms Regulate Diverse Developmental Processes in the Drosophila Nervous System. *Front Neurosci*, *13*, 27. https://doi.org/10.3389/fnins.2019.00027

Dharmaratne, N., Glendining, K. A., Young, T. R., Tran, H., Sawatari, A., & Leamey, C. A. (2012). Ten-m3 is required for the development of topography in the ipsilateral retinocollicular pathway. *PLoS One*, *7*(9), e43083. https://doi.org/10.1371/journal.pone.0043083

Drabikowski, K., Trzebiatowska, A., & Chiquet-Ehrismann, R. (2005). ten-1, an essential gene for germ cell development, epidermal morphogenesis, gonad migration, and neuronal pathfinding in Caenorhabditis elegans. *Dev Biol*, *282*(1), 27-38. https://doi.org/10.1016/j.ydbio.2005.02.017

Edgley, M. L., & Riddle, D. L. (2001). LG II balancer chromosomes in Caenorhabditis elegans: mT1(II;III) and the mIn1 set of dominantly and recessively marked inversions. *Mol Genet Genomics*, *266*(3), 385-395. https://doi.org/10.1007/s004380100523

Feng, K., Zhou, X. H., Oohashi, T., Mörgelin, M., Lustig, A., Hirakawa, S.,…Fässler, R. (2002). All four members of the Ten-m/Odz family of transmembrane proteins form dimers. *J Biol Chem*, *277*(29), 26128-26135. https://doi.org/10.1074/jbc.M203722200

Ferralli, J., Tucker, R. P., & Chiquet-Ehrismann, R. (2018). The teneurin C-terminal domain possesses nuclease activity and is apoptogenic. *Biol Open*, *7*(3). https://doi.org/10.1242/bio.031765

Ferrarelli, F. (2020). Sleep disturbances in schizophrenia and psychosis. *Schizophr Res*, *221*, 1-3. https://doi.org/10.1016/j.schres.2020.05.022

Gatsogiannis, C., Merino, F., Roderer, D., Balchin, D., Schubert, E., Kuhlee, A.,…Raunser, S. (2018). Tc toxin activation requires unfolding and refolding of a β-propeller. *Nature*, *563*(7730), 209-213. https://doi.org/10.1038/s41586-018-0556-6

Gogou, C., Beugelink, J. W., Frias, C. P., Kresik, L., Jaroszynska, N., Drescher, U.,…Meijer, D. H. (2024). Alternative splicing controls teneurin-3 compact dimer formation for neuronal recognition. *Nat Commun*, *15*(1), 3648. https://doi.org/10.1038/s41467-024-47763-x

Graumann, R., Di Capua, G. A., Oyarzún, J. E., Vásquez, M. A., Liao, C., Brañes, J. A.,…Ziegler, A. (2017). Expression of teneurins is associated with tumor differentiation and patient survival in ovarian cancer. *PLoS One*, *12*(5), e0177244. https://doi.org/10.1371/journal.pone.0177244

Hobson, R. J., Geng, J., Gray, A. D., & Komuniecki, R. W. (2003). SER-7b, a constitutively active Galphas coupled 5-HT7-like receptor expressed in the Caenorhabditis elegans M4 pharyngeal motorneuron. *J Neurochem*, *87*(1), 22-29. https://doi.org/10.1046/j.1471-4159.2003.01967.x

Hogg, D. W., Casatti, C. C., Belsham, D. D., Baršytė-Lovejoy, D., & Lovejoy, D. A. (2022). Distal extracellular teneurin region (teneurin C-terminal associated peptide; TCAP) possesses independent intracellular calcium regulating actions,in vitro: A potential

antagonist of corticotropin-releasing factor (CRF). *Biochem Biophys Rep, 32*, 101397. https://doi.org/10.1016/j.bbrep.2022.101397

Hogg, D. W., Husić, M., Wosnick, D., Dodsworth, T., D'Aquila, A. L., & Lovejoy, D. A. (2019). Activity of the Carboxy-Terminal Peptide Region of the Teneurins and Its Role in Neuronal Function and Behavior in Mammals. *Front Neurosci, 13*, 581. https://doi.org/10.3389/fnins.2019.00581

Hogg, D. W., Reid, A. L., Dodsworth, T. L., Chen, Y., Reid, R. M., Xu, M.,…Lovejoy, D. A. (2022). Skeletal muscle metabolism and contraction performance regulation by teneurin C-terminal-associated peptide-1. *Front Physiol, 13*, 1031264. https://doi.org/10.3389/fphys.2022.1031264

Hong, W., Mosca, T. J., & Luo, L. (2012). Teneurins instruct synaptic partner matching in an olfactory map. *Nature, 484*(7393), 201-207. https://doi.org/10.1038/nature10926

Hor, H., Francescatto, L., Bartesaghi, L., Ortega-Cubero, S., Kousi, M., Lorenzo-Betancor, O.,…Estivill, X. (2015). Missense mutations in TENM4, a regulator of axon guidance and central myelination, cause essential tremor. *Hum Mol Genet, 24*(20), 5677-5686. https://doi.org/10.1093/hmg/ddv281

Huang, Y. C., Luo, J., Huang, W., Baker, C. M., Gomes, M. A., Meng, B.,…Flavell, S. W. (2023). A single neuron in C. elegans orchestrates multiple motor outputs through parallel modes of transmission. *Curr Biol, 33*(20), 4430-4445.e4436. https://doi.org/10.1016/j.cub.2023.08.088

Hurst, M. R., Jones, S. A., Binglin, T., Harper, L. A., Jackson, T. A., & Glare, T. R. (2011). The main virulence determinant of Yersinia entomophaga MH96 is a broad-host-range toxin complex active against insects. *J Bacteriol, 193*(8), 1966-1980. https://doi.org/10.1128/JB.01044-10

Husić, M., Barsyte-Lovejoy, D., & Lovejoy, D. A. (2019). Teneurin C-Terminal Associated Peptide (TCAP)-1 and Latrophilin Interaction in HEK293 Cells: Evidence for Modulation of Intercellular Adhesion. *Front Endocrinol (Lausanne), 10*, 22. https://doi.org/10.3389/fendo.2019.00022

Iossifov, I., O'Roak, B. J., Sanders, S. J., Ronemus, M., Krumm, N., Levy, D.,…Wigler, M. (2014). The contribution of de novo coding mutations to autism spectrum disorder. *Nature, 515*(7526), 216-221. https://doi.org/10.1038/nature13908

Jackson, V. A., Meijer, D. H., Carrasquero, M., van Bezouwen, L. S., Lowe, E. D., Kleanthous, C.,…Seiradake, E. (2018). Structures of Teneurin adhesion receptors reveal an ancient fold for cell-cell interaction. *Nat Commun, 9*(1), 1079. https://doi.org/10.1038/s41467-018-03460-0

Keeley, D. P., Hastie, E., J ayadev, R., Kelley, L. C., Chi, Q., Payne, S. G.,…Sherwood, D. R. (2020). Comprehensive Endogenous Tagging of Basement Membrane Components Reveals Dynamic Movement within the Matrix Scaffolding. *Developmental cell, 54*(1). https://doi.org/10.1016/j.devcel.2020.05.022

Kenzelmann, D., Chiquet-Ehrismann, R., Leachman, N. T., & Tucker, R. P. (2008). Teneurin-1 is expressed in interconnected regions of the developing brain and is processed in vivo. *BMC Dev Biol, 8*, 30. https://doi.org/10.1186/1471-213X-8-30

Lang, A. E., Schmidt, G., Schlosser, A., Hey, T. D., Larrinua, I. M., Sheets, J. J.,…Aktories, K. (2010). Photorhabdus luminescens toxins ADP-ribosylate actin and RhoA to force actin clustering. *Science, 327*(5969), 1139-1142. https://doi.org/10.1126/science.1184557

Langenhan, T., Prömel, S., Mestek, L., Esmaeili, B., Waller-Evans, H., Hennig, C.,…Russ, A. P. (2009). Latrophilin signaling links anterior-posterior tissue polarity and oriented cell divisions in the C. elegans embryo. *Dev Cell*, *17*(4), 494-504. https://doi.org/10.1016/j.devcel.2009.08.008

Leamey, C. A., Merlin, S., Lattouf, P., Sawatari, A., Zhou, X., Demel, N.,…Fässler, R. (2007). Ten_m3 regulates eye-specific patterning in the mammalian visual pathway and is required for binocular vision. *PLoS Biol*, *5*(9), e241. https://doi.org/10.1371/journal.pbio.0050241

Li, J., Bandekar, S. J., & Araç, D. (2023). The structure of fly Teneurin-m reveals an asymmetric self-assembly that allows expansion into zippers. *EMBO Rep*, *24*(6), e56728. https://doi.org/10.15252/embr.202256728

Li, J., Shalev-Benami, M., Sando, R., Jiang, X., Kibrom, A., Wang, J.,…Araç, D. (2018). Structural Basis for Teneurin Function in Circuit-Wiring: A Toxin Motif at the Synapse. *Cell*, *173*(3), 735-748.e715. https://doi.org/10.1016/j.cell.2018.03.036

Li, J., Xie, Y., Cornelius, S., Jiang, X., Sando, R., Kordon, S. P.,…Araç, D. (2020). Alternative splicing controls teneurin-latrophilin interaction and synapse specificity by a shape-shifting mechanism. *Nat Commun*, *11*(1), 2140. https://doi.org/10.1038/s41467-020-16029-7

Li, S., DeLisi, L. E., & McDonough, S. I. (2021). Rare germline variants in individuals diagnosed with schizophrenia within multiplex families. *Psychiatry Res*, *303*, 114038. https://doi.org/10.1016/j.psychres.2021.114038

Liang, D., Zhao, Y., Pan, H., Zhou, X., He, R., Yang, J.,…Sun, Q. (2021). Rare variant analysis of essential tremor-associated genes in early-onset Parkinson's disease. *Ann Clin Transl Neurol*, *8*(1), 119-125. https://doi.org/10.1002/acn3.51248

Lossie, A. C., Nakamura, H., Thomas, S. E., & Justice, M. J. (2005). Mutation of l7Rn3 shows that Odz4 is required for mouse gastrulation. *Genetics*, *169*(1), 285-299. https://doi.org/10.1534/genetics.104.034967

Lu, Y. C., Nazarko, O. V., Sando, R., Salzman, G. S., Li, N. S., Südhof, T. C., & Araç, D. (2015). Structural Basis of Latrophilin-FLRT-UNC5 Interaction in Cell Adhesion. *Structure*, *23*(9), 1678-1691. https://doi.org/10.1016/j.str.2015.06.024

MacNeil, L. T., Hardy, W. R., Pawson, T., Wrana, J. L., & Culotti, J. G. (2009). UNC-129 regulates the balance between UNC-40 dependent and independent UNC-5 signaling pathways. *Nat Neurosci*, *12*(2), 150-155. https://doi.org/10.1038/nn.2256

Matúš, D., Post, W. B., Groß, V. E., Knierim, A. B., Kuhn, C. K., Fiedler, F.,…Prömel, S. (2024). The N terminus-only (trans) function of the adhesion G protein-coupled receptor latrophilin-1 controls multiple processes in reproduction of Caenorhabditis elegans. *G3 (Bethesda)*, *14*(11). https://doi.org/10.1093/g3journal/jkae206

Matúš, D., Post, W. B., Horn, S., Schöneberg, T., & Prömel, S. (2022). Latrophilin-1 drives neuron morphogenesis and shapes chemo- and mechanosensation-dependent behavior in C. elegans via a trans function. *Biochem Biophys Res Commun*, *589*, 152-158. https://doi.org/10.1016/j.bbrc.2021.12.006

Meijer, D. H., Frias, C. P., Beugelink, J. W., Deurloo, Y. N., & Janssen, B. J. C. (2022). Teneurin4 dimer structures reveal a calcium-stabilized compact conformation supporting homomeric trans-interactions. *EMBO J*, *41*(9), e107505. https://doi.org/10.15252/embj.2020107505

Meusch, D., Gatsogiannis, C., Efremov, R. G., Lang, A. E., Hofnagel, O., Vetter, I. R.,…Raunser, S. (2014). Mechanism of Tc toxin action revealed in molecular detail. *Nature*, *508*(7494), 61-65. https://doi.org/10.1038/nature13015

Mosca, T. J., Hong, W., Dani, V. S., Favaloro, V., & Luo, L. (2012). Trans-synaptic Teneurin signalling in neuromuscular synapse organization and target choice. *Nature*, *484*(7393), 237-241. https://doi.org/10.1038/nature10923

Mueller, L. E., Wexler, R. S., Lovejoy, D. A., Stein, R. B., & Slee, A. M. (2024). Teneurin C-terminal associated peptide (TCAP)-1 attenuates the development and expression of naloxone-precipitated morphine withdrawal in male Swiss Webster mice. *Psychopharmacology (Berl)*, *241*(8), 1565-1575. https://doi.org/10.1007/s00213-024-06582-0

Mörck, C., Axäng, C., & Pilon, M. (2003). A genetic analysis of axon guidance in the C elegans pharynx. *Dev Biol*, *260*(1), 158-175. https://doi.org/10.1016/s0012-1606(03)00238-0

Mörck, C., Vivekanand, V., Jafari, G., & Pilon, M. (2010). C. elegans ten-1 is synthetic lethal with mutations in cytoskeleton regulators, and enhances many axon guidance defective mutants. *BMC Dev Biol*, *10*, 55. https://doi.org/10.1186/1471-213X-10-55

Nakamura, H., Cook, R. N., & Justice, M. J. (2013). Mouse Tenm4 is required for mesoderm induction. *BMC Dev Biol*, *13*, 9. https://doi.org/10.1186/1471-213X-13-9

Nunes, S. M., Ferralli, J., Choi, K., Brown-Luedi, M., Minet, A. D., & Chiquet-Ehrismann, R. (2005). The intracellular domain of teneurin-1 interacts with MBD1 and CAP/ponsin resulting in subcellular codistribution and translocation to the nuclear matrix. *Exp Cell Res*, *305*(1), 122-132. https://doi.org/10.1016/j.yexcr.2004.12.020

Oohashi, T., Zhou, X. H., Feng, K., Richter, B., Mörgelin, M., Perez, M. T.,…Fässler, R. (1999). Mouse ten-m/Odz is a new family of dimeric type II transmembrane proteins expressed in many tissues. *J Cell Biol*, *145*(3), 563-577. https://doi.org/10.1083/jcb.145.3.563

Pinheiro, V. B., & Ellar, D. J. (2007). Expression and insecticidal activity of Yersinia pseudotuberculosis and Photorhabdus luminescens toxin complex proteins. *Cell Microbiol*, *9*(10), 2372-2380. https://doi.org/10.1111/j.1462-5822.2007.00966.x

Prömel, S., Frickenhaus, M., Hughes, S., Mestek, L., Staunton, D., Woollard, A.,…Langenhan, T. (2012). The GPS motif is a molecular switch for bimodal activities of adhesion class G protein-coupled receptors. *Cell Rep*, *2*(2), 321-331. https://doi.org/10.1016/j.celrep.2012.06.015

Pu, J. L., Gao, T., Si, X. L., Zheng, R., Jin, C. Y., Ruan, Y.,…Zhang, B. R. (2020). Parkinson's Disease in Teneurin Transmembrane Protein 4 (TENM4) Mutation Carriers. *Front Genet*, *11*, 598064. https://doi.org/10.3389/fgene.2020.598064

Reid, R. M., Freij, K. W., Maples, J. C., & Biga, P. R. (2019). Teneurins and Teneurin C-Terminal Associated Peptide (TCAP) in Metabolism: What's Known in Fish? *Front Neurosci*, *13*, 177. https://doi.org/10.3389/fnins.2019.00177

Rubin, B. P., Tucker, R. P., Brown-Luedi, M., Martin, D., & Chiquet-Ehrismann, R. (2002). Teneurin 2 is expressed by the neurons of the thalamofugal visual system in situ and promotes homophilic cell-cell adhesion in vitro. *Development*, *129*(20), 4697-4705. https://doi.org/10.1242/dev.129.20.4697

Sando, R., Jiang, X., & Südhof, T. C. (2019). Latrophilin GPCRs direct synapse specificity by coincident binding of FLRTs and teneurins. *Science*, *363*(6429), eaav7969. https://doi.org/doi:10.1126/science.aav7969

Sando, R., & Südhof, T. C. (2021). Latrophilin GPCR signaling mediates synapse formation. *Elife*, *10*. https://doi.org/10.7554/eLife.65717
Schöler, J., Ferralli, J., Thiry, S., & Chiquet-Ehrismann, R. (2015). The intracellular domain of teneurin-1 induces the activity of microphthalmia-associated transcription factor (MITF) by binding to transcriptional repressor HINT1. *J Biol Chem*, *290*(13), 8154-8165. https://doi.org/10.1074/jbc.M114.615922
Schöneberg, T., & Prömel, S. (2019). Latrophilins and Teneurins in Invertebrates: No Love for Each Other? *Front Neurosci*, *13*, 154. https://doi.org/10.3389/fnins.2019.00154
Suzuki, N., Fukushi, M., Kosaki, K., Doyle, A. D., de Vega, S., Yoshizaki, K.,…Yamada, Y. (2012). Teneurin-4 is a novel regulator of oligodendrocyte differentiation and myelination of small-diameter axons in the CNS. *J Neurosci*, *32*(34), 11586-11599. https://doi.org/10.1523/JNEUROSCI.2045-11.2012
Südhof, T. C. (2017). Synaptic Neurexin Complexes: A Molecular Code for the Logic of Neural Circuits. *Cell*, *171*(4), 745-769. https://doi.org/10.1016/j.cell.2017.10.024
Tan, L. A., Al Chawaf, A., Vaccarino, F. J., Boutros, P. C., & Lovejoy, D. A. (2011). Teneurin C-terminal associated peptide (TCAP)-1 modulates dendritic morphology in hippocampal neurons and decreases anxiety-like behaviors in rats. *Physiol Behav*, *104*(2), 199-204. https://doi.org/10.1016/j.physbeh.2011.03.015
Taylor, S. R., Santpere, G., Weinreb, A., Barrett, A., Reilly, M. B., Xu, C.,…Miller, D. M. (2021). Molecular topography of an entire nervous system. *Cell*, *184*(16), 4329-4347.e4323. https://doi.org/10.1016/j.cell.2021.06.023
Tennant, S. M., Skinner, N. A., Joe, A., & Robins-Browne, R. M. (2005). Homologues of insecticidal toxin complex genes in Yersinia enterocolitica biotype 1A and their contribution to virulence. *Infect Immun*, *73*(10), 6860-6867. https://doi.org/10.1128/IAI.73.10.6860-6867.2005
Tessarin, G. W. L., Michalec, O. M., Torres-da-Silva, K. R., Da Silva, A. V., Cruz-Rizzolo, R. J., Gonçalves, A.,…Casatti, C. A. (2019). A Putative Role of Teneurin-2 and Its Related Proteins in Astrocytes. *Front Neurosci*, *13*, 655. https://doi.org/10.3389/fnins.2019.00655
Topf, U., & Chiquet-Ehrismann, R. (2011). Genetic interaction between Caenorhabditis elegans teneurin ten-1 and prolyl 4-hydroxylase phy-1 and their function in collagen IV-mediated basement membrane integrity during late elongation of the embryo. *Mol Biol Cell*, *22*(18), 3331-3343. https://doi.org/10.1091/mbc.E10-10-0853
Topf, U., & Drabikowski, K. (2019). Ancient Function of Teneurins in Tissue Organization and Neuronal Guidance in the Nematode. *Front Neurosci*, *13*, 205. https://doi.org/10.3389/fnins.2019.00205
Trzebiatowska, A., Topf, U., Sauder, U., Drabikowski, K., & Chiquet-Ehrismann, R. (2008). Caenorhabditis elegans teneurin, ten-1, is required for gonadal and pharyngeal basement membrane integrity and acts redundantly with integrin ina-1 and dystroglycan dgn-1. *Mol Biol Cell*, *19*(9), 3898-3908. https://doi.org/10.1091/mbc.e08-01-0028
Tucker, R. P. (2013). Horizontal gene transfer in choanoflagellates. *J Exp Zool B Mol Dev Evol*, *320*(1), 1-9. https://doi.org/10.1002/jez.b.22480
Tucker, R. P. (2018). Teneurins: Domain Architecture, Evolutionary Origins, and Patterns of Expression. *Front Neurosci*, *12*, 938. https://doi.org/10.3389/fnins.2018.00938
Tucker, R. P., Beckmann, J., Leachman, N. T., Schöler, J., & Chiquet-Ehrismann, R. (2012). Phylogenetic analysis of the teneurins: conserved features and premetazoan ancestry. *Mol Biol Evol*, *29*(3), 1019-1029. https://doi.org/10.1093/molbev/msr271

Tucker, R. P., & Chiquet-Ehrismann, R. (2006). Teneurins: a conserved family of transmembrane proteins involved in intercellular signaling during development. *Dev Biol*, *290*(2), 237-245. https://doi.org/10.1016/j.ydbio.2005.11.038

Tucker, R. P., Chiquet-Ehrismann, R., Chevron, M. P., Martin, D., Hall, R. J., & Rubin, B. P. (2001). Teneurin-2 is expressed in tissues that regulate limb and somite pattern formation and is induced in vitro and in situ by FGF8. *Dev Dyn*, *220*(1), 27-39. https://doi.org/10.1002/1097-0177(2000)9999:9999<::AID-DVDY1084>3.0.CO;2-B

Uhlen, M., Zhang, C., Lee, S., Sjöstedt, E., Fagerberg, L., Bidkhori, G.,…Ponten, F. (2017). A pathology atlas of the human cancer transcriptome. *Science*, *357*(6352). https://doi.org/10.1126/science.aan2507

Vysokov, N. V., Silva, J. P., Lelianova, V. G., Ho, C., Djamgoz, M. B., Tonevitsky, A. G., & Ushkaryov, Y. A. (2016). The Mechanism of Regulated Release of Lasso/Teneurin-2. *Front Mol Neurosci*, *9*, 59. https://doi.org/10.3389/fnmol.2016.00059

Vysokov, N. V., Silva, J. P., Lelianova, V. G., Suckling, J., Cassidy, J., Blackburn, J. K.,…Ushkaryov, Y. A. (2018). Proteolytically released Lasso/teneurin-2 induces axonal attraction by interacting with latrophilin-1 on axonal growth cones. *Elife*, *7*. https://doi.org/10.7554/eLife.37935

Waggoner, L. E., Zhou, G. T., Schafer, R. W., & Schafer, W. R. (1998). Control of alternative behavioral states by serotonin in Caenorhabditis elegans. *Neuron*, *21*(1), 203-214. https://doi.org/10.1016/s0896-6273(00)80527-9

Wang, J., Cheng, G., Li, H., & Yang, W. (2024). Effects of cognitive training and behavior modification on aggressive behavior and sleep quality in schizophrenia. *Front Psychiatry*, *15*, 1363547. https://doi.org/10.3389/fpsyt.2024.1363547

Wang, L., Rotzinger, S., Al Chawaf, A., Elias, C. F., Barsyte-Lovejoy, D., Qian, X.,…Lovejoy, D. A. (2005). Teneurin proteins possess a carboxy terminal sequence with neuromodulatory activity. *Brain Res Mol Brain Res*, *133*(2), 253-265. https://doi.org/10.1016/j.molbrainres.2004.10.019

Wang, S., DeLeon, C., Sun, W., Quake, S. R., Roth, B. L., & Südhof, T. C. (2024). Alternative splicing of latrophilin-3 controls synapse formation. *Nature*, *626*(7997), 128-135. https://doi.org/10.1038/s41586-023-06913-9

Waterfield, N. R., Bowen, D. J., Fetherston, J. D., Perry, R. D., & ffrench-Constant, R. H. (2001). The tc genes of Photorhabdus: a growing family. *Trends Microbiol*, *9*(4), 185-191. https://doi.org/10.1016/s0966-842x(01)01978-3

Willson, J., Amliwala, K., Davis, A., Cook, A., Cuttle, M. F., Kriek, N.,…Holden-Dye, L. (2004). Latrotoxin receptor signaling engages the UNC-13-dependent vesicle-priming pathway in C. elegans. *Curr Biol*, *14*(15), 1374-1379. https://doi.org/10.1016/j.cub.2004.07.056

Xu, C., Li, Z., Lyu, C., Hu, Y., McLaughlin, C. N., Wong, K. K. L.,…Luo, L. (2024). Molecular and cellular mechanisms of teneurin signaling in synaptic partner matching. *Cell*, *187*(18), 5081-5101.e5019. https://doi.org/10.1016/j.cell.2024.06.022

Xue, C. B., Xu, Z. H., Zhu, J., Wu, Y., Zhuang, X. H., Chen, Q. L.,…Chen, J. H. (2018). Exome Sequencing Identifies TENM4 as a Novel Candidate Gene for Schizophrenia in the SCZD2 Locus at 11q14-21. *Front Genet*, *9*, 725. https://doi.org/10.3389/fgene.2018.00725

Yi, X., Li, M., He, G., Du, H., Li, X., Cao, D.,…Zhou, D. (2021). Genetic and functional analysis reveals TENM4 contributes to schizophrenia. *iScience*, *24*(9), 103063. https://doi.org/10.1016/j.isci.2021.103063

Young, T. R., Black, D., Mansuri, H., Oohashi, T., Zhou, X. H., Sawatari, A., & Leamey, C. A. (2023). Ten-m4 plays a unique role in the establishment of binocular visual circuits. *Dev Neurobiol*, *83*(3-4), 104-124. https://doi.org/10.1002/dneu.22912

Young, T. R., Bourke, M., Zhou, X., Oohashi, T., Sawatari, A., Fässler, R., & Leamey, C. A. (2013). Ten-m2 is required for the generation of binocular visual circuits. *J Neurosci*, *33*(30), 12490-12509. https://doi.org/10.1523/JNEUROSCI.4708-12.2013

Zhang, M., Chung, S. H., Fang-Yen, C., Craig, C., Kerr, R. A., Suzuki, H.,…Schafer, W. R. (2008). A self-regulating feed-forward circuit controlling C. elegans egg-laying behavior. *Curr Biol*, *18*(19), 1445-1455. https://doi.org/10.1016/j.cub.2008.08.047

Zhang, X., Chen, X., Matúš, D., & Südhof, T. C. (2025). Reconstitution of synaptic junctions orchestrated by teneurin-latrophilin complexes. *Science*, *387*(6731), 322-329. https://doi.org/10.1126/science.adq3586

Zhang, X., Lin, P. Y., Liakath-Ali, K., & Südhof, T. C. (2022). Teneurins assemble into presynaptic nanoclusters that promote synapse formation via postsynaptic non-teneurin ligands. *Nat Commun*, *13*(1), 2297. https://doi.org/10.1038/s41467-022-29751-1

Zheng, L., Michelson, Y., Freger, V., Avraham, Z., Venken, K. J., Bellen, H. J.,…Wides, R. (2011). Drosophila Ten-m and filamin affect motor neuron growth cone guidance. *PLoS One*, *6*(8), e22956. https://doi.org/10.1371/journal.pone.0022956

*Figures 1.1A, 1.2, 2.2A, 2.6A, 2.7A, 3.2 created with Biorender.com.